5. Derivation of PMF (Probable Maximum Flood)

5.1 General Procedure of PMF

PMF analysis aims to estimate the maximum flood considered probable in a particular basin. In the analysis, in general, typical storms which have been taken place in the past are collected in the area covering not only the basin in question but also adjacent areas, or in the area where the climate condition is similar. Then such collected storms are adjusted and maximized so as to be adaptable in the said basin. The maximized storms are called PMP (Probable Maximum Precipitation). Based on the PMP derived, PMF is estimated.

In this Nam Yuam project, since most of the data collected were limited within the basin itself, the typical storms were searched for mainly in the basin and were adjusted.

5.2 Selection of precedent typical storms

Storms here are defined that s sequence of rainfall taking for a certain period with considerable amount of precipitation. Twenty-five storms were selected, looking over the past daily precipitation data recorded at four observatories in the basin as shown in Fig. 5.1 (Mas La Luang, Cham Chaeng, Sop Han and Ban Tha Rua) as well as another observatory in the adjacent basin (Salween). In the selection, following points were considered.

° The storm should be relatively independent from the sequence.

° The storm should contain sufficient amount of precipitation.

° The storm should be the one occuring in wide area preferably covering the whole basin.
(In other words, such storms that found at the five observatories on the same day, during the same period in a similar patter of sequence)

Followings are the storms picked up from the past rainfall data, judging from the said condition.

1.	1967,	Aug.	1	to	Aug.	9
2.	1968,	Jul.	24	to	Jul.	30
3.	"	Aug.	10	to	Aug.	17
4.	1969,	May	26	to	Jun.	2
5.	"	Sep.	2	to	Sep.	7
6.*	1970,	May	15	to	May	18
7.*	1971,	Jul.	16	to	Jul.	22
8.	1972,	Jul.	9	to	Jul.	18
9.	"	Aug.	21	to	Aug.	26
10.	1973,	May	3	to	May	7
11.*	1974,	Aug.	8	to	Aug.	13
12.	1975,	Jul.	13	to	Jul.	18
13.	1976,	Jul.	2	to	Jul.	11
14.	1977,	Jun.	21	to	Jun.	27
15.	"	Jul.	20	to	Jul.	24
16.*	"	Sep.	4	to	Sep.	8
17.*	1978,	Aug.	12	to	Aug.	16
18.*	"	Sep.	20	to	Sep.	23
19.	1979,	Aug.	2	to	Aug.	8
20.*	"	Aug.	11	to	Aug.	17
21.(1)*	1980,	May	20	to	May	25
21.(2)	"	May	26	to	May	28
22.	"	Aug.	22	to	Aug.	27
23.(1)	"	Aug.	31	to	Sep.	5
23.(2)*	"	Sep.	6	to	Sep.	9

Upon these twenty-five storms, average precipitation during the storm period and daily total precipitation of all obser-vaatories were respectively examined so that more competent storms were chosen to the nine storms indicated above by "*".

5.3 DAD (Depth-Area-Duration) analysis

DAD operation was conducted for the selected nine storms, thus the original spot precipitation was converted to areal precipitation. In the operation, hypothetical isohyetal map was elaborated as shown in Fig. 5.2, taking into account rainfall distribution pattern in the basin. An assumption was set that the isohyets would not change the shape regardless of storms or days in the sequence of a storm. On the other hand, rainfall amount represented by the isohyets was properly given in each day in the sequence of a storm. This means that the area surrounded by the isohyet was represented by the observatory located solely in the area and was assumed to have precipitation given as an average of the observatory's and isohyet's.

Fig. 5.3 shows an instance of the DAD operation together with the isohyetal map, which was performed upon the assumption described above. Fig. 5.4 gives an example of DAD curves which was obtained in the analysis.

5.4 Dew point

The observatories in the basin are not recording dew points. Therefore, dew points were obtained from relative humidity and temperature which were available as data, making use of table 5.1. The equation below is the definition of relative humidity.

$$H = \frac{e}{e_s} \times 100\%$$

where, H: relative humidity

e: vapour pressure

e_s: saturation vapor pressure at a particular temperature

Since relative humidity H and temperature are known, vapour pressure e could be obtained, refering saturation vapour pressure e_s at the temperature to the said table. Then, knowing e, dew point could be found, refering again to the table, for dew point is the temperature where the said vapour pressure e is to be saturation vapour pressure e_s.

Temperature data available in this study was daily max. or min., therefore the average of them was utilized in the said procedure.

As a result, dew points had been obtained at three observatories; Sop Han, Ban Tha Rua and Salween. However dew point at Ban Tha Rua was decided to be used in the analysis, considering length of data period and rainfall pattern of the baisn.

5.5 Adjustment and maximization of the storms

Since the typical storms were in this study selected from the rainfalls taking place in the basin now in consideration, the elevation adjustment and barrier adjustment were judged unnecessary, which are taken into account in general procedure of PMP analysis. Another adjustmenth; moisture adjustment, was considered, but was in fact involved in the maximization, because the selected storms were ones in the basin itself.

This maximization of the storms were achieved on the basis of precipitable water (total amount of moisture contained in a column stood vertically on the ground surface of unit area), which was derived from dew point. This precipitable water was known by the figure prepared by the U.S. National Weather Service.

An example of maximization is shown in Table 5.2. In the table, precipitation of line (1) is the one conducted DAD operation, thus, having been converted to areal precipitation. Dew point of line (3) is the highest one taking place at Ban Tha Rua during the particular storm interval. Line (5) indicated the highest dew point having occurred at Ban Tha Rau in the past. Corresponding the dew points given in the line (3) and (5), precipitable waters were respectively obtained. Then, by the propotion between (3) and (5), the observed precipitation in the line (1) was maximized.

The maximized precipitation was shown in the Fig. 5.5 in terms of the persistent period. As seen in the figure, the Storm No.21(1) (1980, May 21 to 24) gives extraordinary large magnitude, thus this storm was employed as PMP.

5.6 Estimation of daily runoff caused by PMP

While searching for PMP as mentioned above, relationship between a sequence of rainfall and the resultant runoff was studied based on the past recorded data of daily precipitation and discharge.

Here, the term "a sequence of rainfall" means the rainfall lasted for several days with remarkable amount and thus caused considerable discharge in the river. Looking over the past records, remarkable sequences of rainfall and the following discharges were selected. And the total amount of rainfall in the sequence and the maximum daily discharge in the discharges followingly caused were studied. Taking unit rainfall to be 10 mm, the resultant maximum daily discharge is 93 m^3/s as an average, is 128 m^3/s as the highest, which occurred generally with time lag of one day. It is shown in Fig. 5.6 and 5.7. Discharge against the unit rainfall varies greatly with the seasons, i.e. rainy and dry seasons. In other words, it varies with the amount of moisture kept in the ground. Fig.5.7 clearly shows that discharges taken place in July and August indicated by circle are consisting a group in the figure. since the PMP is now considered occur in July and August which are middle of rainy season, the ground is to be fully saturated. Therefore, the resultant maximum daily discharge was decided to be 128 m^3/s of the highest against the unit rainfall.

Assuming basin retention of 5% for the four-day persistent rainfall of PMP, rainfall excess becomes 257 mm. the maximum daily discharge thereby is then 3,290 m^3/s. On the other hand, it is notable that the sequence of rainfall takes place continually in July and August where the present study focusses. Therefore a precedent storm and the following discharge should be involved. As the precedent discharge, the maximum experienced discharge at Ban Tha Rua (1791, Aug. 30, Q = 925 m^3/s) was considered. Setting the precedent discharge three days before, the maximum daily discharge becomes 3,790 m^3/s resulted from PMP.

It should be reminded that all the analyses described above are based upon the daily data, thus the obtained maximum discharge is also a daily average. However, it is obvious that flood discharge in fact changes the amount considerably in hours so that actual peak discharge is much larger than the daily average. Examination of observed record at Ban Tha Rua revealed that the ratio between daily average and hourly peak discharges is 1.17 as an average, and is 1.64 as the maximum. Taking the maximum of 1.64, the PMF is concluded to be 6,216 $m^3/s \fallingdotseq$ 6,200 m^3/s as an hourly peak discharge.

Hydrograph of the PMF was formed in the similitude of the envelop of floods recorded in the past. The obtained PMF is given in Fig. 5.8.

References

(1) "Manual for Estimation of Probable Maximum Precipitation", WMO-No.332, Operational Hydrology Report No.1, 1973, WMO, Geneva, Switzerland.

(2) "Hydrological Survey of Iraq, Probable Maximum Flood at Bekhme damsite", EPDC Ltd. Design Sec., Dec. 1979, Tokyo.

(3) "Huai Saphan Hin Project Feasibility Report", Appendix C, Hydrology Part II, Probable Maximum Precipitation, National Energy Administration, Aug. 1977, Thailand.

Table 5.1 Relationship between Temperature and Saturated Vapour Pressure

(Unit: mb)

Temperature (°C)	x 0.1 °C									
	0	1	2	3	4	5	6	7	8	9
50	123.40	124.01	124.63	125.25	125.87	126.49	127.12	127.75	128.38	129.01
49	117.40	117.99	118.58	119.17	119.77	120.37	120.97	121.57	122.18	122.79
48	111.66	112.22	112.79	113.36	113.93	114.50	115.07	115.65	116.23	116.82
47	106.16	106.70	107.24	107.78	108.33	108.88	109.43	109.98	110.54	111.10
46	100.89	101.41	101.93	102.45	102.97	103.50	104.03	104.56	105.09	105.62
45	95.86	96.35	96.85	97.34	97.84	98.34	98.85	99.36	99.87	100.38
44	91.03	91.51	91.98	92.46	92.94	93.42	93.90	94.39	94.87	95.36
43	86.42	86.88	87.33	87.79	88.24	88.70	89.17	89.63	90.10	90.56
42	82.02	82.45	82.88	83.32	83.75	84.19	84.64	85.08	85.53	85.97
41	77.80	78.22	78.63	79.05	79.46	79.88	80.31	80.73	81.63	81.59
40	73.78	74.17	74.57	74.97	75.37	75.77	76.17	76.58	76.98	77.39
39	69.93	70.31	70.69	71.07	71.45	71.83	72.22	72.61	73.00	73.39
38	66.26	66.62	66.98	67.35	67.71	68.08	68.45	68.82	69.19	69.56
37	62.76	63.11	63.45	63.80	64.14	64.49	64.84	65.20	65.55	65.91
36	59.42	59.75	60.08	60.41	60.74	61.07	61.41	61.74	62.08	62.42
35	56.24	56.55	56.86	57.18	57.49	57.81	58.13	58.45	58.77	59.10
34	53.20	53.50	53.80	54.10	54.40	54.70	55.00	55.31	55.62	55.93
33	50.31	50.59	50.87	51.16	51.45	51.74	52.03	52.32	52.61	52.90
32	47.55	47.82	48.09	48.36	48.64	48.91	49.19	49.47	49.75	50.03
31	44.93	45.18	45.44	45.70	45.96	46.22	46.49	46.75	47.02	47.28
30	42.43	42.67	42.92	43.17	43.41	43.66	43.91	44.17	44.42	44.67
29	20.05	40.29	40.52	40.76	40.99	41.23	41.47	41.71	41.95	42.19
28	37.80	38.02	38.24	38.46	38.69	38.91	39.14	39.36	39.59	39.82
27	35.65	35.86	36.07	36.28	36.49	36.71	36.92	37.14	37.36	37.58
26	33.61	33.81	34.01	34.21	34.41	34.62	34.82	35.03	35.23	35.44
25	31.67	31.86	32.05	32.24	32.43	32.63	32.82	33.02	33.21	33.41
24	29.83	30.01	30.19	30.37	30.56	30.74	30.92	31.11	31.30	31.48
23	28.09	28.26	28.43	28.60	28.77	28.95	29.12	29.30	29.48	29.65
22	26.43	26.59	26.75	26.92	27.08	27.25	27.41	27.58	27.75	27.92
21	24.86	25.01	25.17	25.32	25.48	25.64	25.79	25.95	26.11	26.27
20	23.37	23.52	23.66	23.81	23.96	24.11	24.26	24.41	24.56	24.71
19	21.96	22.10	22.24	22.38	22.52	22.66	22.80	22.94	23.08	23.23
18	20.63	20.76	20.89	21.02	21.15	21.29	21.42	21.56	21.69	21.83
17	19.37	19.49	19.61	19.74	19.86	19.99	20.12	20.24	20.37	20.50
16	18.17	18.29	18.41	18.52	18.64	18.76	18.88	19.00	19.12	19.24
15	17.04	17.15	17.46	17.38	17.49	17.60	17.71	17.83	17.94	18.06
14	15.98	16.08	16.19	16.29	16.40	16.50	16.61	16.72	16.83	16.93
13	14.97	15.07	15.17	15.27	15.37	15.47	15.57	15.67	15.77	15.87
12	14.02	14.11	14.20	14.30	14.39	14.49	14.58	14.68	14.77	14.87
11	13.12	13.21	13.29	13.38	13.47	13.56	13.65	13.74	13.83	13.93
10	12.27	12.35	12.44	12.52	12.60	12.69	12.77	12.86	12.95	13.03

Table 5. 2 Maximization of Storms

MAXIMIZATION OF RAINFALL

Storm No.17

Period: 1978, 8/12 - 8/16

		UNIT	STORM PERIOD						REMARKS
			1 day	2 day	3 day	4 day	5 day	6 day	
(1)	Precipitation for C.A. 5,920 km^2	mm	33.2	42.7	52.2	59.0	63.7		
(2)	Date	-	8/14	13 - 14	13 - 15	12 - 15	12 - 16		
(3)	Max. Dew Point at Ban Tha Rua	°C	26.1	26.1	26.1	26.1	26.1		
(4)	Precipitable Water corresp. to the dew point (3) above	mm	90.2	90.2	90.2	90.2	90.2		
(5)	Max. recorded dew point in the whole data (Ban Tha Rua)	°C	33.6	33.6	33.6	33.6	33.6	33.6	
(6)	Precipitable Water corresp. to the dew point in (5) above	mm	164.8	164.8	164.8	164.8	164.8	164.8	
(7)	Max. Factor		1.827	1.827	1.827	1.827	1.827		
(8)	Max. Precipitation	mm	60.7	78.0	95.4	107.8	116.4		

Fig. 5. 1 Observatory and Gaging Stations with the Covering Area

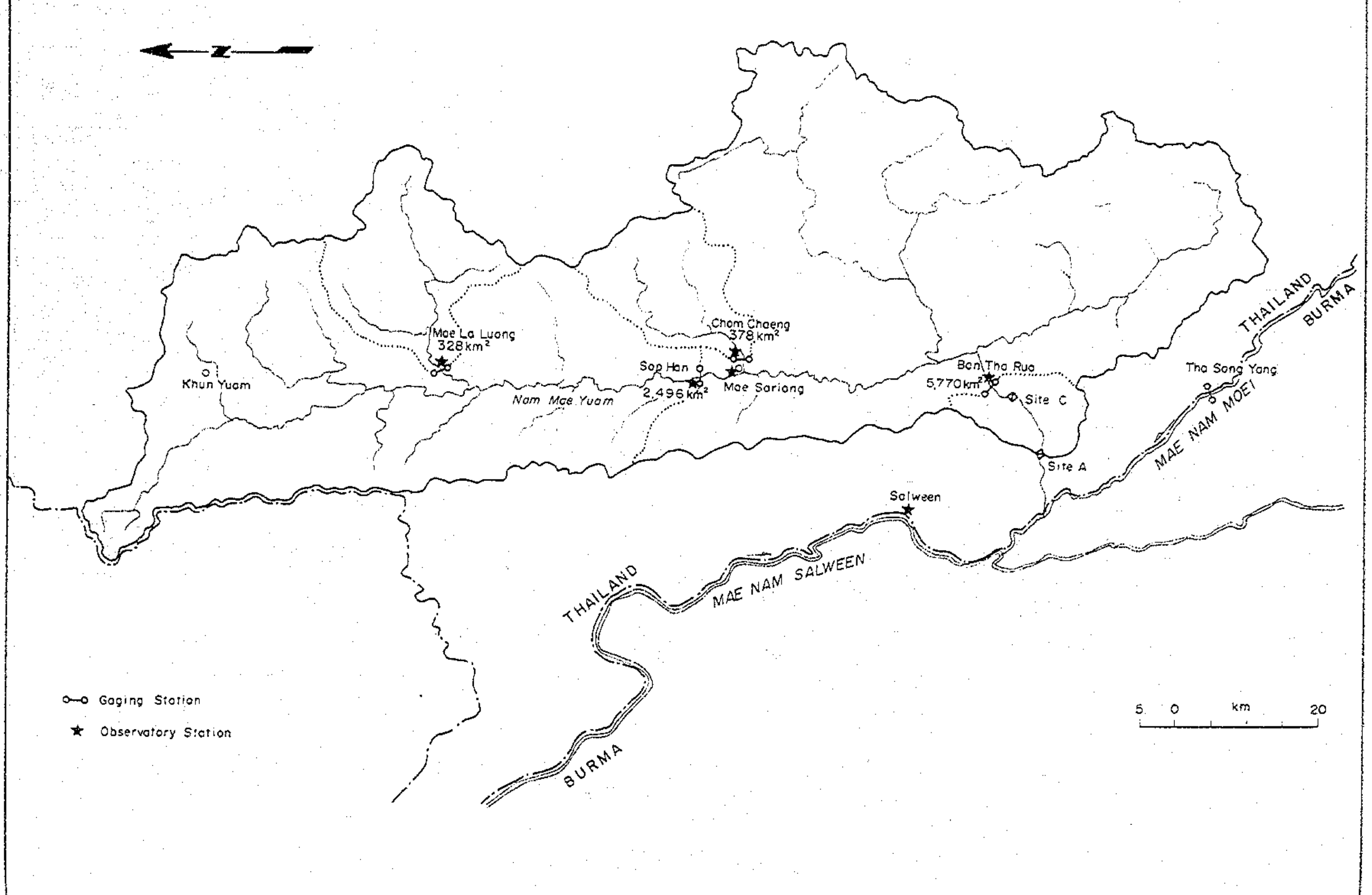

Fig. 5.2 Hypothetical Isohyetal Map with Corresponding O. S.

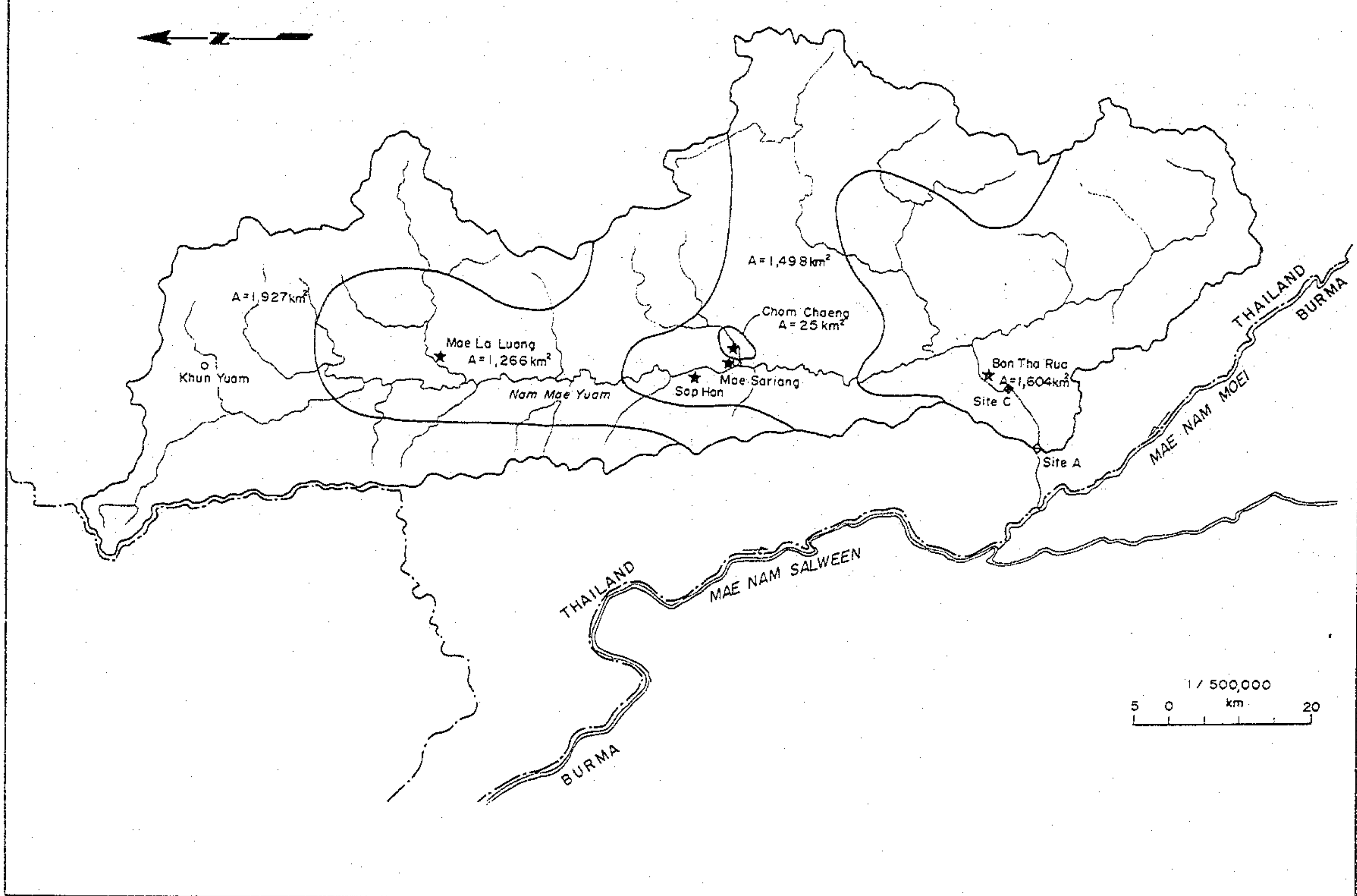

Fig. 5. 3 Hypothetical Isohyetal Map with Corresponding O. S.

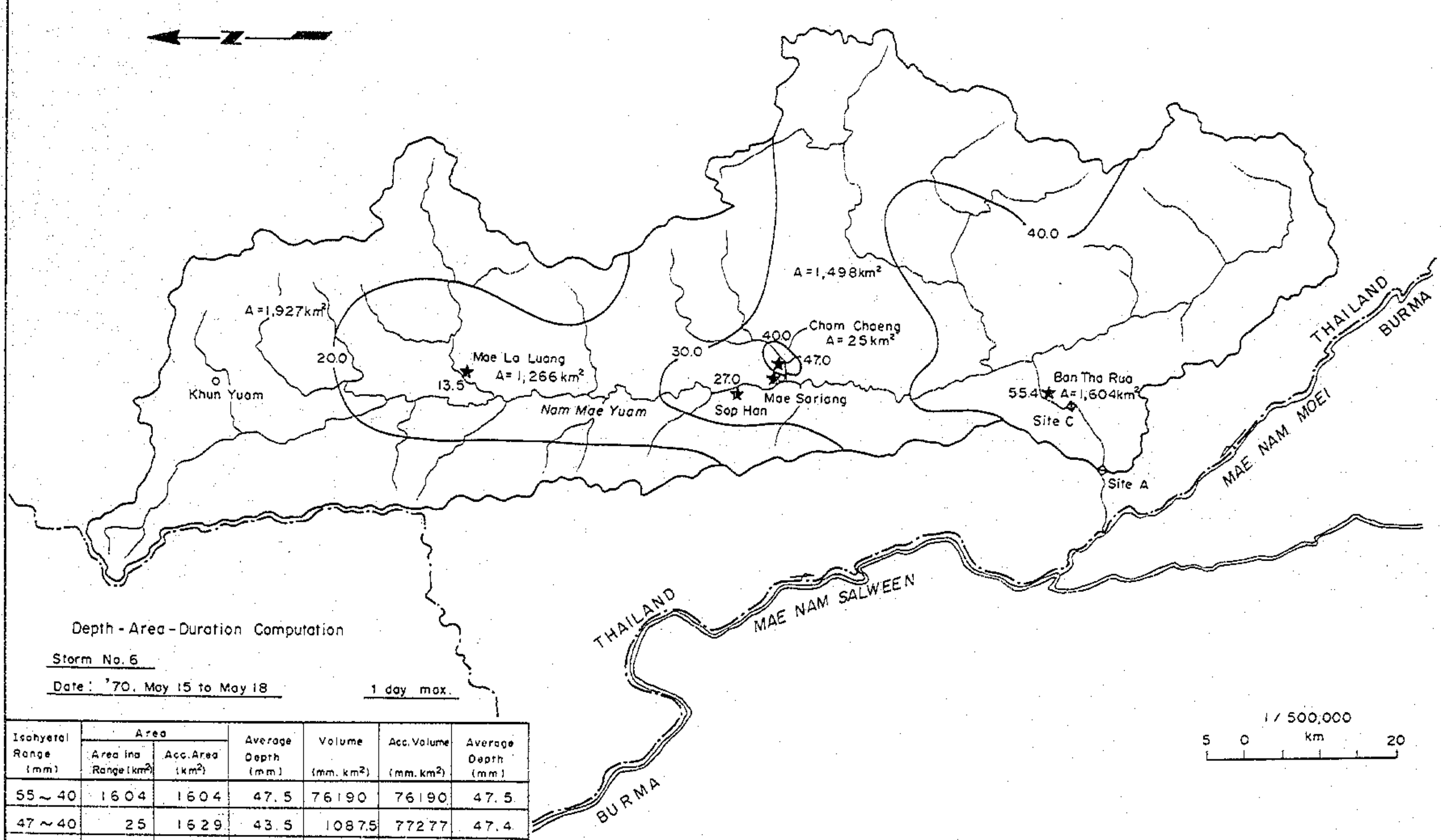

Depth - Area - Duration Computation

Storm No. 6

Date : '70. May 15 to May 18   1 day max.

Isohyetal Range (mm)	Area: Area ina Range (km²)	Area: Acc. Area (km²)	Average Depth (mm)	Volume (mm. km²)	Acc. Volume (mm. km²)	Average Depth (mm)
55 ~ 40	1604	1604	47.5	76190	76190	47.5
47 ~ 40	25	1629	43.5	1087.5	77277	47.4
40 ~ 30	1498	3127	35.0	52430	129707	41.5
30 ~ 20	1266	4393	25.0	31650	161357	36.7
20 ~ 0	1527	5920	10.0	15270	176627	29.8

Fig. 5.4 DAD Curves

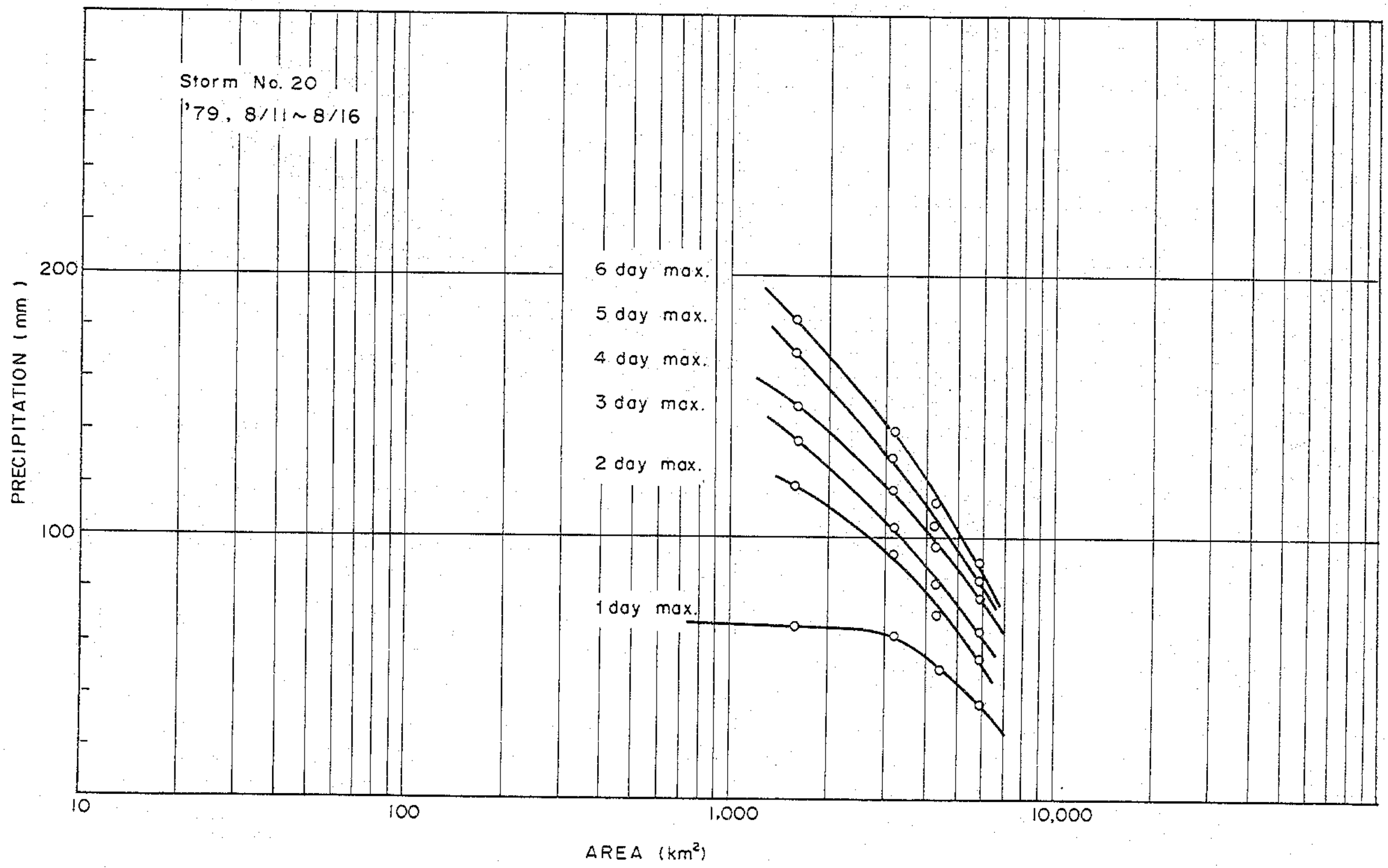

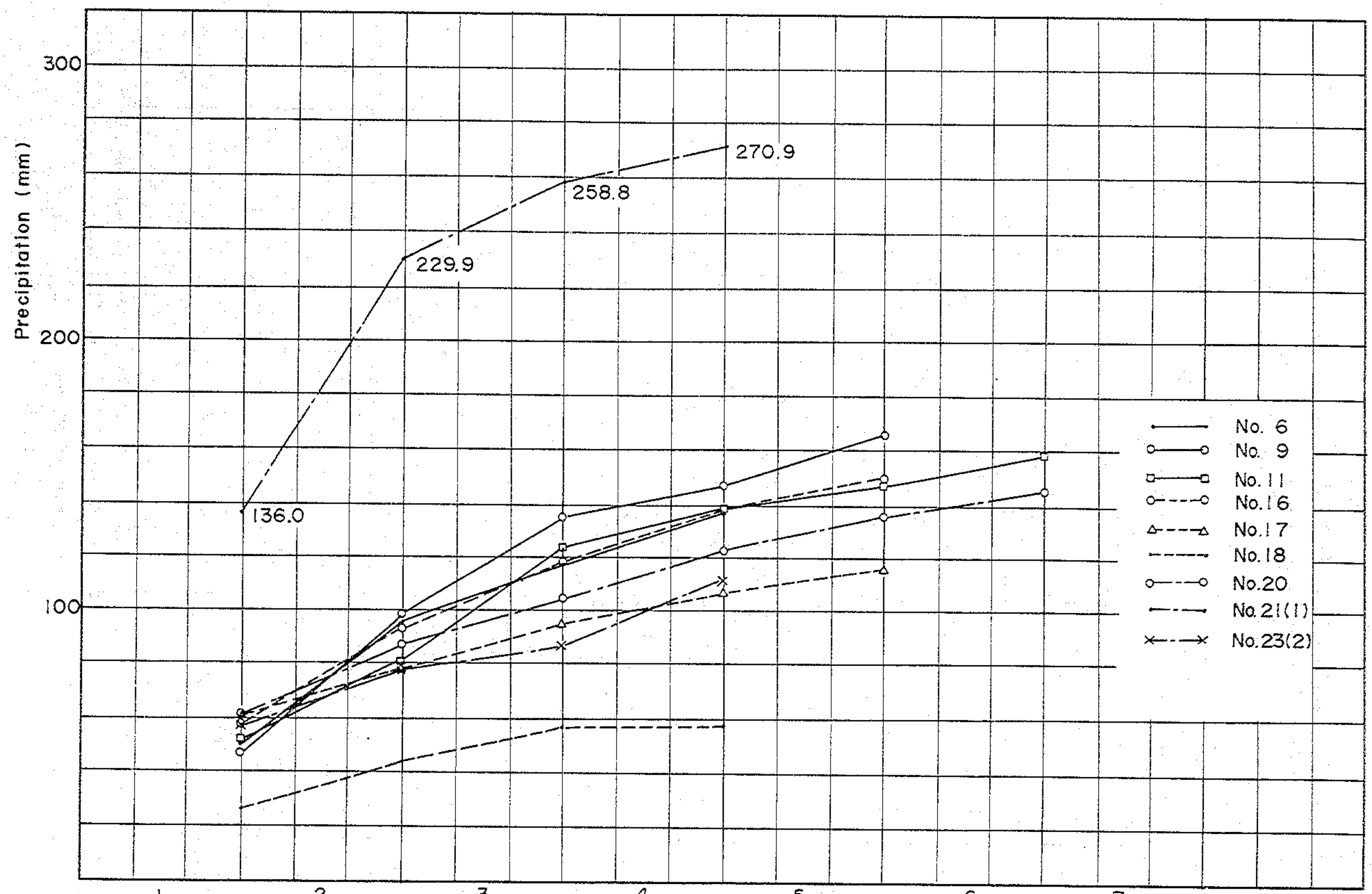

Fig. 5.5 Maximised Precipitation of Storms

Fig. 5. 6 Precipitation and Discharge
1970

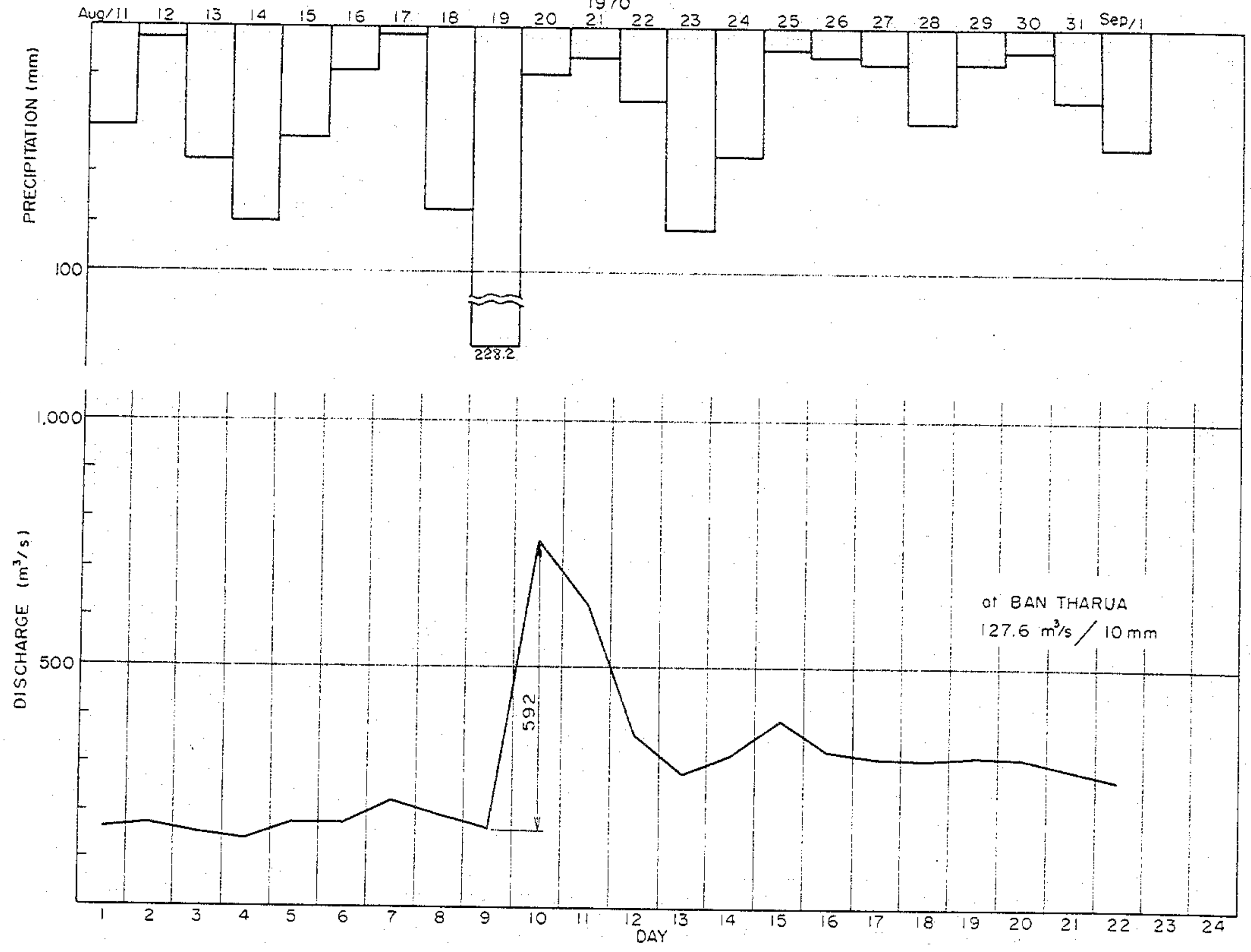

Fig. 5.7 Relationship Between Increment of Discharge and Day Rainfall

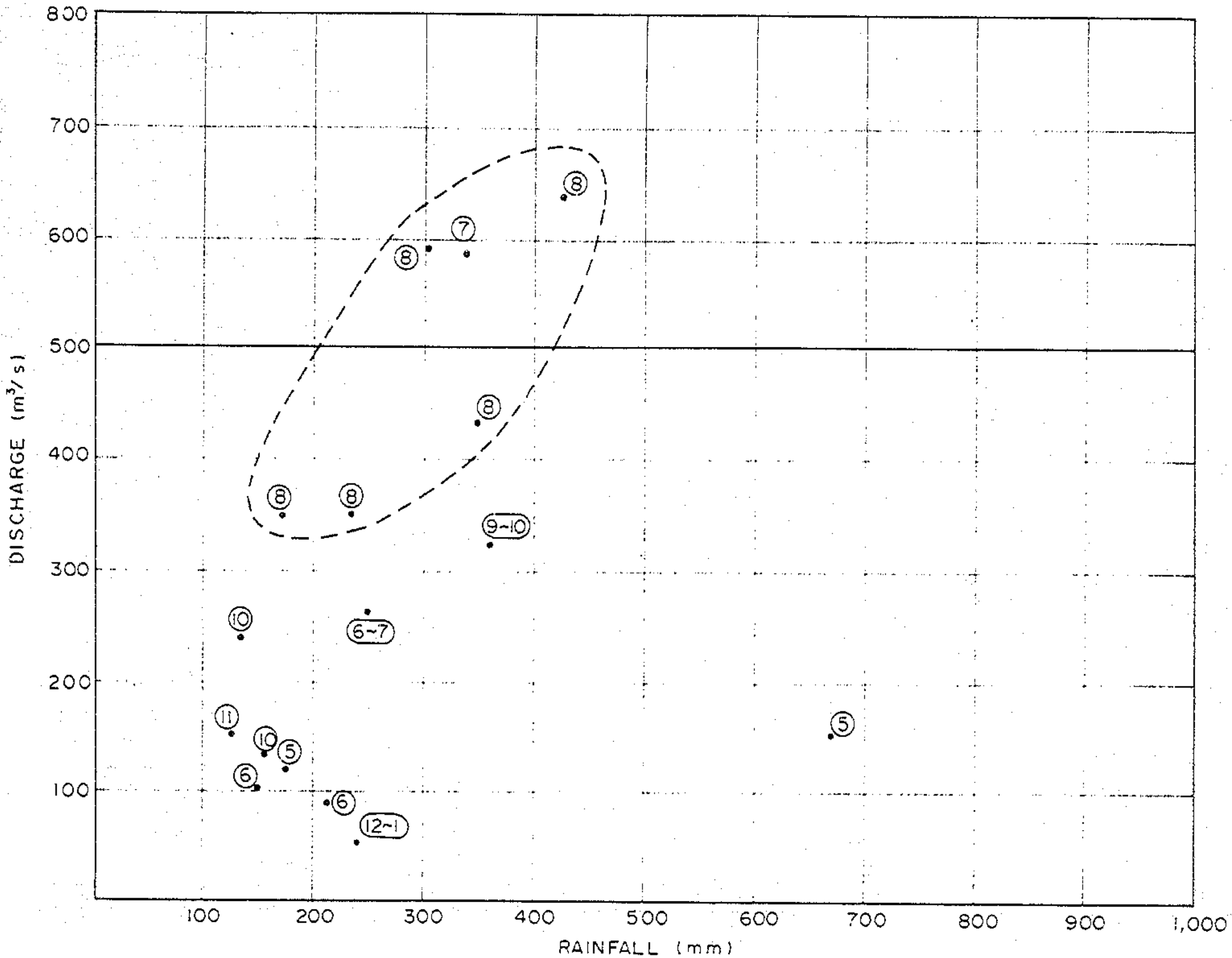

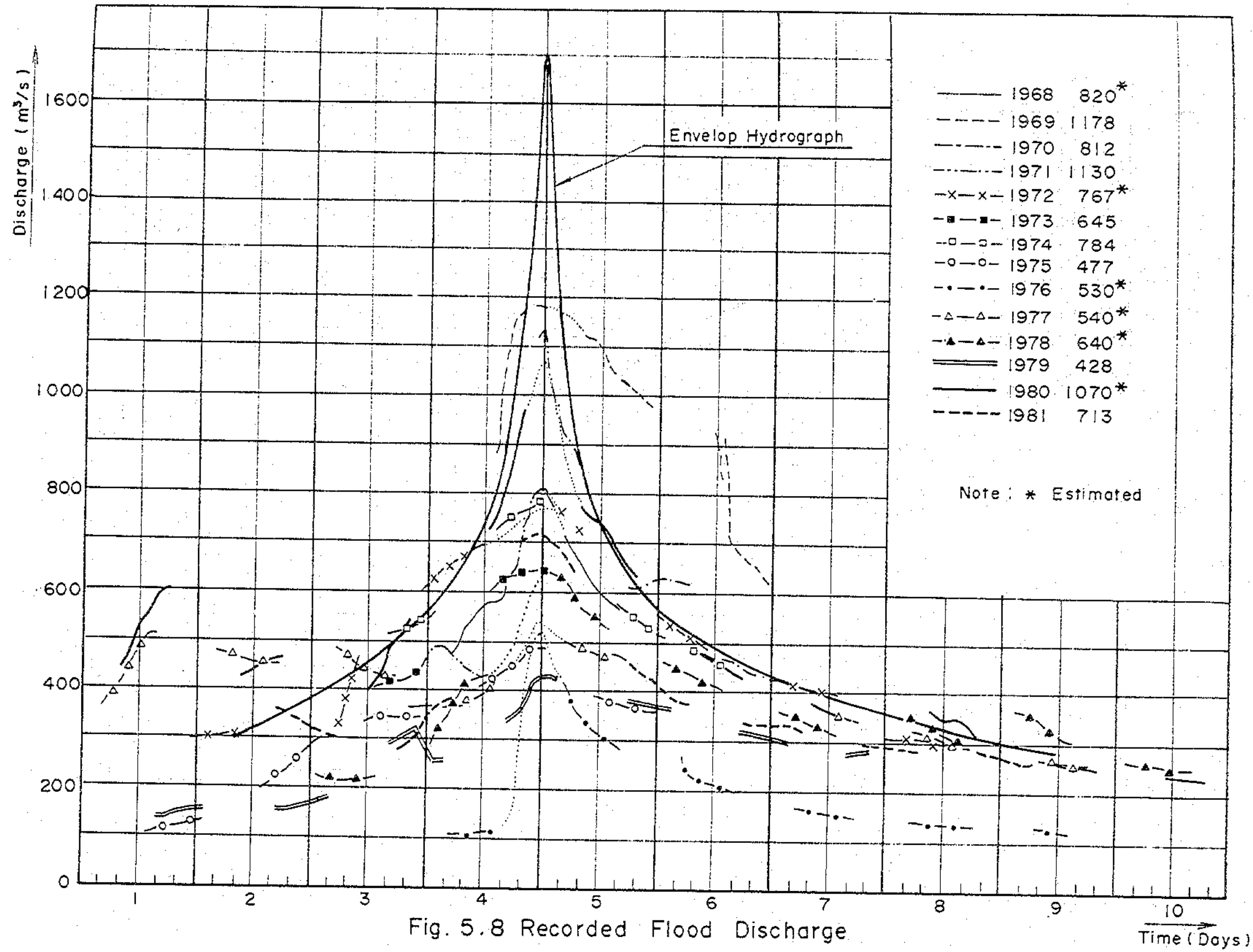

Fig. 5.8 Recorded Flood Discharge

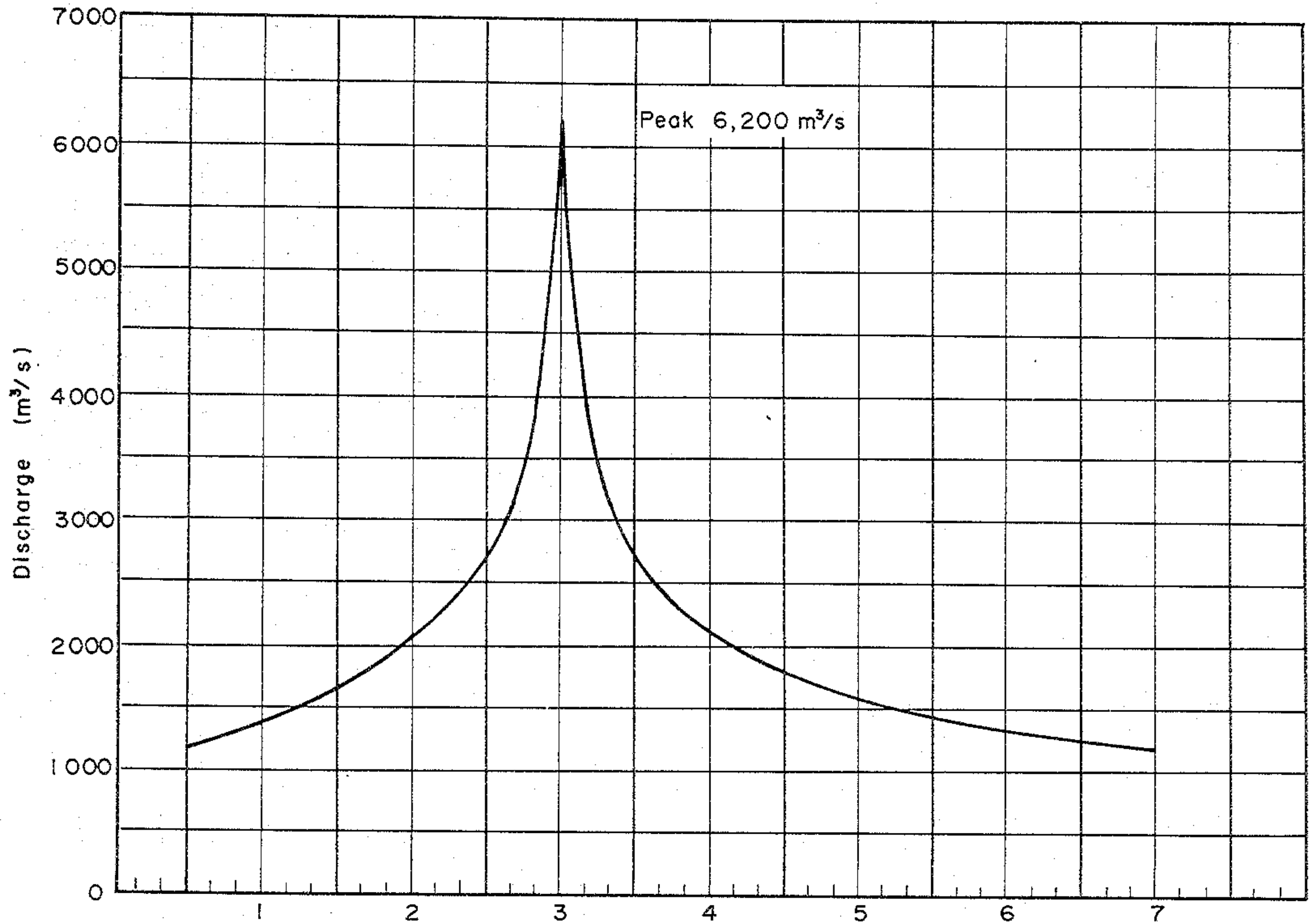

Fig. 5.9 PMF Discharge

A 3 DESIGN

1. Flood Routing

1.1 General

According to the proposed scheme, Nam Yuam dam site has topographical feature of the considerably large reservoir area and hydrological feature of sharpness of the design flood curve. Concerning such a dam site, it is advantageous that the scale of spillway should be reduced to an adequate extent with some of flood volume stored in the reservoir. The flood routing has been done under the below-mentioned conditions.

1.2 Conditions

Design flood inflow

Probable maximum flood (Qmax = 6,200 m^3/sec)

See Fig. 1

Reservoir storage capacity

See Fig. 2

Dimensions of spillway

See Fig. 3, 4

Initial reservoir water level

EL 170.00 (High water level)

Operation rule

i) As far as flood inflow does not exceed discharge capacity of spillway at high water level of EL. 170.00, spillway gates are partially opened with reservoir water level kept the high water level.

ii) If flood inflow exceeds discharge capacity of spillway at high water level, spillway gates are fully opened.

1.3 Calculations

Discharge capacity of spillway is given on the following formula.

$$Q = N \cdot C \cdot (B-2Kh) \cdot h^{3/2}$$

where;

Q: discharge (m^3/sec)

C: coefficient of discharge

K: coefficient of contraction due to pier

N: number of gates = 4

B: width of crest = 12.00 m

h: head on crest (m)

Value of C is determined on Iwasaki's formula in case of idealy shaped crest.

$$C = 1.60 \frac{1 + 2a(h/hd)}{1 + a\ (h/hd)}$$

$$Cd = 2.20 - 0.0416\ (hd/w)^{0.99}$$

where;

hd: design head = 12.00 m

W: height of weir = 8.00 m

Cd: coefficient of overflow at design head

therefore

Cd: 2.138

a = 0.5063

$$C = 1.60 \frac{1 + 1.0126\ (h/12.00)}{1 + 0.5063\ (h/12.00)}$$

Value of K is given on Fig. 5.

Consequently results of calculation of spillway capacity are shown on Table 1 and Fig. 6.

1.4 Results

The results of calculations are shown on Fig. 7. It has been evident that surcharge of 0.88 m at the reservoir enables to reduce needed spillway capacity to 77% of maximum flood discharge.

Table 1.1 Spillway Capacity

Reservoir Water Level(m)	h (m)	h/hd	C	K	2Kh (m)	B-2Kh (m)	Q (m^3/sec)
158.00	0.00	0.000	-	-	-	-	0
159.00	1.00	0.083	1.665	0.126	0.26	1.74	78
160.00	2.00	0.167	1.725	0.105	0.42	1.58	226
161.00	3.00	0.250	1.780	0.087	0.52	1.48	425
162.00	4.00	0.333	1.831	0.071	0.57	1.43	670
163.00	5.00	0.417	1.879	0.056	0.56	1.44	961
164.00	6.00	0.500	1.923	0.046	0.56	1.44	1,294
165.00	7.00	0.583	1.965	0.036	0.51	1.49	1,673
166.00	8.00	0.667	2.004	0.029	0.47	1.53	2,091
167.00	9.00	0.750	2.040	0.023	0.42	1.58	2,552
168.00	10.00	0.833	2.075	0.017	0.35	1.65	3,059
169.00	11.00	0.917	2.107	0.011	0.24	1.76	3,618
170.00	12.00	1.000	2.138	0.004	0.11	1.89	4,229
171.00	13.00	1.083	2.167	0.000	0.00	2.00	4,875
172.00	14.00	1.167	2.194	0.000	0.00	2.00	5,517

Fig. 1.1 Design Flood Inflow

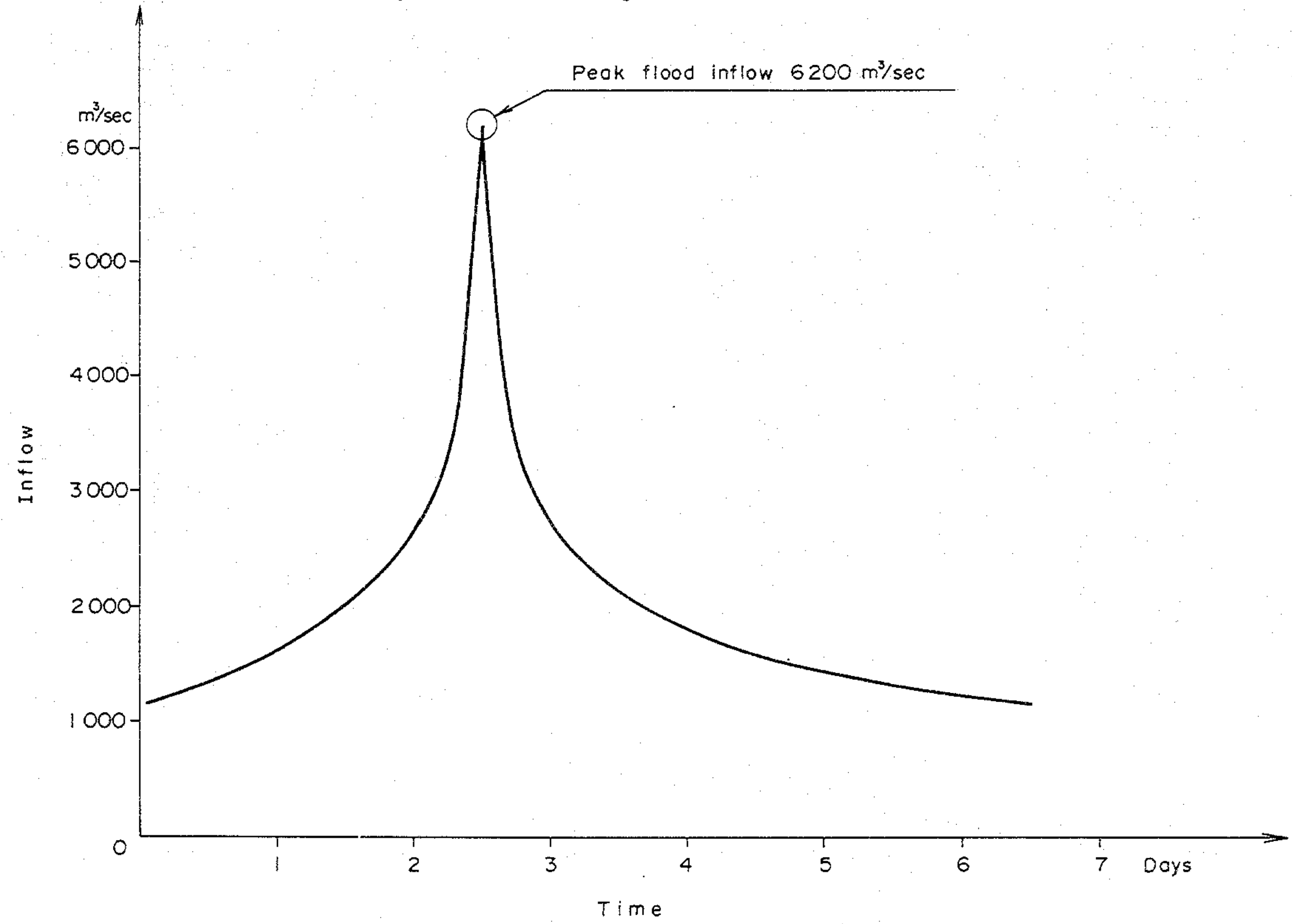

Fig. 1.2 Reservoir Storage Capacity

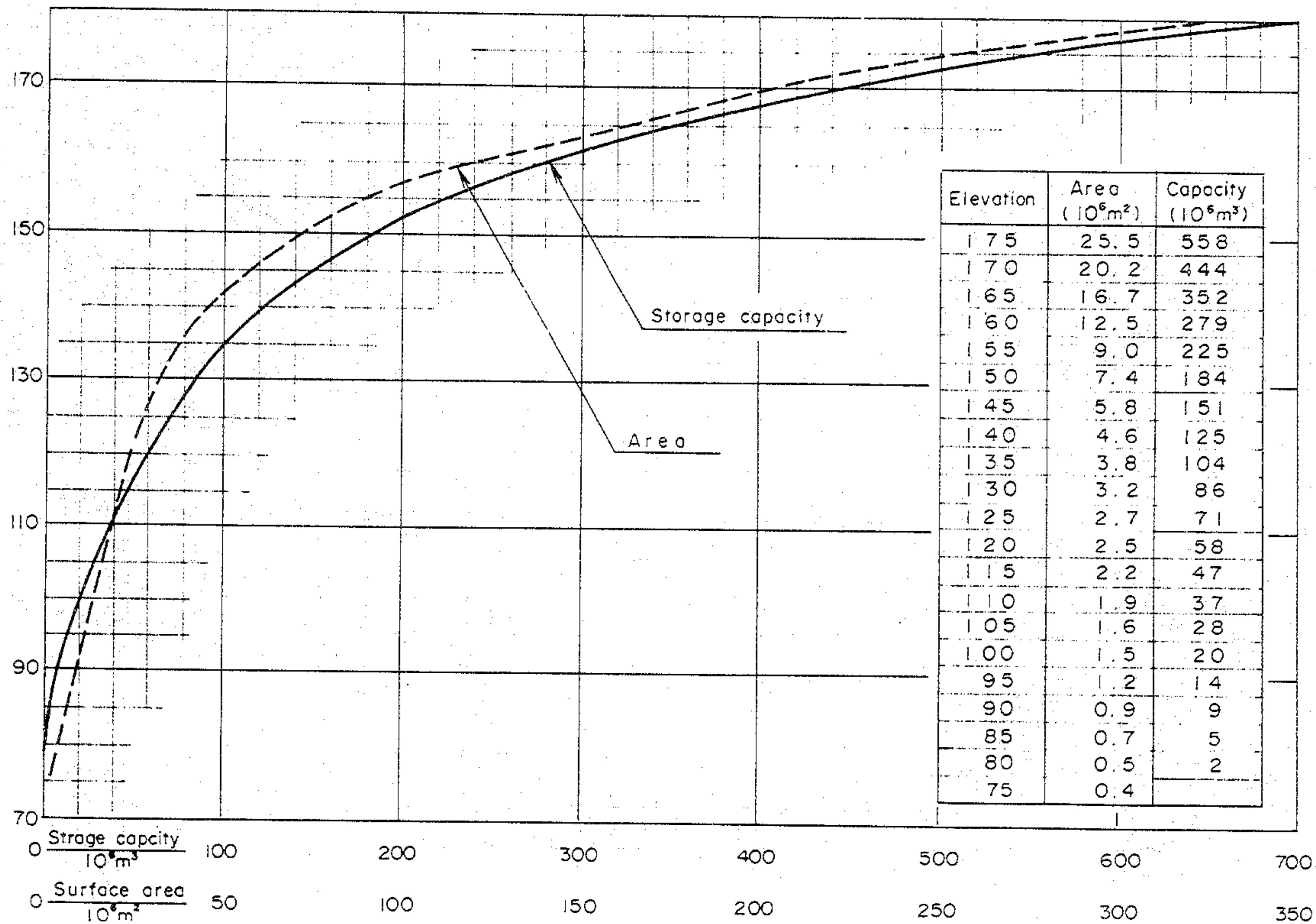

Elevation	Area ($10^6 m^2$)	Capacity ($10^6 m^3$)
175	25.5	558
170	20.2	444
165	16.7	352
160	12.5	279
155	9.0	225
150	7.4	184
145	5.8	151
140	4.6	125
135	3.8	104
130	3.2	86
125	2.7	71
120	2.5	58
115	2.2	47
110	1.9	37
105	1.6	28
100	1.5	20
95	1.2	14
90	0.9	9
85	0.7	5
80	0.5	2
75	0.4	

Fig. 1.3 Upstream View of Spillway

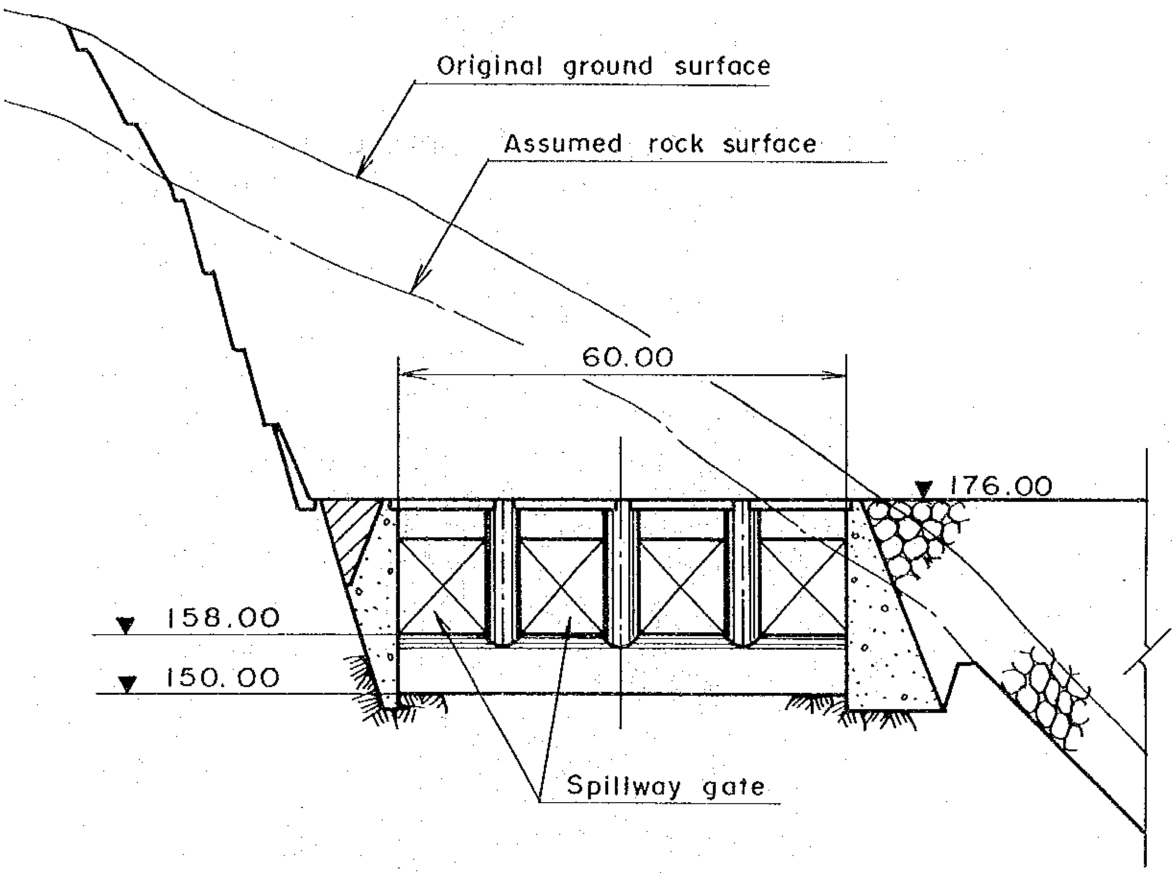

Fig. 1.4 Typical Section of Spillway

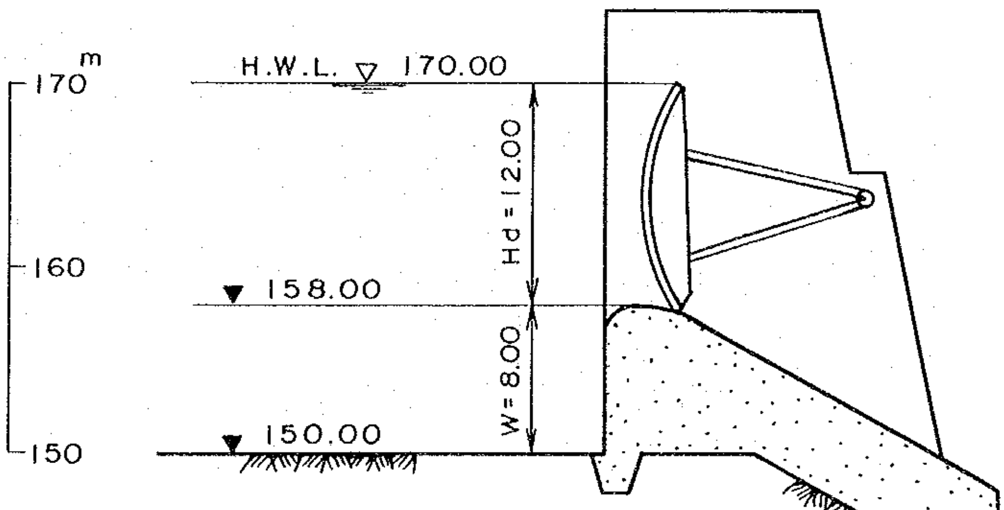

Fig. 1.5 Coefficient of Contraction due to Pier

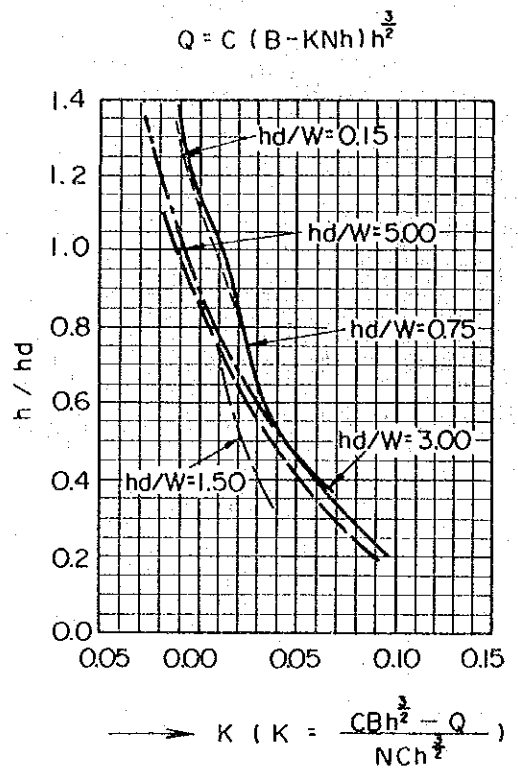

Fig. 1.6 Discharge Capacity of Spillway

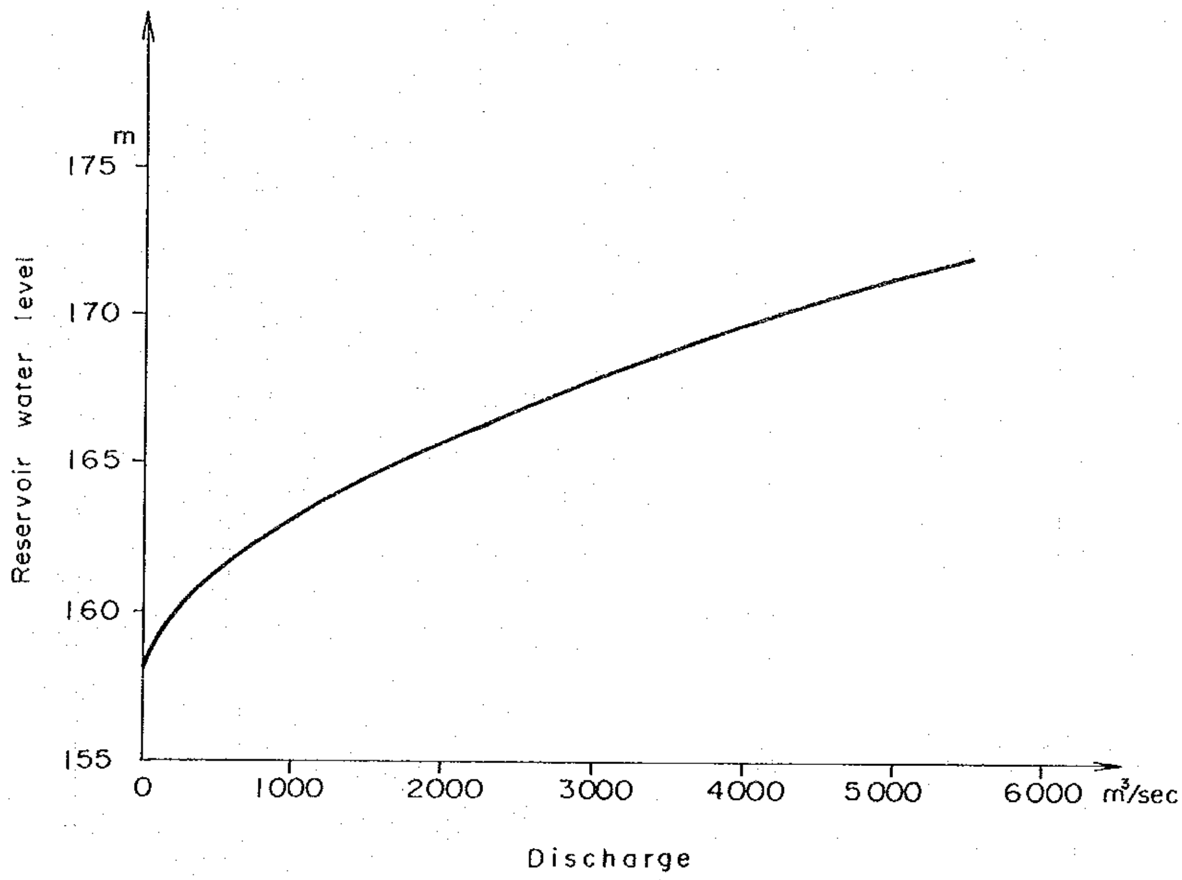

Fig. 1.7 Results of Calculation

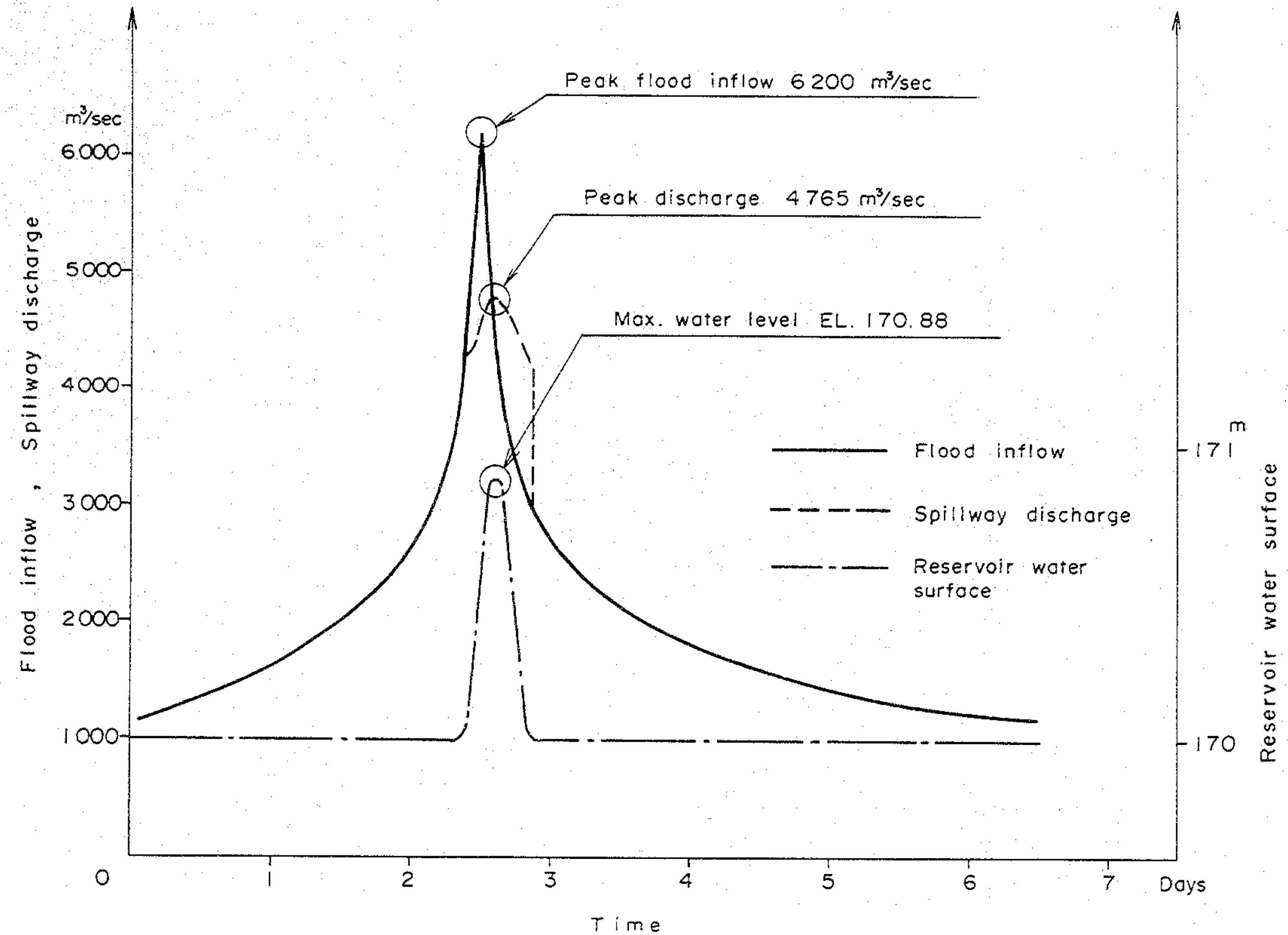

2. Nam Yuam Dam Stability Analysis

2.1 General

Stability analysis was done by the slip circle method for Nam Yuam dam and this analysis was calculated by the computer.

2.2 Stability analysis by slip circle method

The factor of safety against sliding is expressed as follows.

Normal condition:

$$SF(N) = \frac{\Sigma (N + Hn - U)\ \mathrm{ton}\,\phi + \Sigma C \cdot L}{\Sigma (T - Ht)}$$

Earthquake condition:

$$SF(E) = \frac{\Sigma (N + Hn - U)\ \tan\phi - \Sigma Ne\ \mathrm{ton}\,\phi + \Sigma C \cdot L}{\Sigma (T - Ht) + \Sigma Te}$$

where,

- N : normal force
- T : tangential force
- $\tan\phi$: coefficient of internal friction
- Hn : normal component of hydrostatic pressure
- Ht : tangential component of hydrostatic pressure
- U : pore water pressure
- L : length of sliding circle
- Ne : normal component of seismic force
- Te : tangential component of seismic force
- C : cohesion force

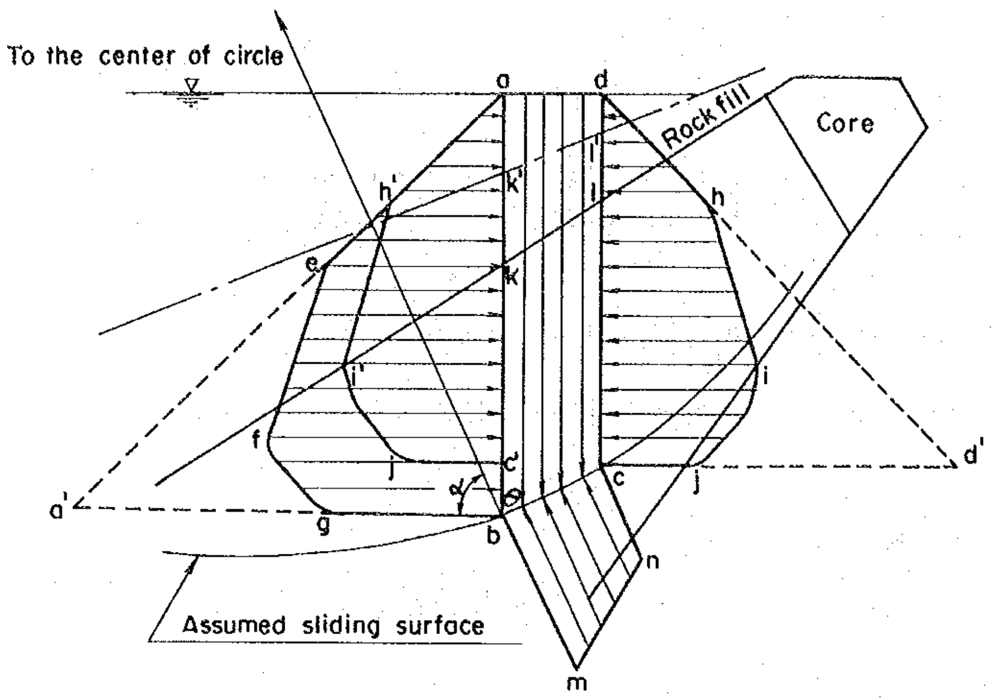

$\Sigma N \cdot \tan\phi = \Sigma\{\gamma(k'bcl') + \gamma w(abcd)\}\cos\theta \tan\phi$

$\Sigma Hn \cdot \tan\phi = \Sigma(efgbc'j'i'j')\cos\alpha \tan\phi$

$\Sigma U \tan\phi = \Sigma(bmnc)\tan\phi$

$\Sigma T = \Sigma\{\gamma(k'bcl') + \gamma n(abcd)\}\sin\theta$

$\Sigma Ht = \Sigma(efgbc'j'i'h')\sin\alpha$

$\Sigma Ne \tan\phi = \Sigma\beta(k'bcl')K \sin\theta \tan\phi$

$\Sigma Te = \Sigma\beta(k'bcl')K \cos\theta$

γ : unit weight in normal condition

β : unit weight in earthquake condition

abcd : a piece of slice

bmnc : porefluid pressure to the sliding surface

efgbc'j'i'h' : total of horizontal hydrostatic pressure to the slice

K : seismic coefficient

2.3 Conditions of Calculation

Design values of embankment materials

Zone	Material	Specific gravity	Unit weight t/m^3			Coefficient	
			Dry	Wet	Saturated	tan ϕ	C
1	Impervious core	2.65	1.80	2.07	2.12	0.45	0
2a	Transition fill	2.63	1.95	2.00	2.20	0.65	0
2b	Filter fill	2.63	1.95	2.00	2.20	0.65	0
3	Smaller size rock fill	2.63	1.80	1.82	2.13	0.70	0
4	Larger size rock fill	2.63	1.75	1.77	2.09	0.80	0

Reservoir water surface level;
EL. 170.00 (Normal high water level)

Seismic coefficient;
K = 0.06

Porefluid pressure;

Porefluid pressure of cofferdam was not taken into account and porefluid pressure in impervious core is assumed as shown in Fig. 1. Materials forms are shown in Fig. 2.

2.4 Result

The safety factor of sliding circles are shown in Fig. 3. From the result of this analysis, the dambody is safe enough under normal and earthquake conditions for assumed design values. But after the determination of the actual design values for the respective tests' results, the safety of dam must be checked in detail.

Fig. 2.1 POREFLUID PRESSURE

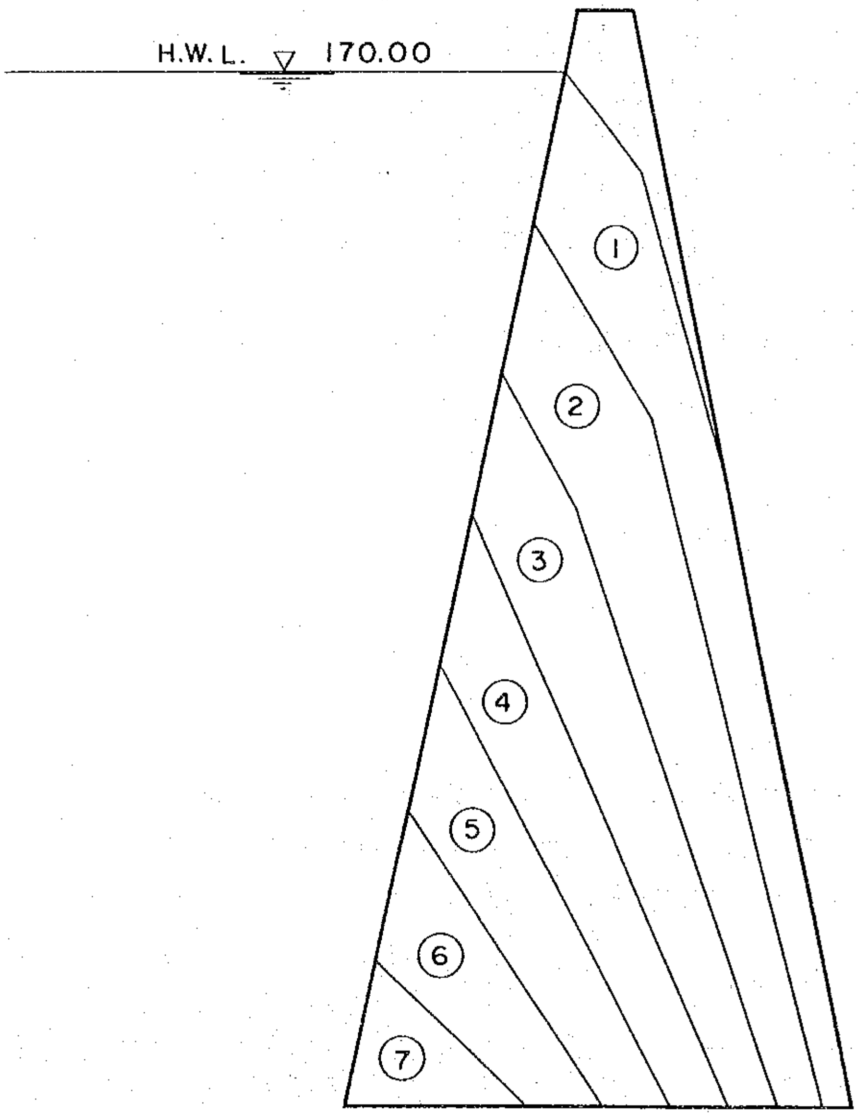

Zone	Porefluid Pressure (t/m^2)
①	7.5
②	22.5
③	37.5
④	52.5
⑤	67.5
⑥	82.5
⑦	97.5

Fig. 2.2 TYPICAL SECTION

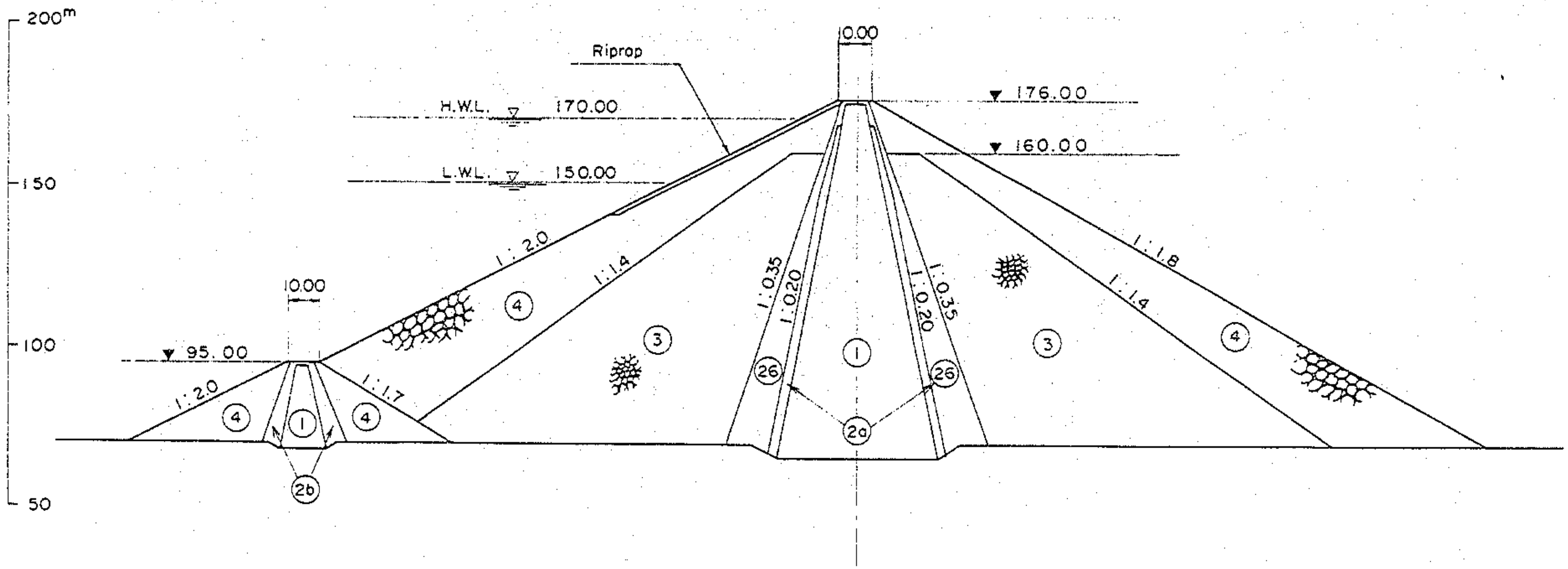

① Impervious core

②a Transition fill

②b Filter fill

③ Smaller size rock fill

④ Larger size rock fill

Fig. 2.3 RESULT OF STABILITY ANALYSIS

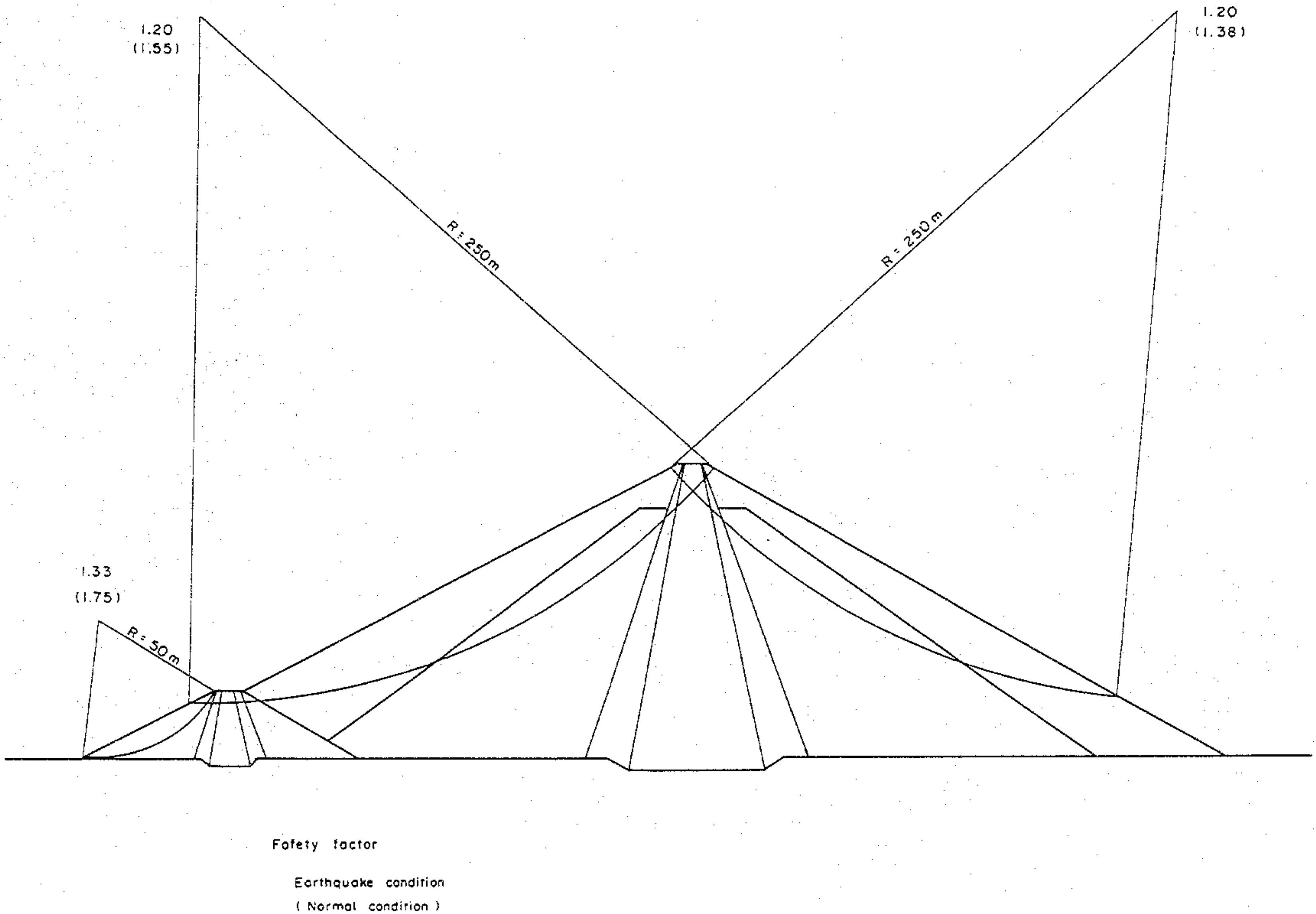

3. Tailwater level

Control section was assumed at Section I, where uniform flow would be formed. Tailwater level was obtained by backwater calculations.

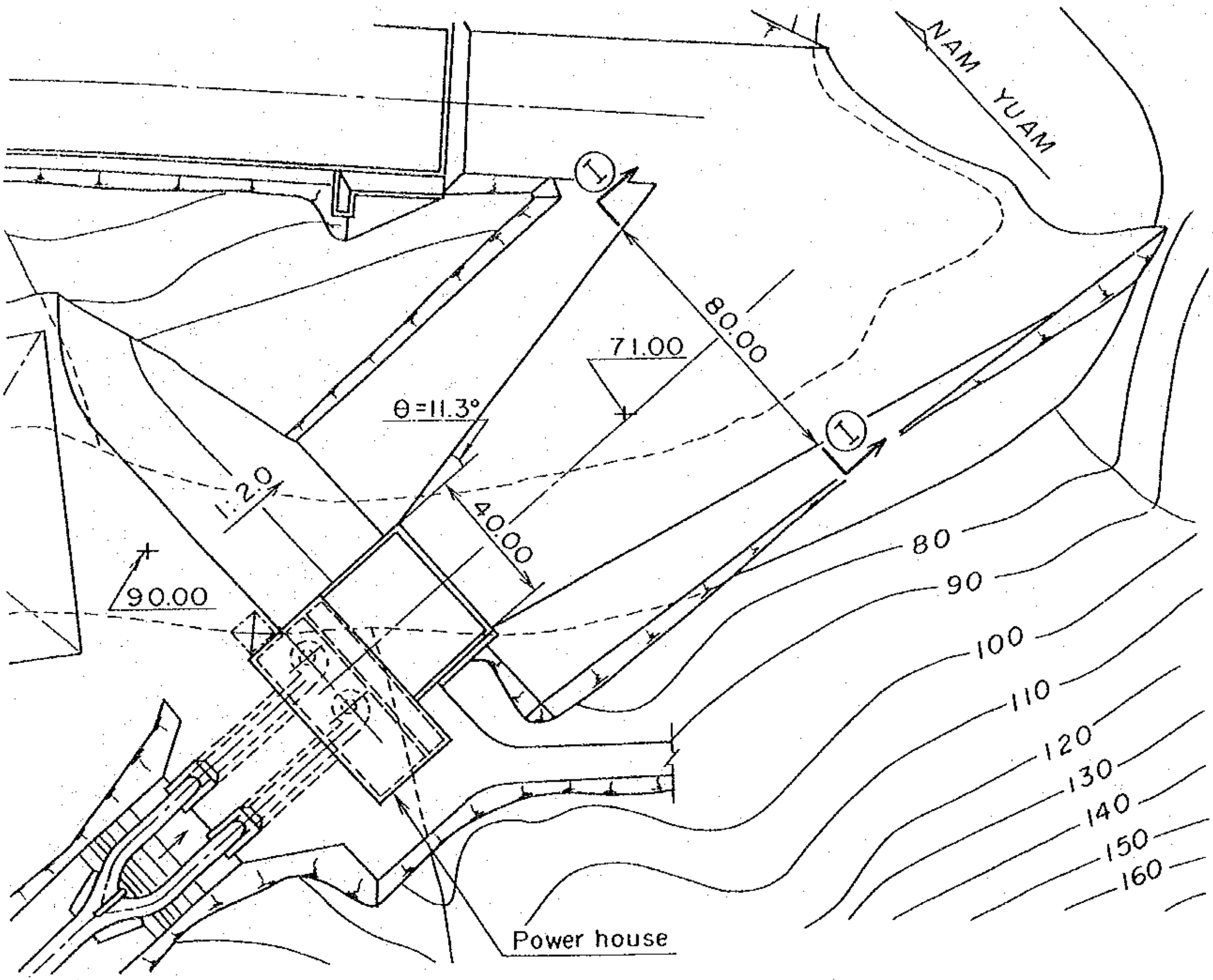

Section I

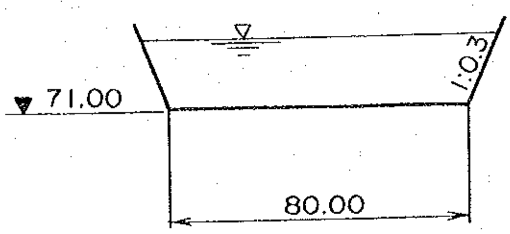

A 4 CONSTRUCTION MATERIAL

Table 4-1 Result of Soil Tests

Sample No.	Depth (m)	Classification of Soils by Unified System	Specific Gravity	Natural Water Content (%)	Atterberg Limits L.L (%)	PL (%)	PI	Gradation Analyses Maximum Grain Size (mm)	-38.1 mm (%)	-19.1 mm (%)	-4.75 mm (%)	-0.425 mm (%)	-0.075 mm (%)	-0.005 mm (%)	Compaction & Permeability Optimum Water Content (%)	Maximum Dry Density (t/m³)	Coefficient of Permeability (cm/sec)	Triaxial Compression Strength ($\overline{CIU}$) Total Stress c (kgf/cm²)	ø (deg.)	Effective Stress $\overline{c}$ (kgf/cm²)	$\overline{ø}$ (deg.)
A-1	1	SC	2.688	8.8	28.6	18.5	10.1	25	100	97	86	48	45	30	13.0	1.850	7.9×10^{-5}	0	27.8	0.48	33.8
A-2	1	SC	2.832	14.0	39.0	23.3	15.7	19	100	100	75	50	44	19	18.2	1.695	3.2×10^{-6}	—	—	—	—
	2	ML	2.788	16.9	39.2	27.0	12.2	25	100	99	93	66	56	22	—	—	—	—	—	—	—
	3	SC	2.841	18.6	38.2	22.9	15.3	25	100	97	91	61	47	18	15.7	1.710	4.4×10^{-6}	1.10	18.4	0.56	26.4
	4	CL	2.826	22.1	43.0	23.7	19.3	19	100	100	84	64	58	23	22.4	1.580	6.7×10^{-6}	—	—	—	—
	5	CL	2.839	24.0	40.9	22.8	18.1	25	100	96	94	74	64	27	22.5	1.585	6.3×10^{-6}	1.00	18.8	0.66	25.5
A-3	1	GC	2.733	10.8	41.2	23.0	18.2	38	100	91	65	39	35	21	—	—	—	—	—	—	—
	2	GC	2.734	10.3	40.8	23.6	17.2	38	100	92	59	35	30	18	12.8	1.930	1.7×10^{-5}	1.00	19.7	0.36	33.8
A-4	1	GC	2.660	8.6	26.2	17.2	9.0	25	100	96	54	25	20	13	—	—	—	—	—	—	—
A-5	1	SC	2.687	9.0	35.2	23.5	11.7	25	100	97	74	48	45	24	—	—	—	—	—	—	—
	2	GC	2.720	8.3	32.8	21.9	10.9	25	100	96	63	31	26	17	11.7	1.990	6.5×10^{-5}	0.67	27.2	0.37	34.8
A-7	1	CL	2.694	25.6	49.3	25.8	23.5				90	78	74		—	—	—		—	—	—
	2	ML	2.612	18.6	40.4	26.2	14.2				84	61	56		15.6	1.762	3.9×10^{-7}	(15.4)	—	—	—
	3	ML	2.656	13.5	44.8	28.5	16.3				—	62	52		17.2	1.757	1.1×10^{-7}	(18.9)	—	—	—
A-8	1	GC	2.773	27.6	38.2	24.1	14.1				73	53	48		—	—	—	—	—	—	—
	2	SM	2.779	24.0	39.1	24.0	15.1				82	54	46		13.4	1.807	3.4×10^{-7}	(14.6)	—	—	—
	3	SC	2.752	10.0	37.0	23.8	13.2				79	55	50		14.8	1.803	2.6×10^{-7}	(14.4)	—	—	—
A-9	1	CL	2.709	19.6	33.4	20.1	13.3				83	75	59		—	—	—	—	—	—	—
	2	CL	2.684	15.1	37.9	22.0	15.9				88	64	51		13.8	1.845	1.6×10^{-7}	(14.0)	—	—	—
	3	CL	2.752	24.2	44.2	26.4	17.8				83	66	58		—	—	—	—	—	—	—
	4	CL	2.669	21.9	44.7	23.8	20.9				88	72	65		16.8	1.762	1.4×10^{-7}	(15.8)	—	—	—
A-10	1	CL	2.610	19.1	36.5	20.8	15.7				82	62	54		—	—	—	—	—	—	—
	2	CL	2.628	29.1	38.2	21.2	17.0								—	—	—	—	—	—	—
	3	CL	2.758	25.7	37.9	21.5	16.4				95	83	71		16.1	1.779	3.1×10^{-8}	(17.1)	—	—	—
	4	CL	2.662	18.6	39.6	21.2	18.4				99	87	75		—	—	—	—	—	—	—
	5	CL	2.788	20.6	39.0	21.0	18.0				95	81	69		15.8	1.782	8.9×10^{-8}	(16.8)	—	—	—

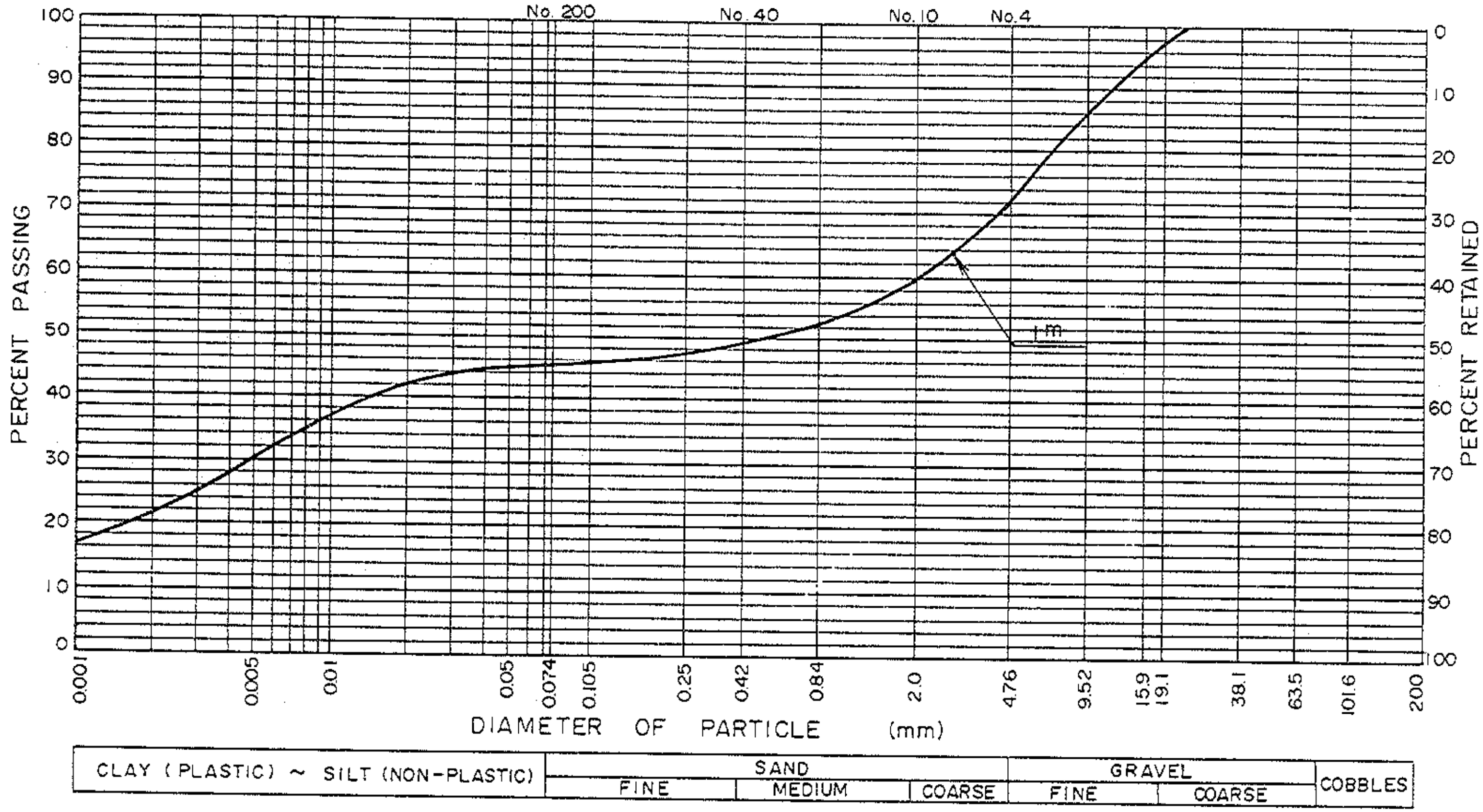

SAMPLE NO.		
MAX GRAIN SIZE		
mm (%)		
mm (%)		
mm 46 (%)		
mm 0.074 (%)		
D_{60} (mm)		
D_{30} (mm)		
D_{10} (mm)		
Cu		
Cc		

$Cu = \frac{D_{60}}{D_{10}}$

COEFFICIENT OF UNIFORMITY

$Cc = \frac{(D_{30})^2}{(D_{60}) \times (D_{10})}$

COEFFICIENT OF CURVATURE

SAMPLE		SOIL CLASSIFICATION		SPECIFIC GRAVITY		ATTERBERG LIMITS			
NUMBER	DEPTH (m)	UNIFIED SYSTEM	REVISED P.R. SYSTEM			LL	PL	PI	SL

Fig. 1-1 Grain Size Distribution Curve Sample A-1

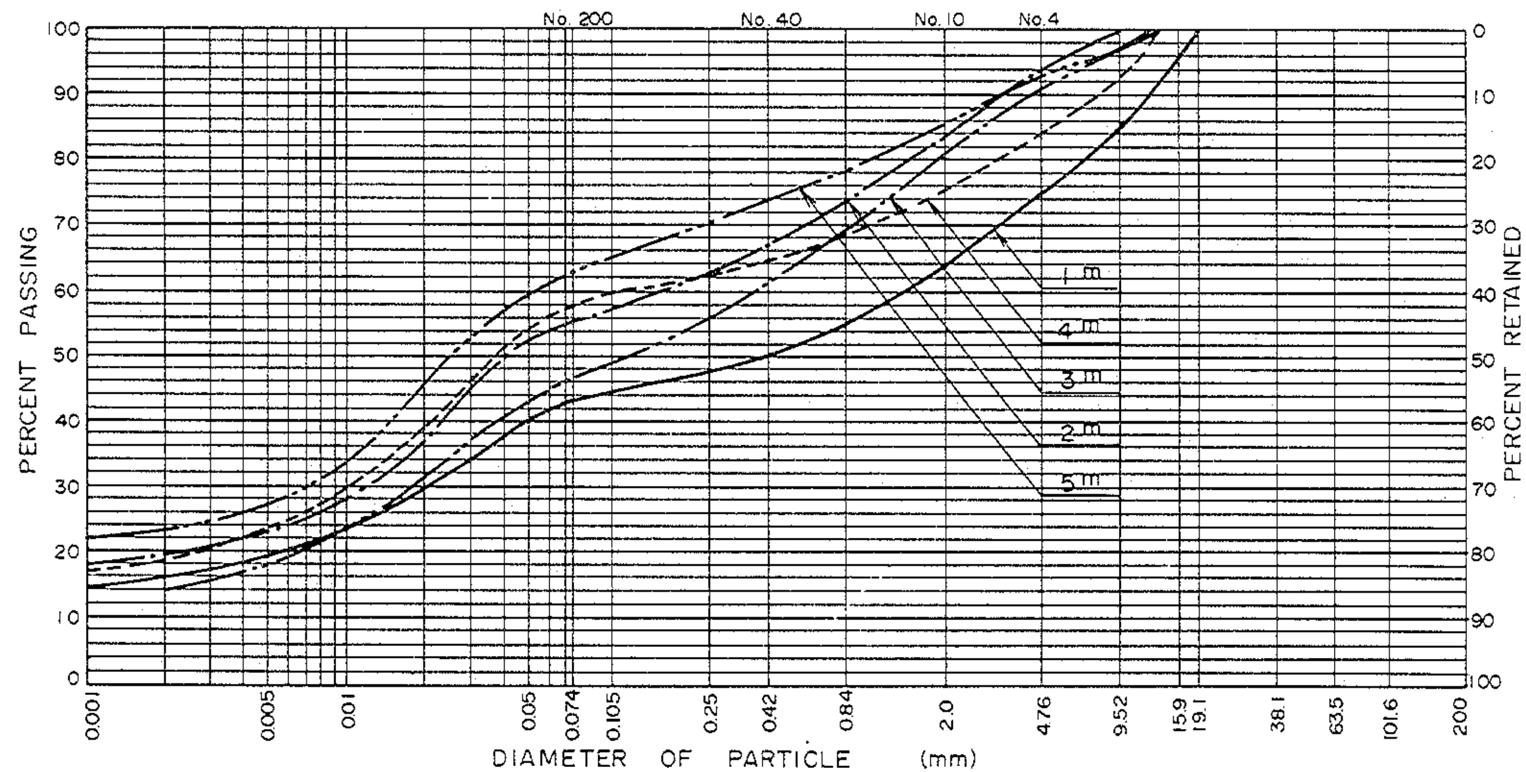

CLAY (PLASTIC) ~ SILT (NON-PLASTIC)	SAND			GRAVEL		COBBLES
	FINE	MEDIUM	COARSE	FINE	COARSE	

SAMPLE NO.		
MAX GRAIN SIZE		
mm (%)		
mm (%)		
mm 46 (%)		
mm 0.074 (%)		
D_{60} (mm)		
D_{30} (mm)		
D_{10} (mm)		
Cu		
Cc		

$$Cu = \frac{D_{60}}{D_{10}}$$

COEFFICIENT OF UNIFORMITY

$$Cc = \frac{(D_{30})^2}{(D_{60}) \times (D_{10})}$$

COEFFICIENT OF CURVATURE

SAMPLE		SOIL CLASSIFICATION		SPECIFIC GRAVITY		ATTERBERG LIMITS			
NUMBER	DEPTH (m)	UNIFIED SYSTEM	REVISED P.R. SYSTEM			LL	PL	PI	SL

Fig. I-2 Grain Size Distribution Curve Sample A-2

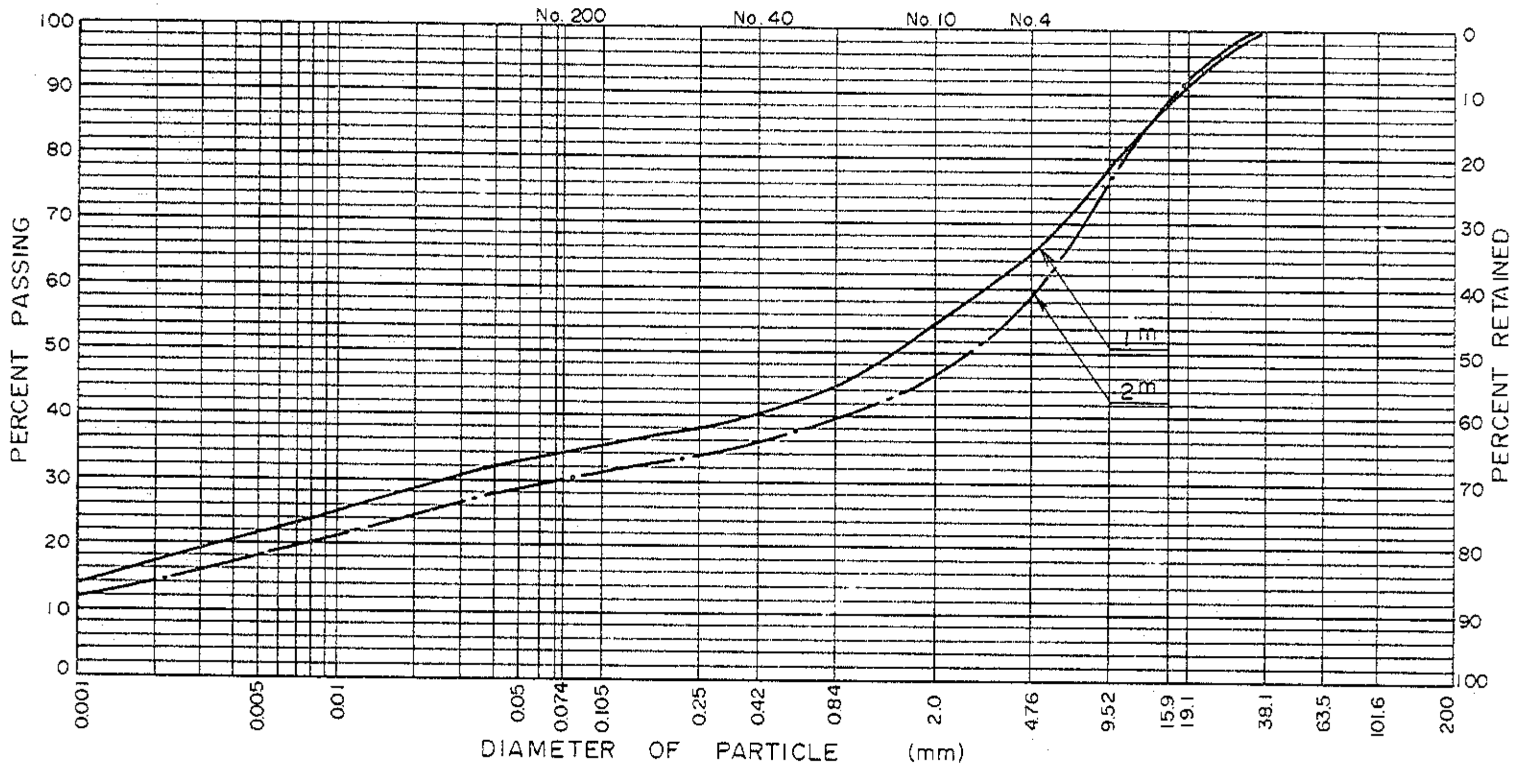

CLAY (PLASTIC) ~ SILT (NON-PLASTIC)	SAND			GRAVEL		COBBLES
	FINE	MEDIUM	COARSE	FINE	COARSE	

SAMPLE NO.		
MAX GRAIN SIZE		
mm (%)		
mm (%)		
mm 4.76 (%)		
mm 0.074 (%)		
D_{60} (mm)		
D_{30} (mm)		
D_{10} (mm)		
Cu		
Cc		

$$Cu = \frac{D_{60}}{D_{10}}$$

COEFFICIENT OF UNIFORMITY

$$Cc = \frac{(D_{30})^2}{(D_{60}) \times (D_{10})}$$

COEFFICIENT OF CURVATURE

SAMPLE		SOIL CLASSIFICATION		SPECIFIC GRAVITY		ATTERBERG LIMITS			
NUMBER	DEPTH (m)	UNIFIED SYSTEM	REVISED PR. SYSTEM			LL	PL	PI	SL

Fig.1-3 Grain Size Distribution Curve Sample A-3

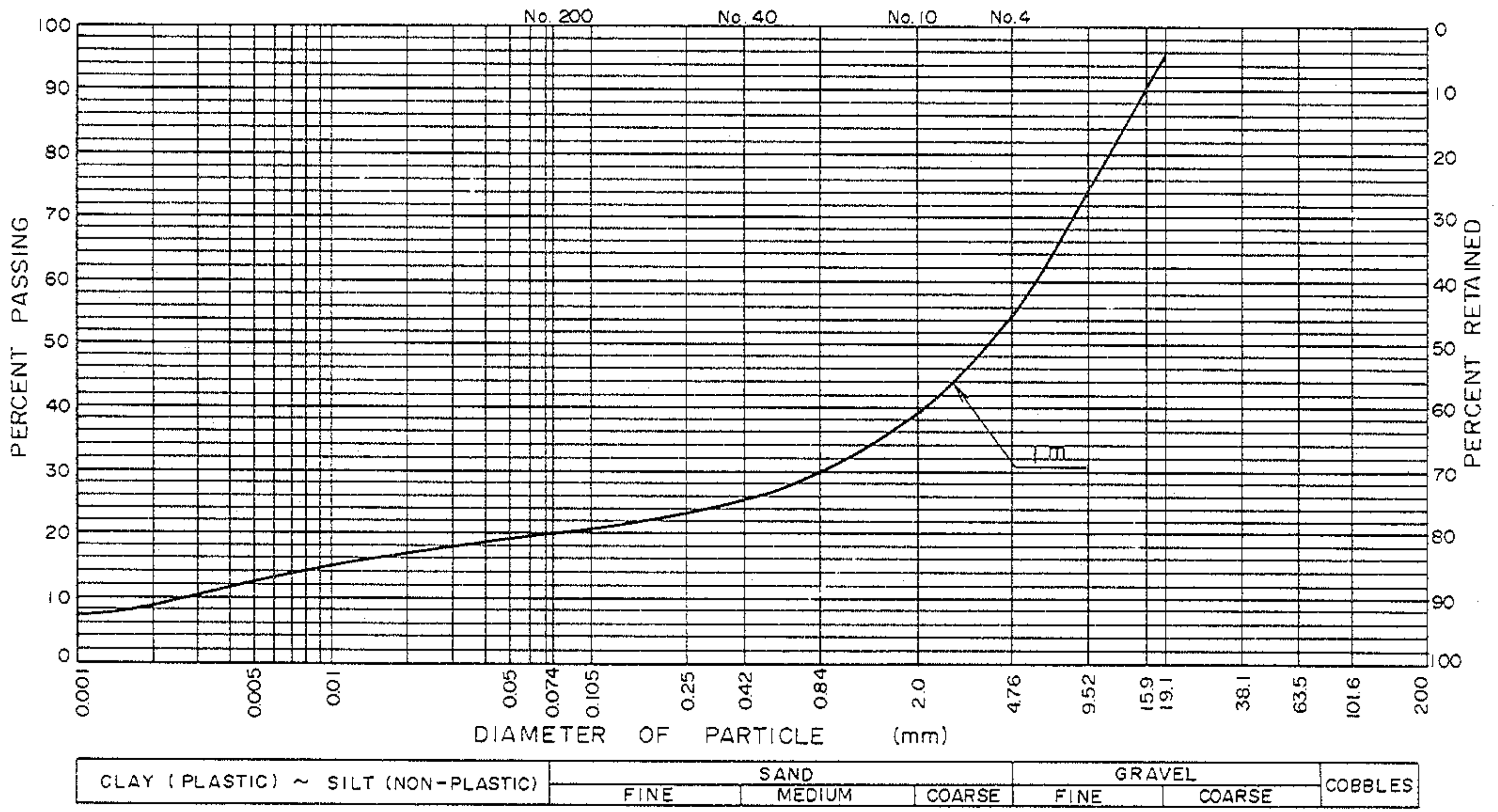

SAMPLE NO.		
MAX GRAIN SIZE		
mm (%)		
mm (%)		
mm 46 (%)		
mm 0.074 (%)		
D_{60} (mm)		
D_{30} (mm)		
D_{10} (mm)		
Cu		
Cc		

$$Cu = \frac{D_{60}}{D_{10}}$$

COEFFICIENT OF UNIFORMITY

$$Cc = \frac{(D_{30})^2}{(D_{60}) \times (D_{10})}$$

COEFFICIENT OF CURVATURE

SAMPLE		SOIL CLASSIFICATION		SPECIFIC GRAVITY		ATTERBERG LIMITS			
NUMBER	DEPTH (m)	UNIFIED SYSTEM	REVISED PR. SYSTEM			LL	PL	PI	SL

Fig. I-4 Grain Size Distribution Curve Sample A-4

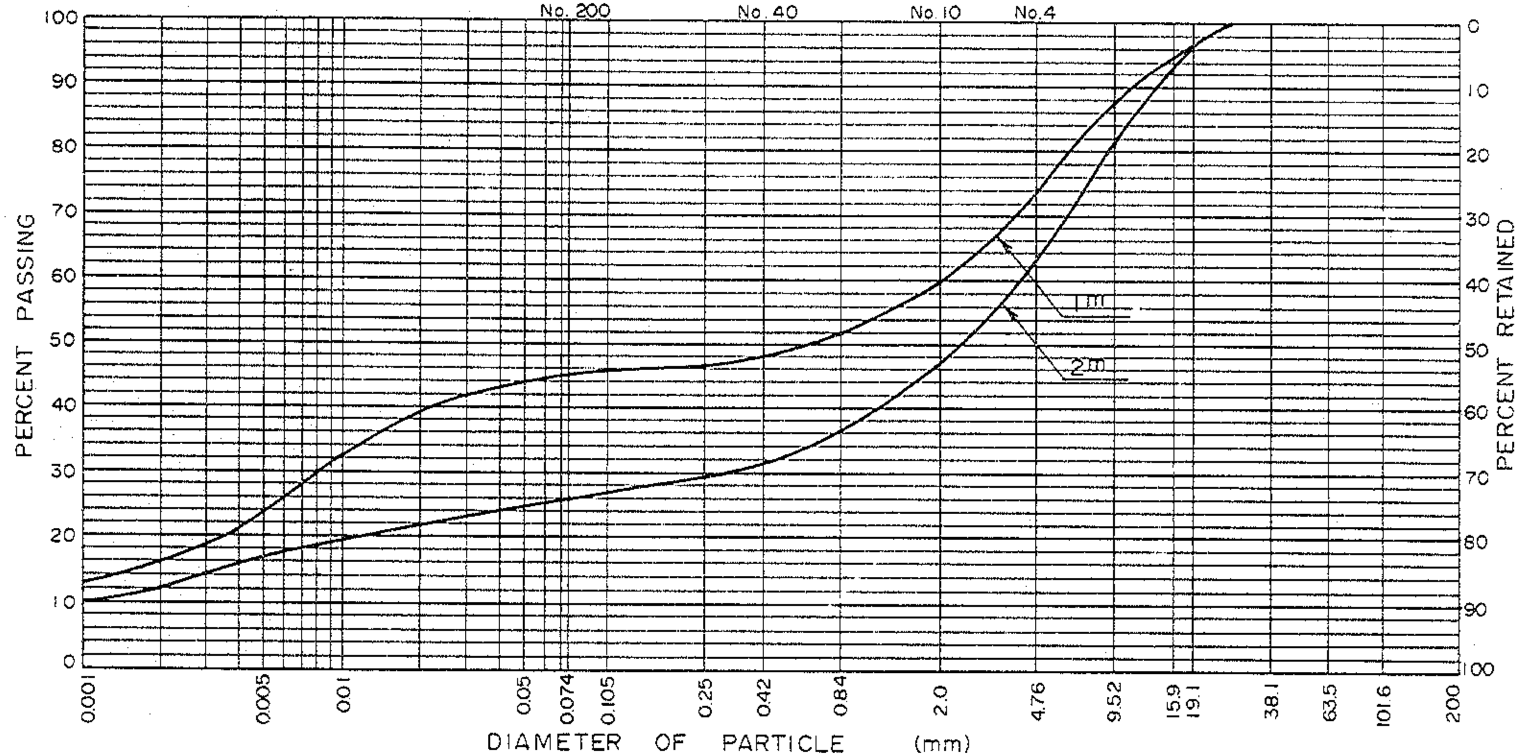

CLAY (PLASTIC) ~ SILT (NON-PLASTIC)	SAND			GRAVEL		COBBLES
	FINE	MEDIUM	COARSE	FINE	COARSE	

SAMPLE NO.		
MAX GRAIN SIZE		
mm (%)		
mm (%)		
mm 46 (%)		
mm 0.074 (%)		
D_{60} (mm)		
D_{30} (mm)		
D_{10} (mm)		
Cu		
Cc		

$Cu = \frac{D_{60}}{D_{10}}$ COEFFICIENT OF UNIFORMITY

$Cc = \frac{(D_{30})^2}{(D_{60}) \times (D_{10})}$ COEFFICIENT OF CURVATURE

SAMPLE		SOIL CLASSIFICATION		SPECIFIC GRAVITY		ATTERBERG LIMITS			
NUMBER	DEPTH (m)	UNIFIED SYSTEM	REVISED PR. SYSTEM			LL	PL	PI	SL

Fig. I-5 Grain Size Distribution Curve Sample A-5

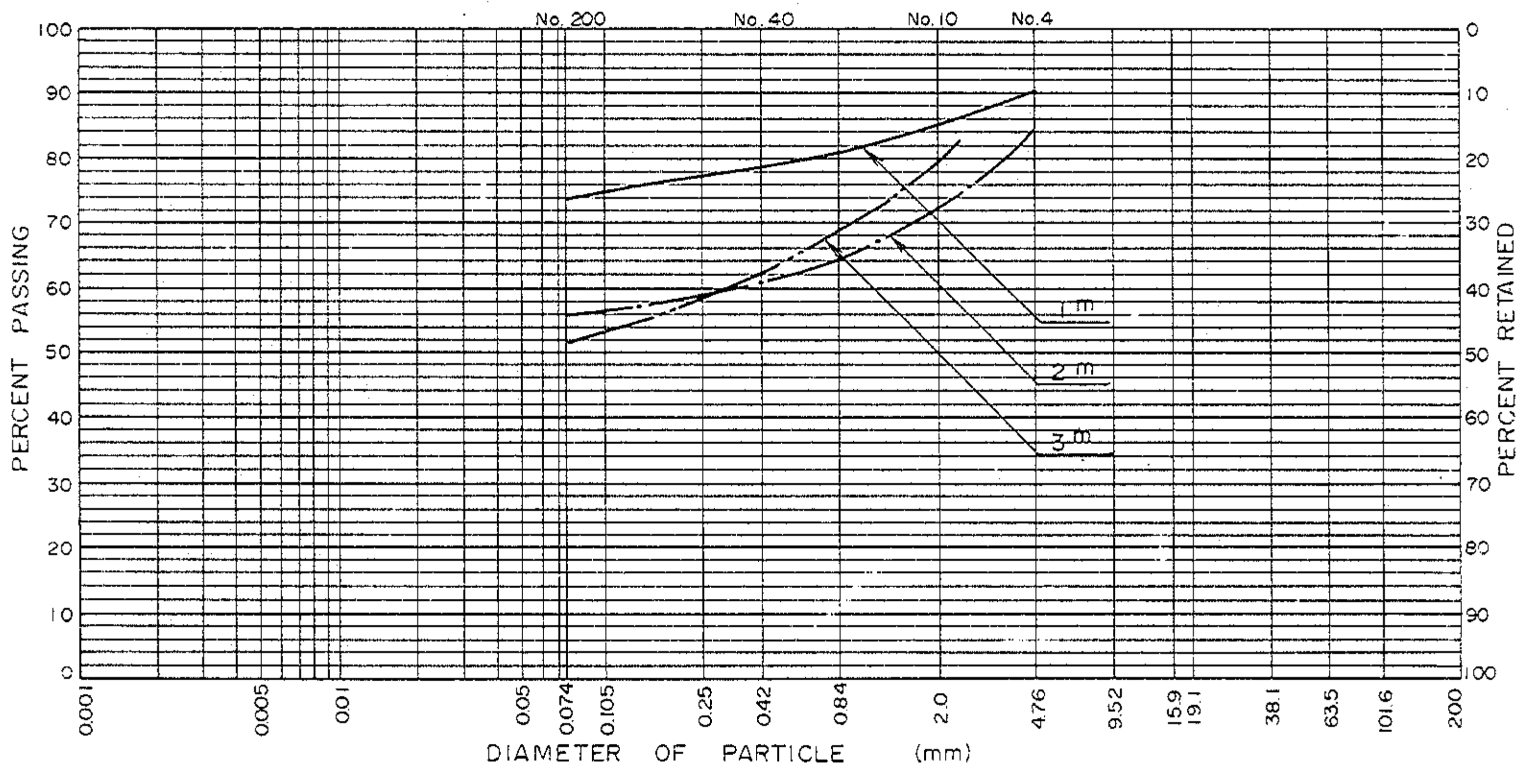

CLAY (PLASTIC) ~ SILT (NON-PLASTIC)	SAND			GRAVEL		COBBLES
	FINE	MEDIUM	COARSE	FINE	COARSE	

SAMPLE NO.		
MAX GRAIN SIZE		
mm (%)		
mm (%)		
mm 46 (%)		
mm 0.074 (%)		
D_{60} (mm)		
D_{30} (mm)		
D_{10} (mm)		
Cu		
Cc		

$$Cu = \frac{D_{60}}{D_{10}}$$

COEFFICIENT OF UNIFORMITY

$$Cc = \frac{(D_{30})^2}{(D_{60}) \times (D_{10})}$$

COEFFICIENT OF CURVATURE

SAMPLE		SOIL CLASSIFICATION		SPECIFIC GRAVITY		ATTERBERG LIMITS			
NUMBER	DEPTH (m)	UNIFIED SYSTEM	REVISED PR. SYSTEM			LL	PL	PI	SL

Fig. I-6 Grain Size Distribution Curve Sample A-7

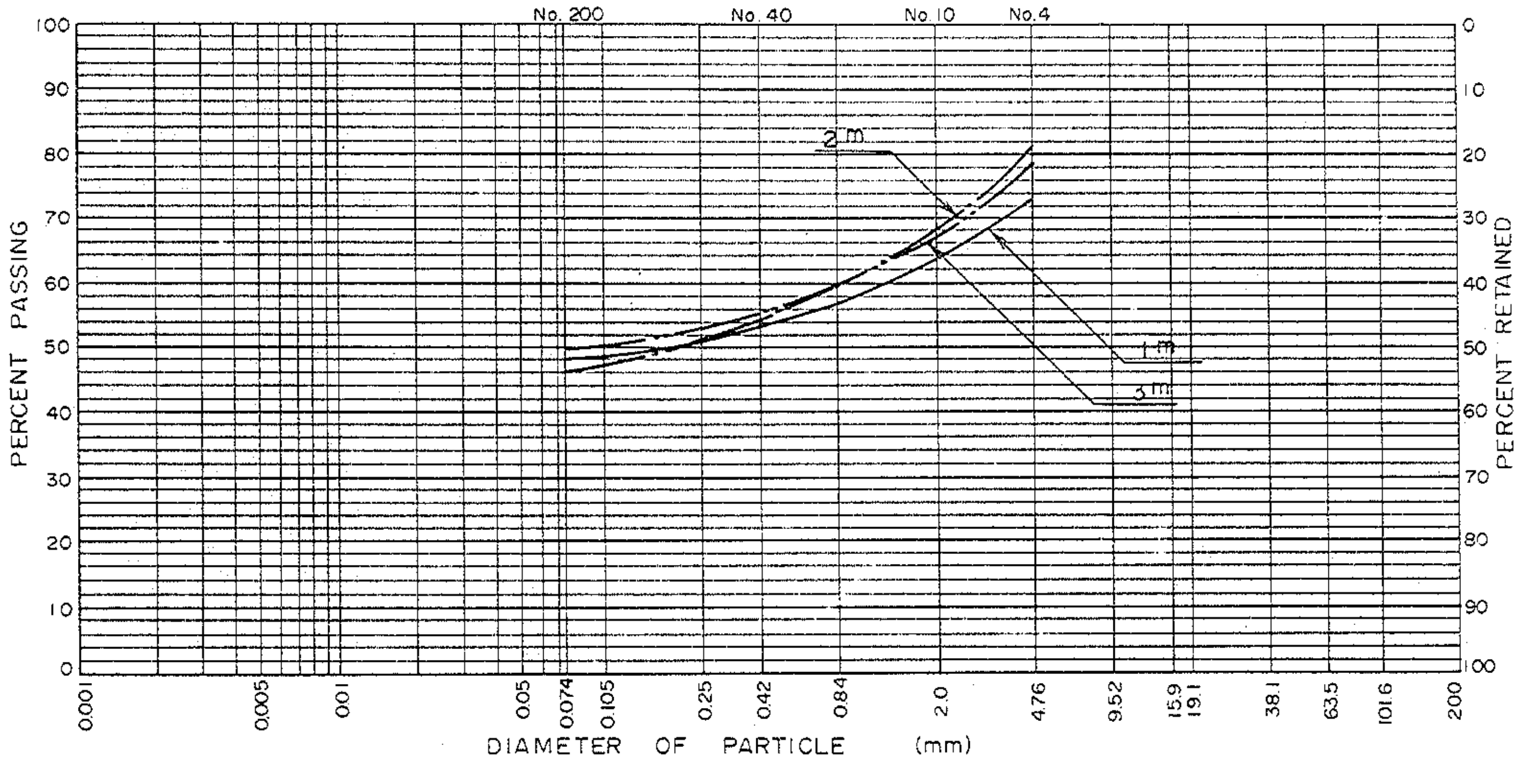

CLAY (PLASTIC) ~ SILT (NON-PLASTIC)	SAND			GRAVEL		COBBLES
	FINE	MEDIUM	COARSE	FINE	COARSE	

SAMPLE NO.		
MAX GRAIN SIZE		
mm (%)		
mm (%)		
mm 46 (%)		
mm 0.074 (%)		
D60 (mm)		
D30 (mm)		
D10 (mm)		
Cu		
Cc		

$Cu = \frac{D_{60}}{D_{10}}$

COEFFICIENT OF UNIFORMITY

$Cc = \frac{(D_{30})^2}{(D_{60}) \times (D_{10})}$

COEFFICIENT OF CURVATURE

SAMPLE		SOIL CLASSIFICATION		SPECIFIC GRAVITY		ATTERBERG LIMITS			
NUMBER	DEPTH (m)	UNIFIED SYSTEM	REVISED P.R. SYSTEM			LL	PL	PI	SL

Fig. I-7 Grain Size Distribution Curve Sample A-8

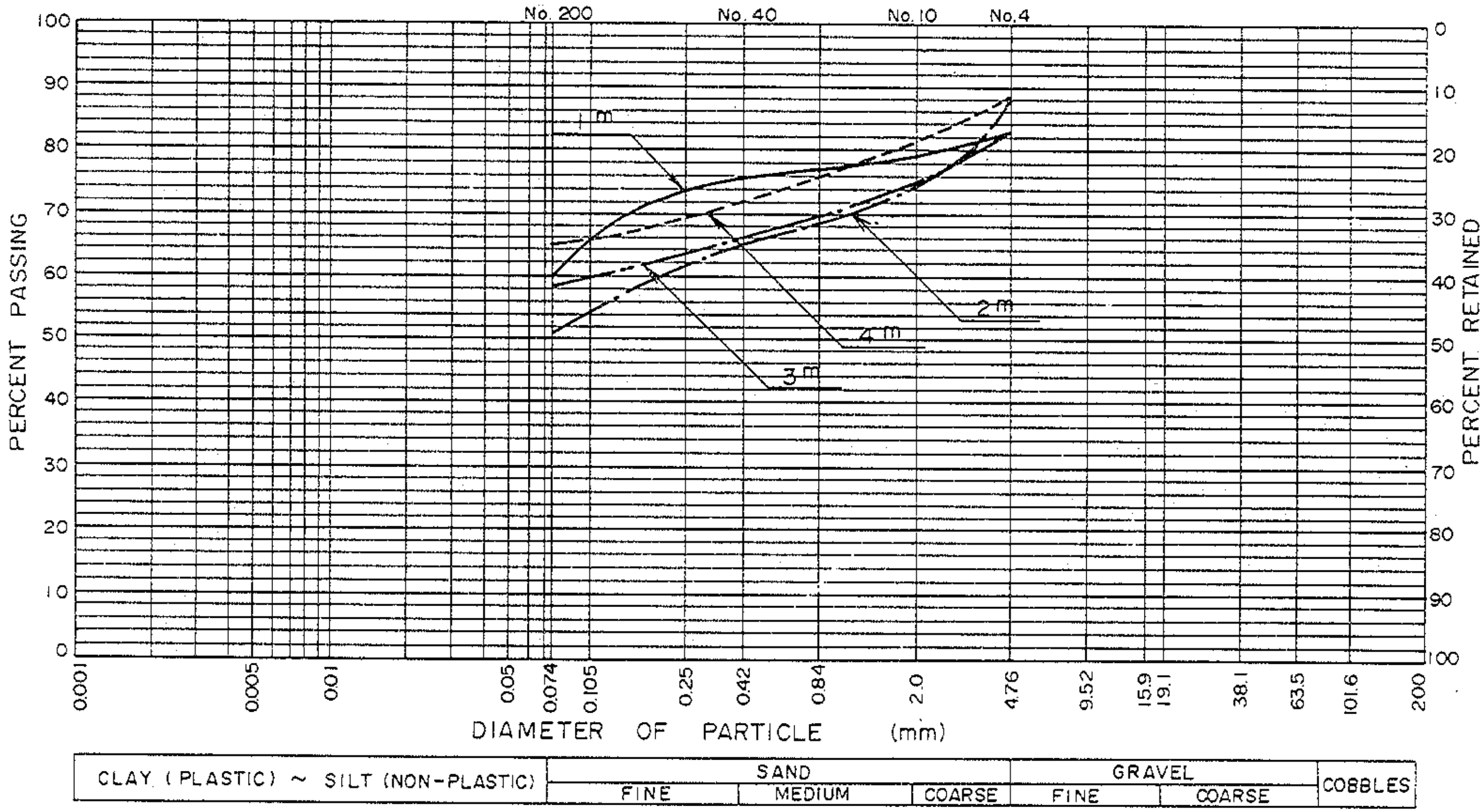

SAMPLE NO.		
MAX GRAIN SIZE		
mm (%)		
mm (%)		
mm 46 (%)		
mm 0.074 (%)		
D_{60} (mm)		
D_{30} (mm)		
D_{10} (mm)		
Cu		
Cc		

$$Cu = \frac{D_{60}}{D_{10}}$$

COEFFICIENT OF UNIFORMITY

$$Cc = \frac{(D_{30})^2}{(D_{60}) \times (D_{10})}$$

COEFFICIENT OF CURVATURE

SAMPLE		SOIL CLASSIFICATION		SPECIFIC GRAVITY		ATTERBERG LIMITS			
NUMBER	DEPTH (m)	UNIFIED SYSTEM	REVISED P.R. SYSTEM			LL	PL	PI	SL

Fig. I-8 Grain Size Distribution Curve Sample A-9

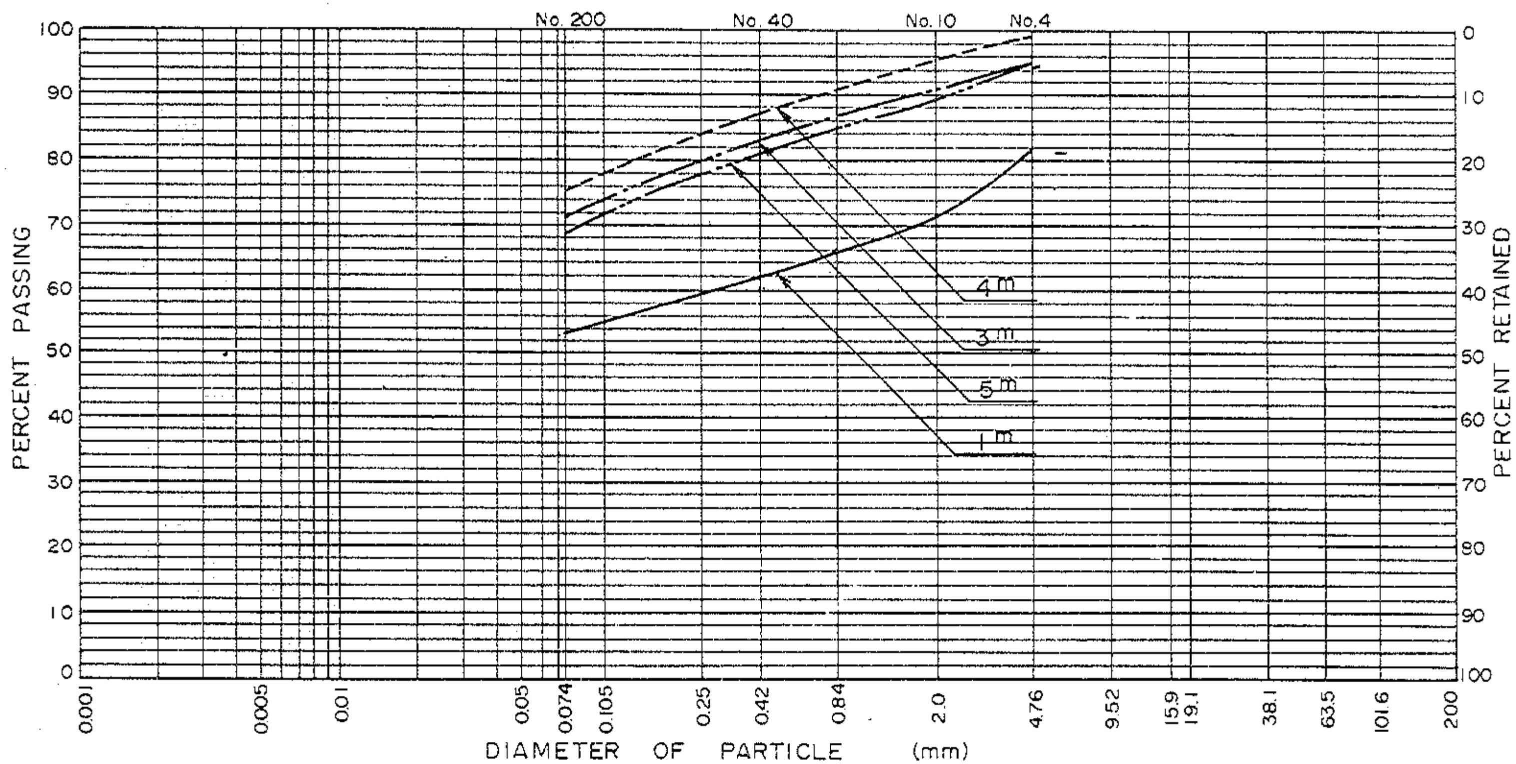

CLAY (PLASTIC) ~ SILT (NON-PLASTIC)	SAND			GRAVEL		COBBLES
	FINE	MEDIUM	COARSE	FINE	COARSE	

SAMPLE NO.		
MAX GRAIN SIZE		
mm (%)		
mm (%)		
mm 46 (%)		
mm 0.074 (%)		
D_{60} (mm)		
D_{30} (mm)		
D_{10} (mm)		
Cu		
Cc		

$$Cu = \frac{D_{60}}{D_{10}}$$

COEFFICIENT OF UNIFORMITY

$$Cc = \frac{(D_{30})^2}{(D_{60}) \times (D_{10})}$$

COEFFICIENT OF CURVATURE

SAMPLE		SOIL CLASSIFICATION		SPECIFIC GRAVITY		ATTERBERG LIMITS			
NUMBER	DEPTH (m)	UNIFIED SYSTEM	REVISED P.R. SYSTEM			LL	PL	PI	SL

Fig. 1-9 Grain Size Distribution Curve Sample A-10

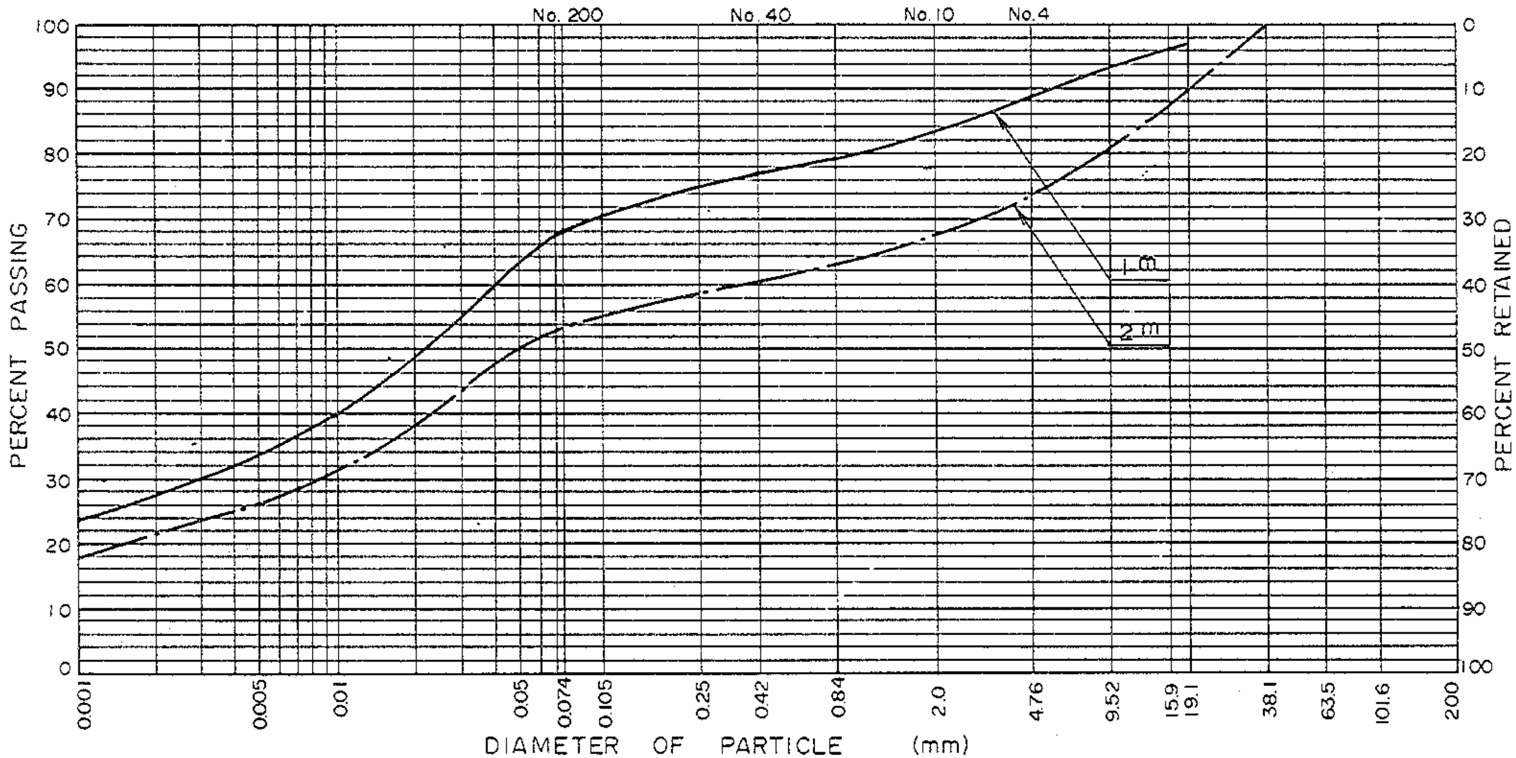

CLAY (PLASTIC) ~ SILT (NON-PLASTIC)	SAND			GRAVEL		COBBLES
	FINE	MEDIUM	COARSE	FINE	COARSE	

SAMPLE NO.		
MAX GRAIN SIZE		
mm (%)		
mm (%)		
mm 4.6 (%)		
mm 0.074 (%)		
D_{60} (mm)		
D_{30} (mm)		
D_{10} (mm)		
Cu		
Cc		

$$Cu = \frac{D_{60}}{D_{10}}$$

COEFFICIENT OF UNIFORMITY

$$Cc = \frac{(D_{30})^2}{(D_{60}) \times (D_{10})}$$

COEFFICIENT OF CURVATURE

SAMPLE		SOIL CLASSIFICATION		SPECIFIC GRAVITY		ATTERBERG LIMITS			
NUMBER	DEPTH (m)	UNIFIED SYSTEM	REVISED PR. SYSTEM			LL	PL	PI	SL

Fig. 1-10 Grain Size Distribution Curve Sample B-1

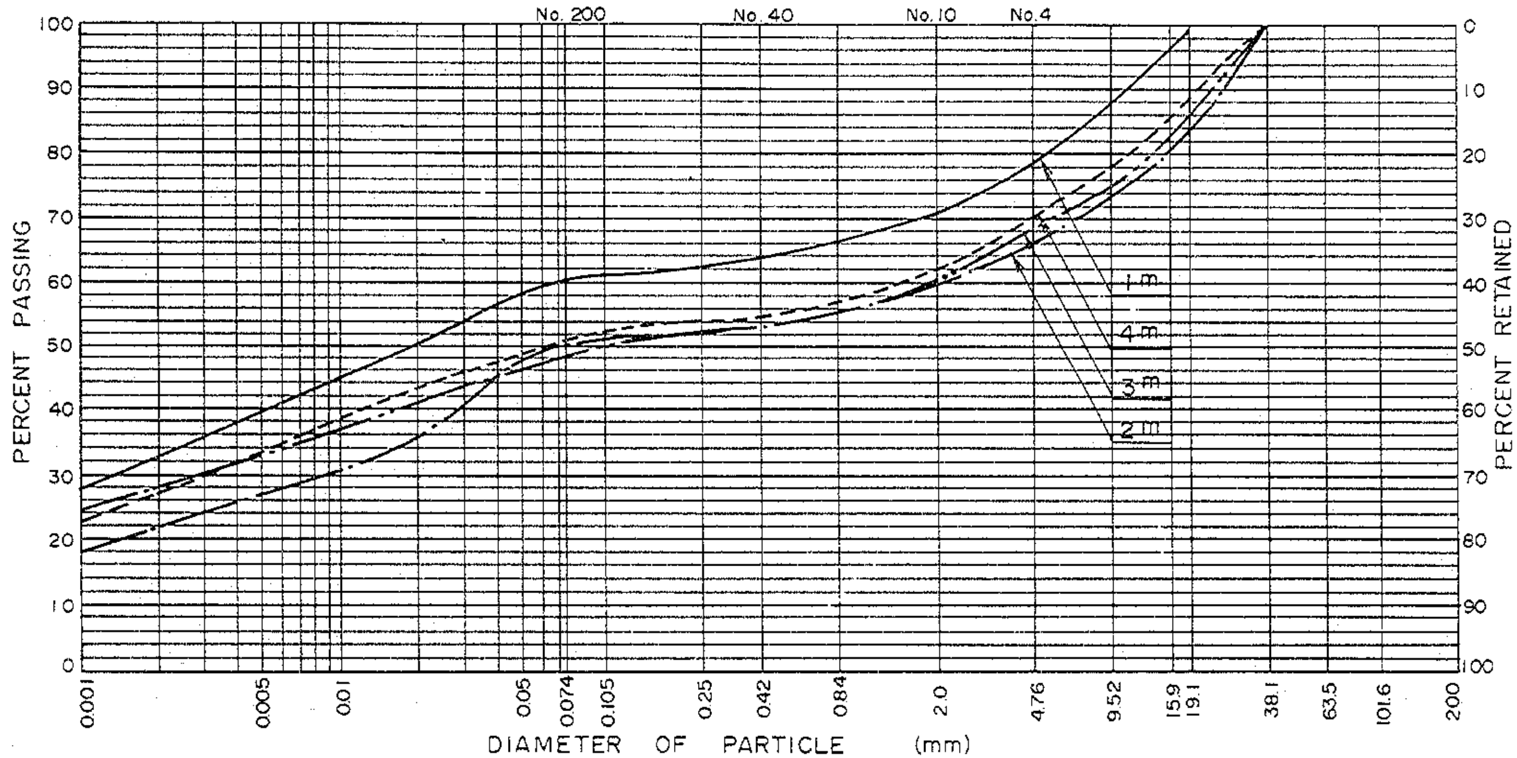

CLAY (PLASTIC) ~ SILT (NON-PLASTIC)	SAND			GRAVEL		COBBLES
	FINE	MEDIUM	COARSE	FINE	COARSE	

SAMPLE NO.		
MAX GRAIN SIZE		
mm (%)		
mm (%)		
mm 46 (%)		
mm 0.074 (%)		
D60 (mm)		
D30 (mm)		
D10 (mm)		
Cu		
Cc		

$Cu = \frac{D_{60}}{D_{10}}$

COEFFICIENT OF UNIFORMITY

$Cc = \frac{(D_{30})^2}{(D_{60}) \times (D_{10})}$

COEFFICIENT OF CURVATURE

SAMPLE		SOIL CLASSIFICATION		SPECIFIC GRAVITY		ATTERBERG LIMITS			
NUMBER	DEPTH (m)	UNIFIED SYSTEM	REVISED PR. SYSTEM			LL	PL	PI	SL

Fig. I-11 Grain Size Distribution Curve Sample C-1

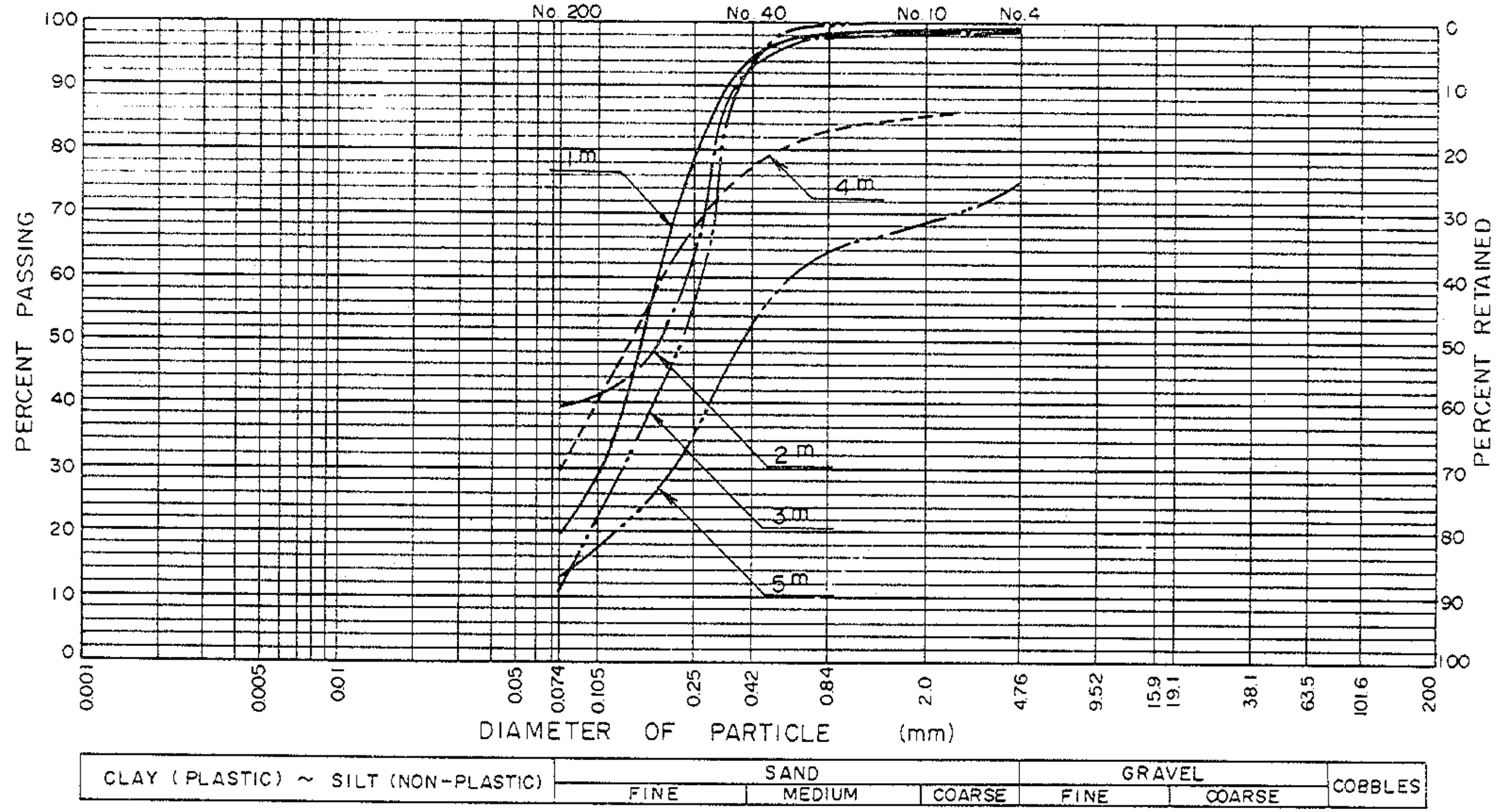

SAMPLE NO.		
MAX GRAIN SIZE		
mm (%)		
mm (%)		
mm 46 (%)		
mm 0.074 (%)		
D60 (mm)		
D30 (mm)		
D10 (mm)		
Cu		
Cc		

$Cu = \frac{D_{60}}{D_{10}}$ COEFFICIENT OF UNIFORMITY

$Cc = \frac{(D_{30})^2}{(D_{60}) \times (D_{10})}$ COEFFICIENT OF CURVATURE

SAMPLE		SOIL CLASSIFICATION		SPECIFIC GRAVITY		ATTERBERG LIMITS			
NUMBER	DEPTH (m)	UNIFIED SYSTEM	REVISED P.R. SYSTEM			LL	PL	PI	SL

Fig. I-12 Grain Size Distribution Curve Sample C-6

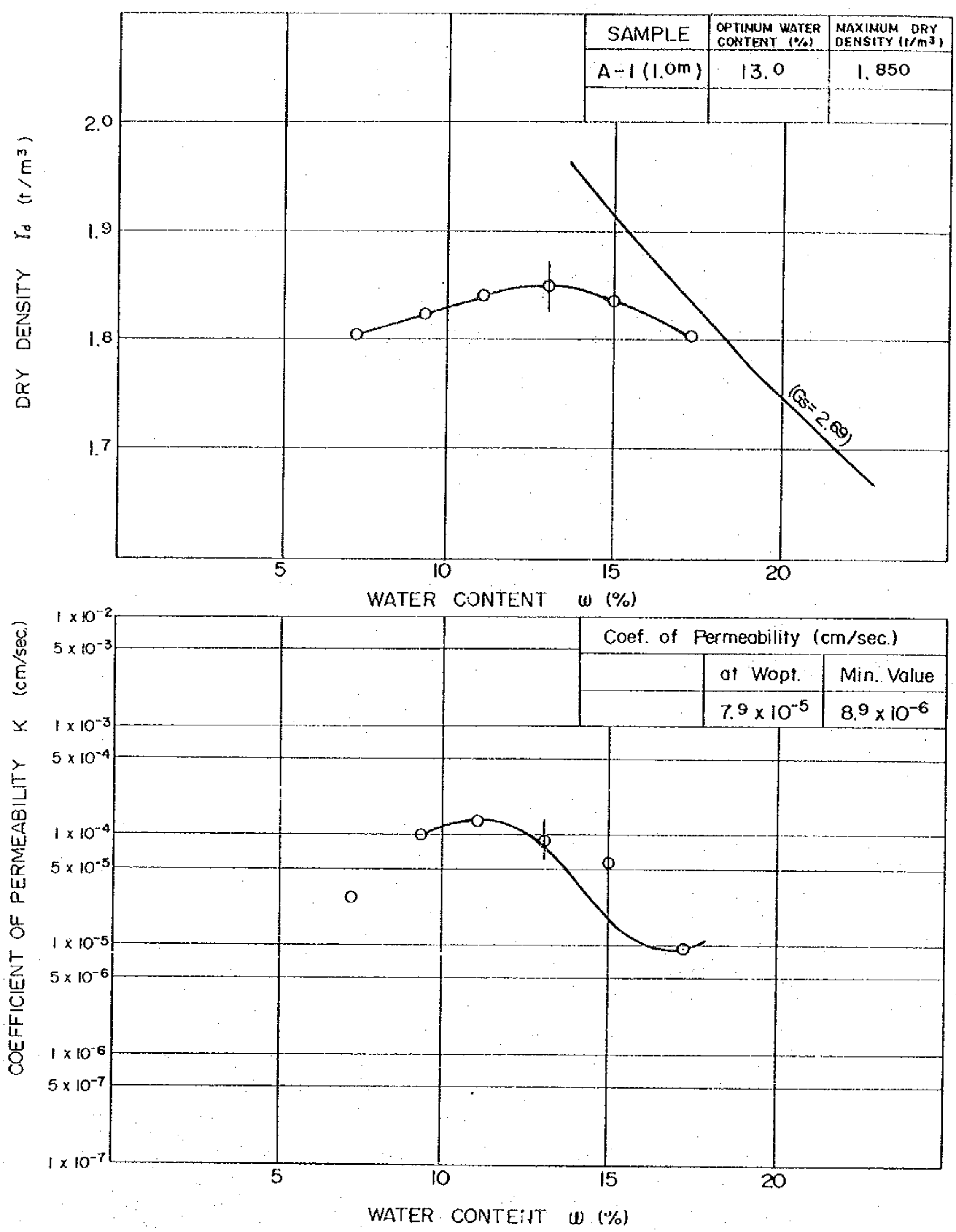

Sample A-1 1.00m

Fig.2-1 Compaction and Permeability Test

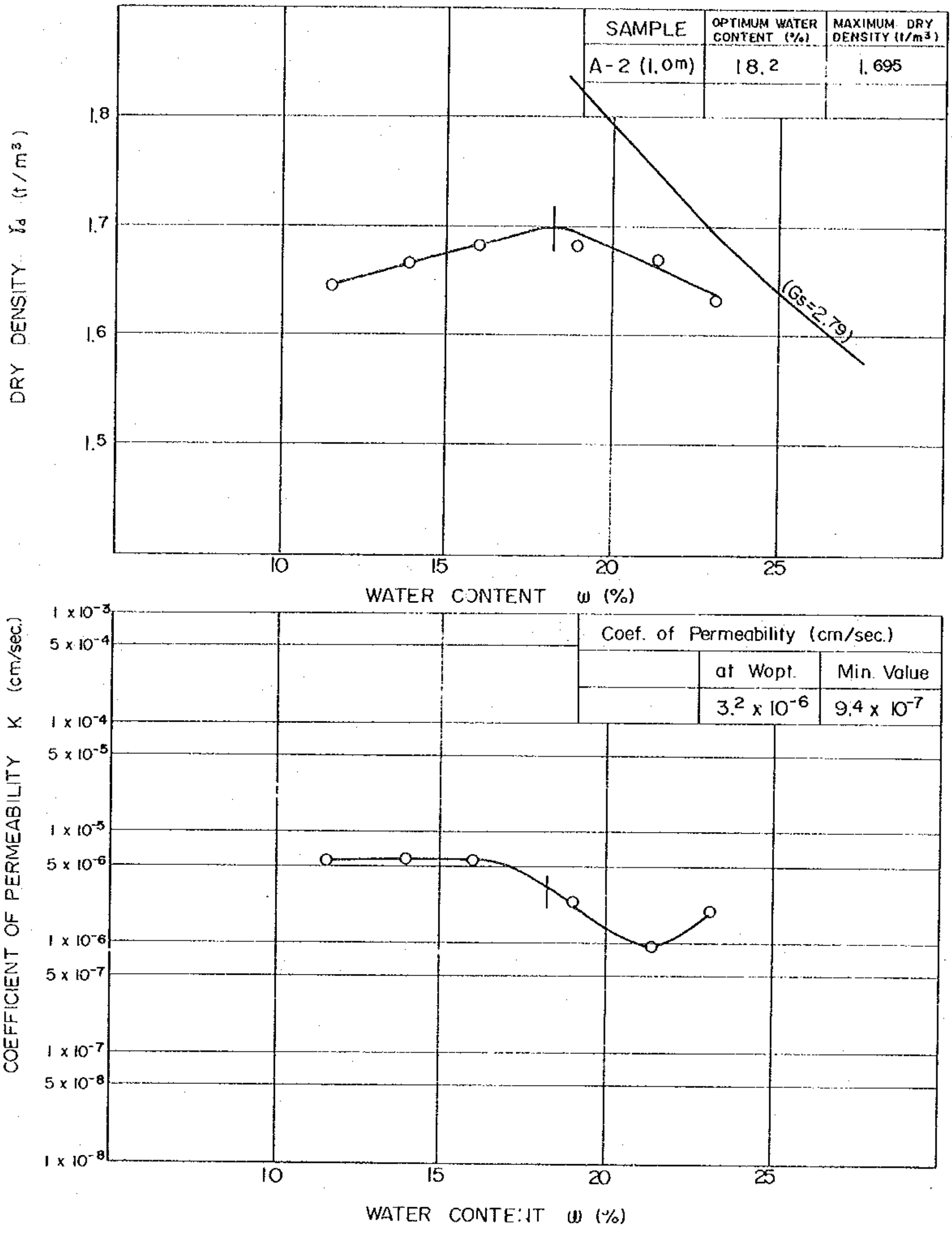

Sample A-2 1.00m

Fig.2-2 Compaction and Permeability Test

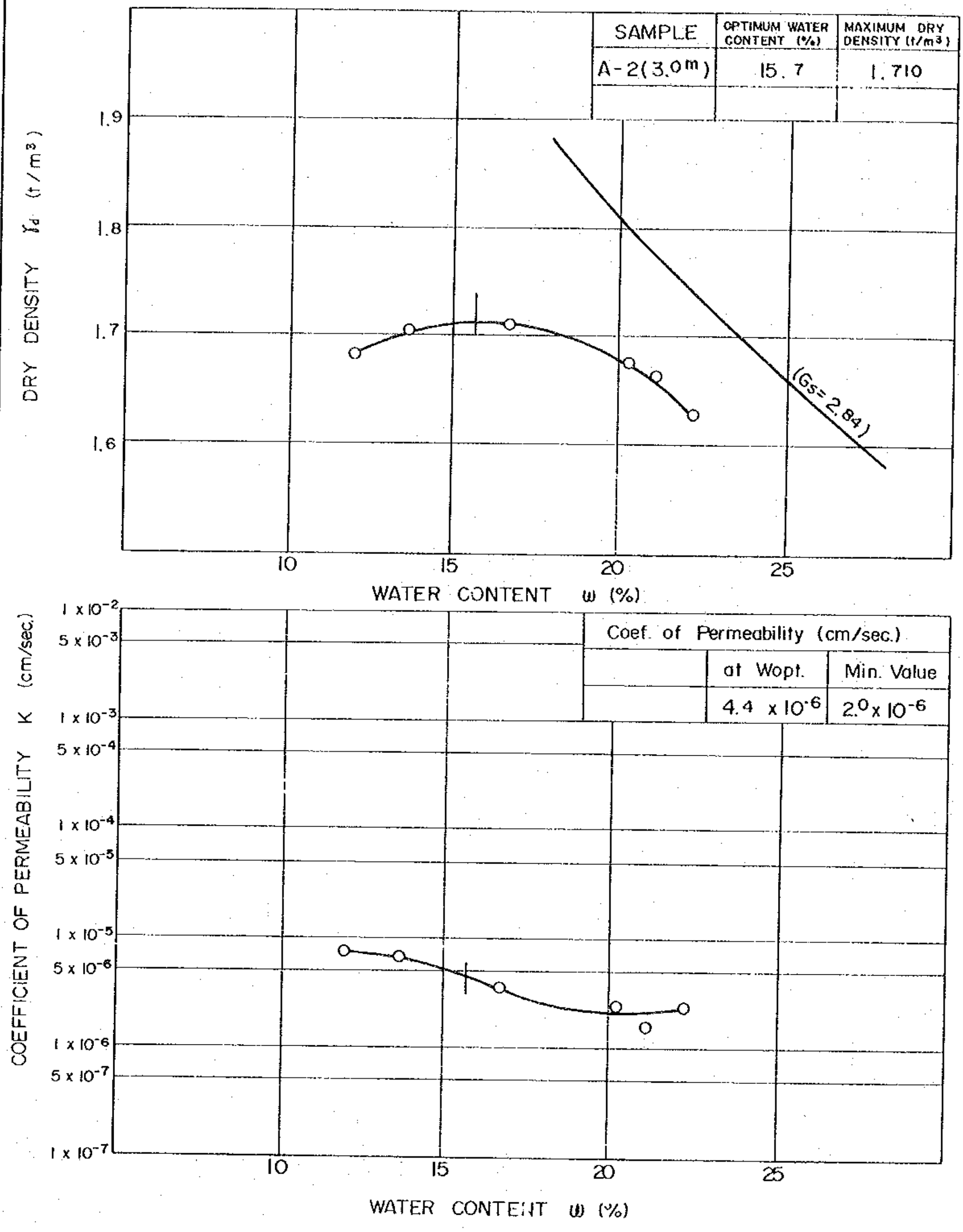

Sample A-2 3.00m

Fig.2-3 Compaction and Permeability Test

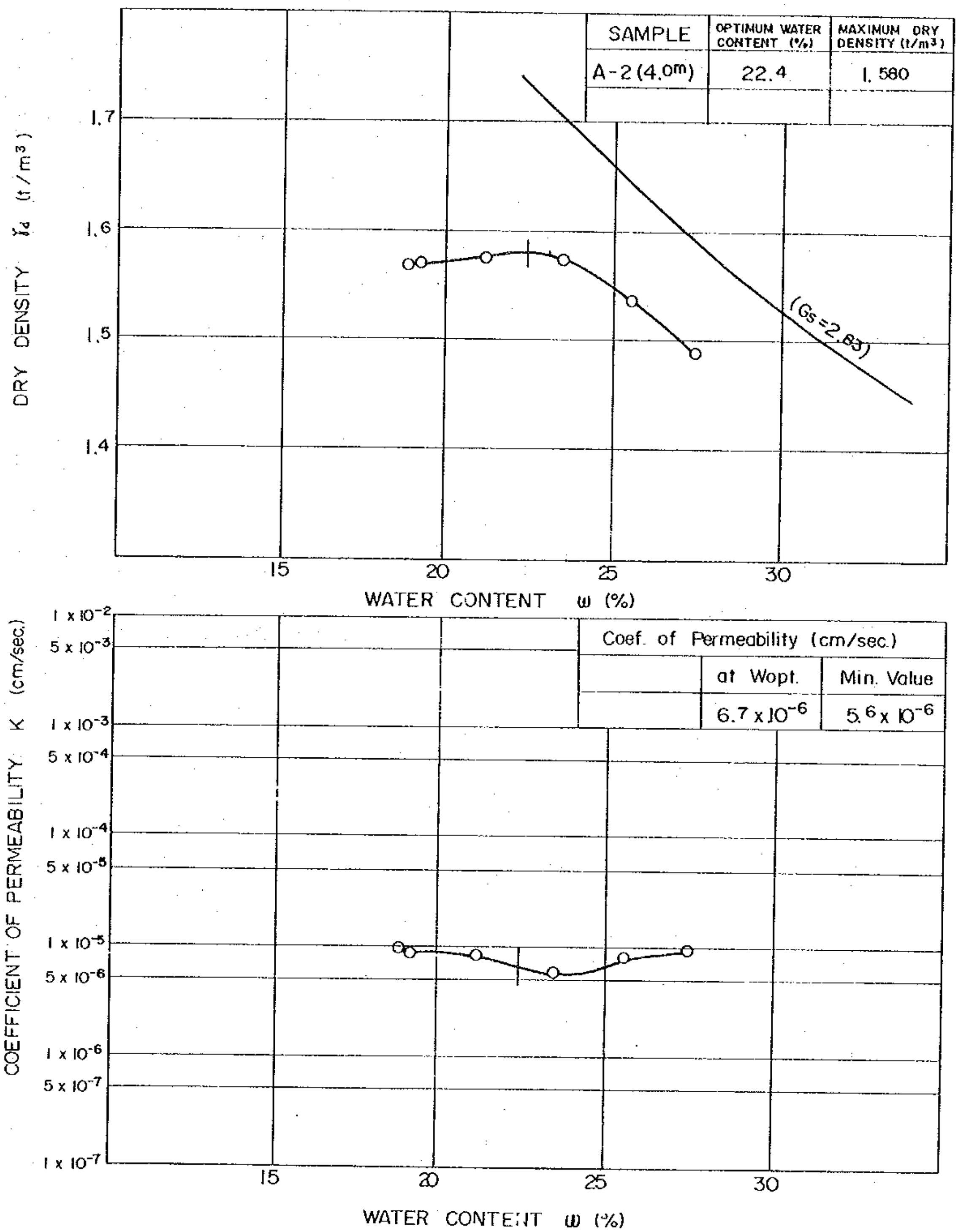

Sample A-2 4.00m

Fig.2-4 Compaction and Permeability Test

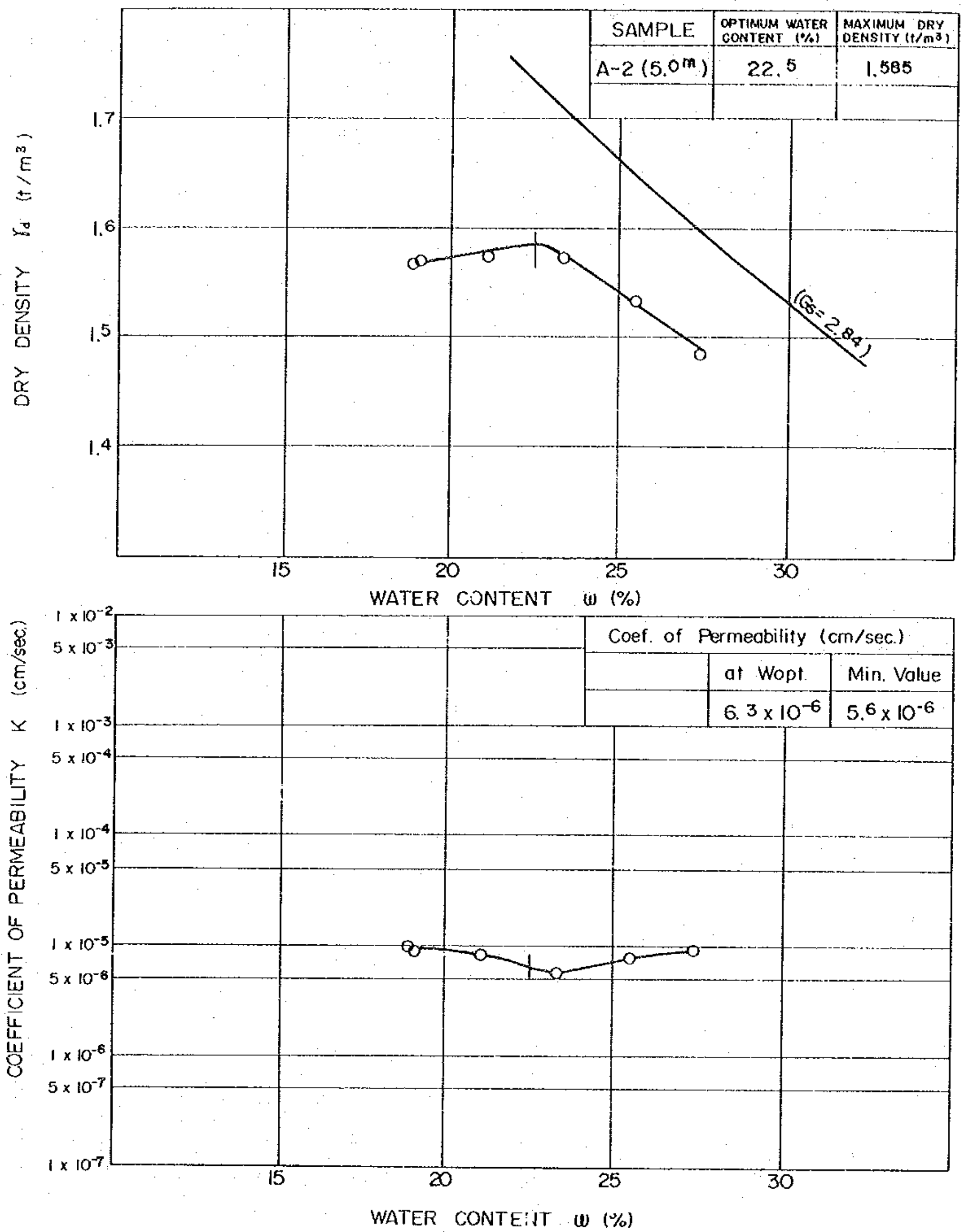

Sample A-2 5,00m

Fig.2-5 Compaction and Permeability Test

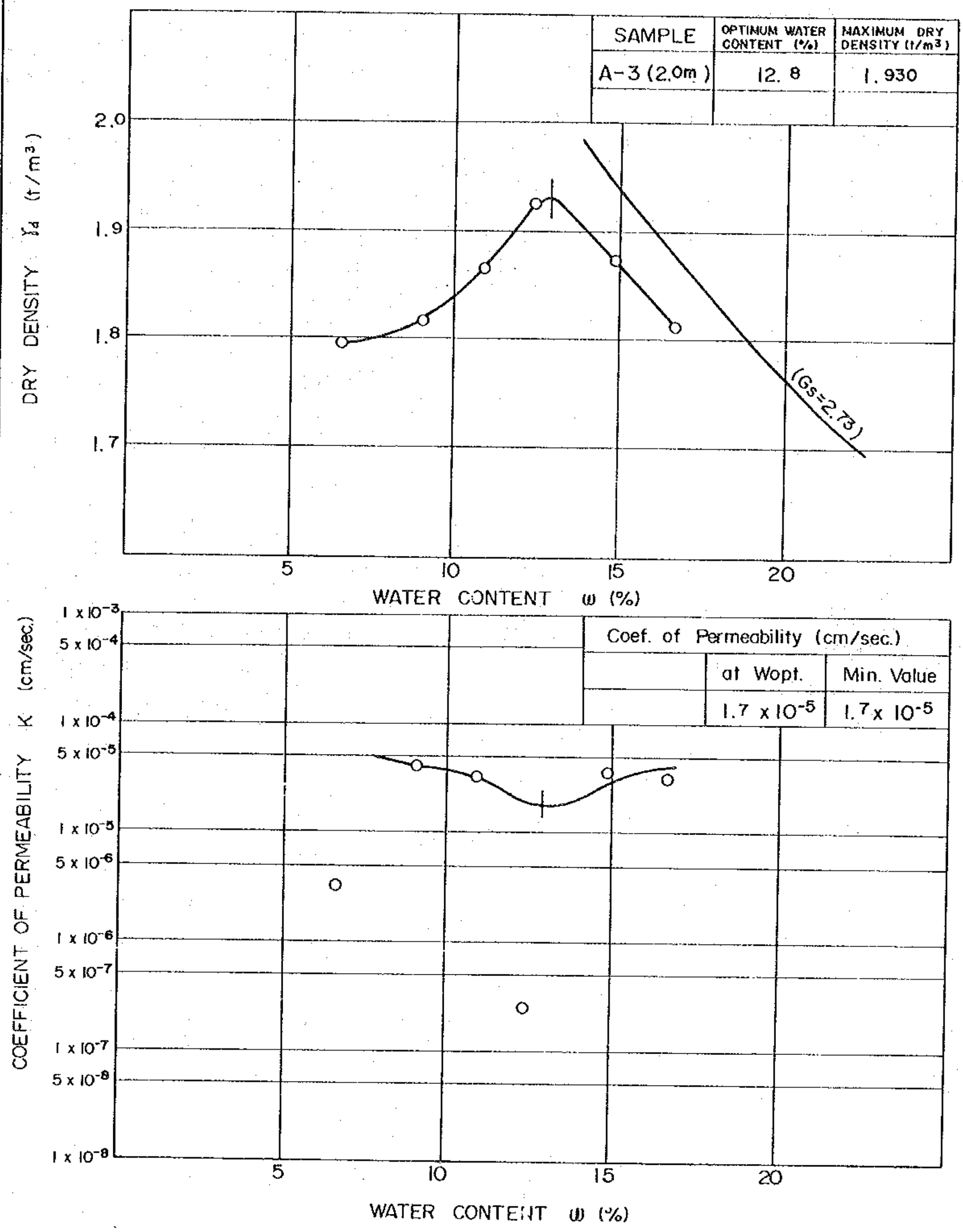

Sample A-3 2.00m

Fig.2-6 Compaction and Permeability Test

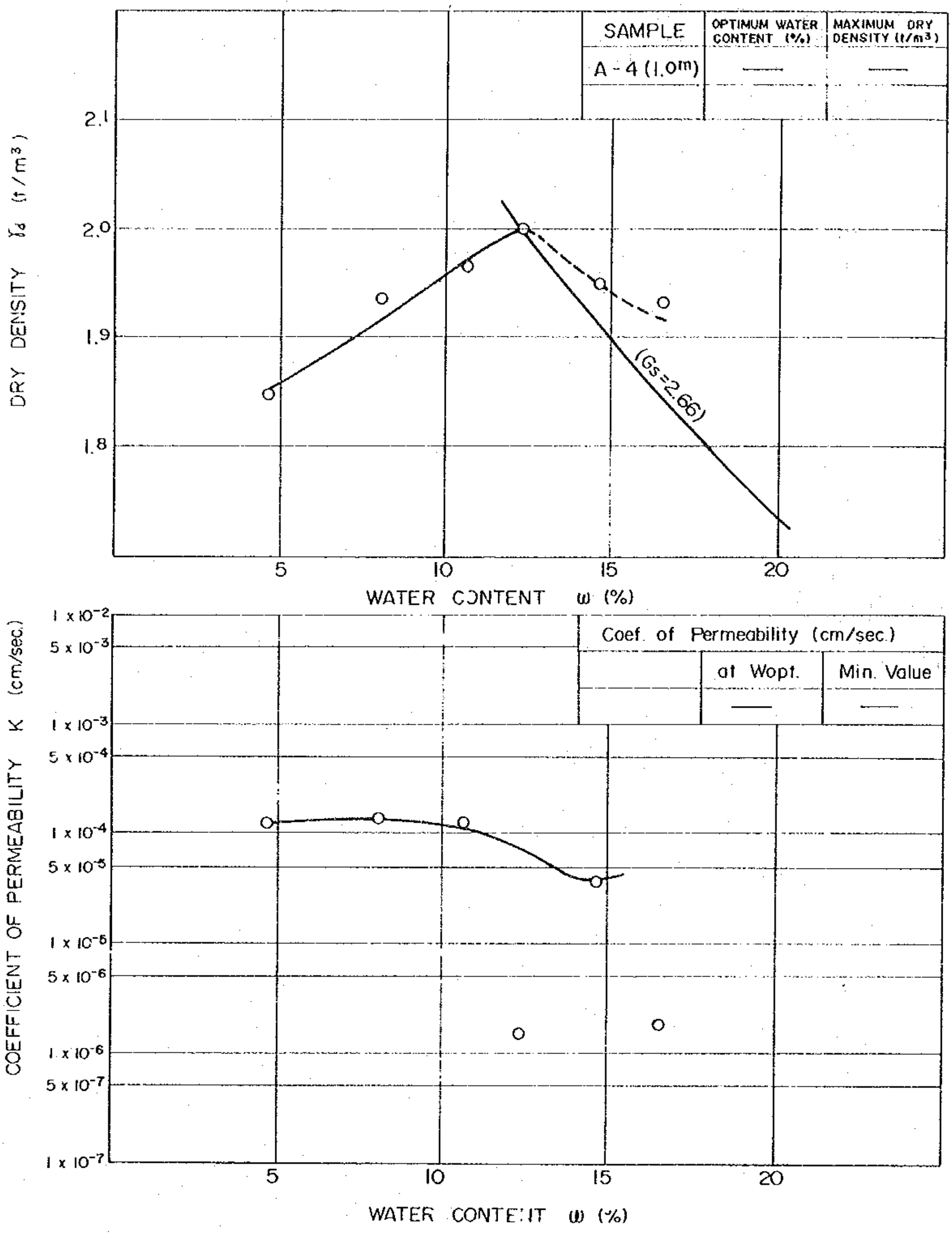

Sample A-4 1.00m

Fig.2-7 Compaction and Permeability Test

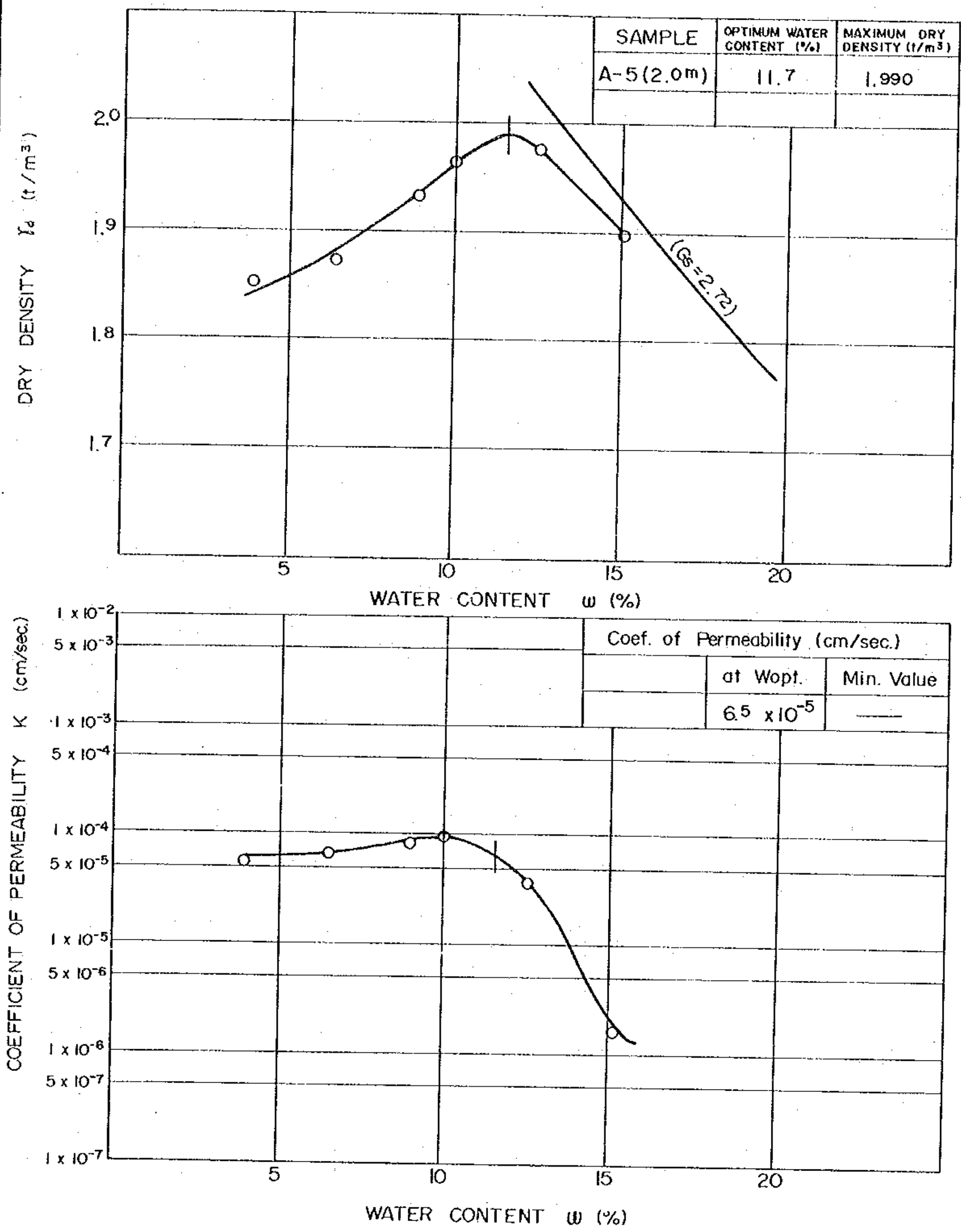

Sample A-5 2.00m

Fig. 2-8 Compaction and Permeability Test

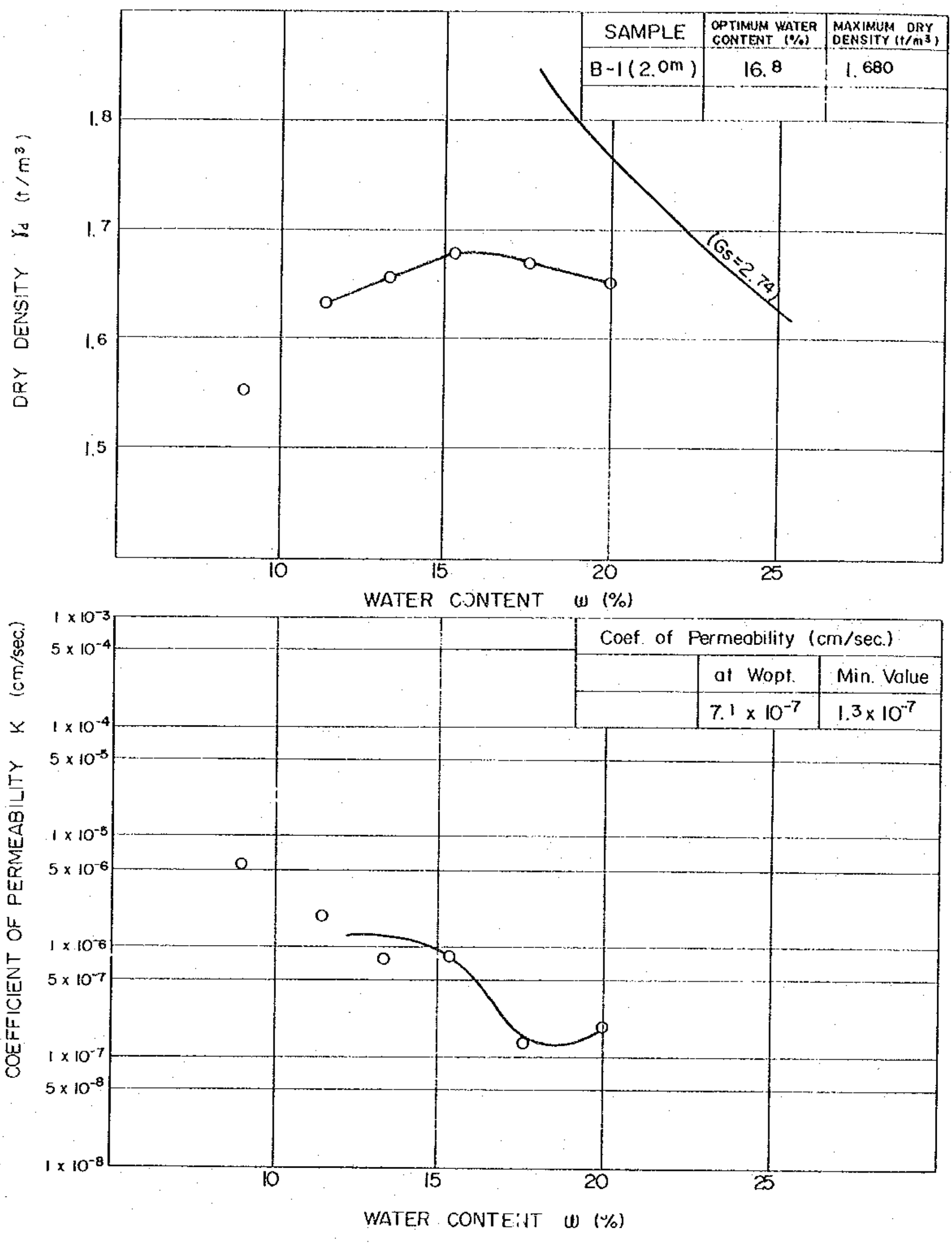

Sample B-1 2.00m

Fig.2-9 Compaction and Permeability Test

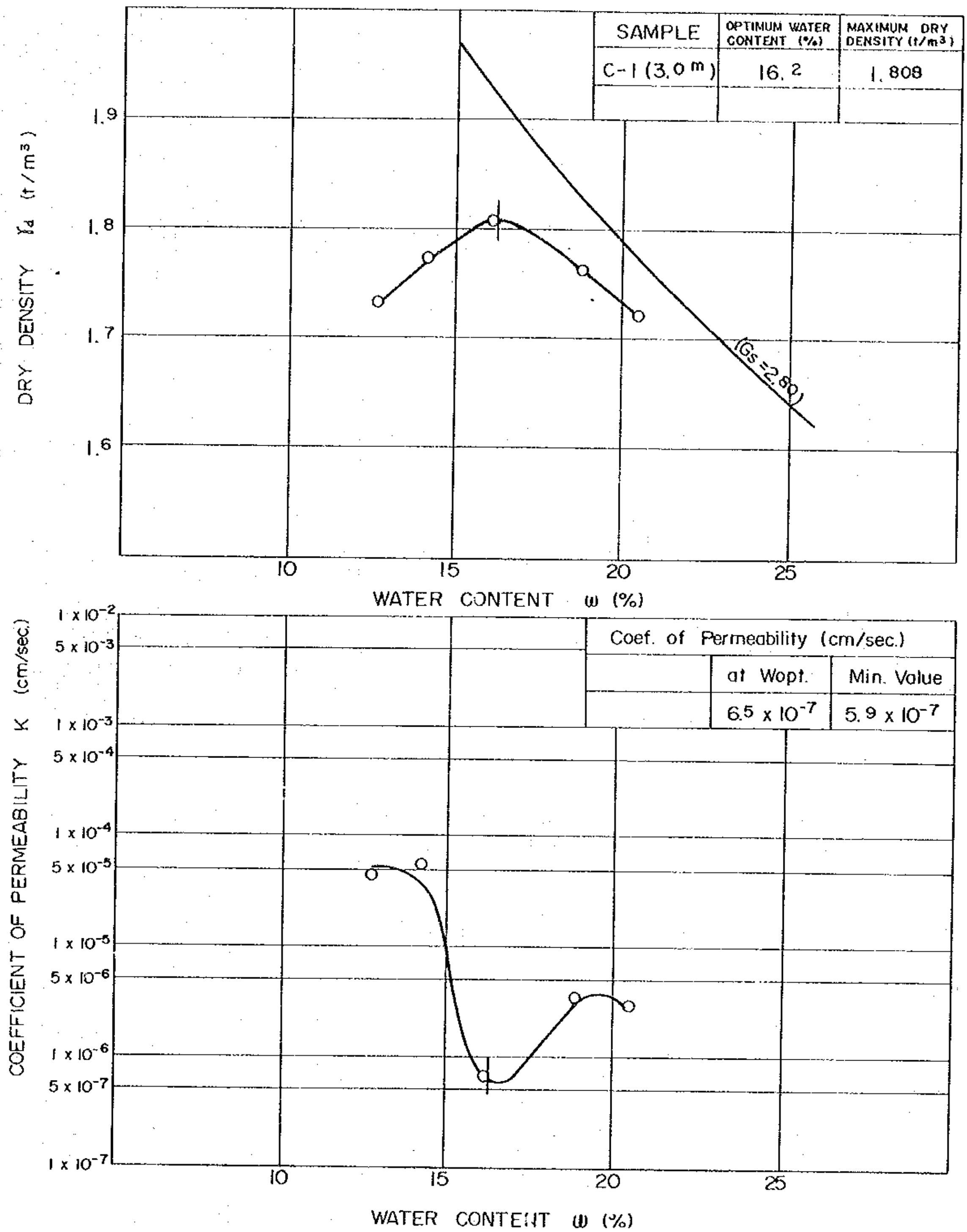

Sample C-1 3.00m

Fig.2-10 Compaction and Permeability Test

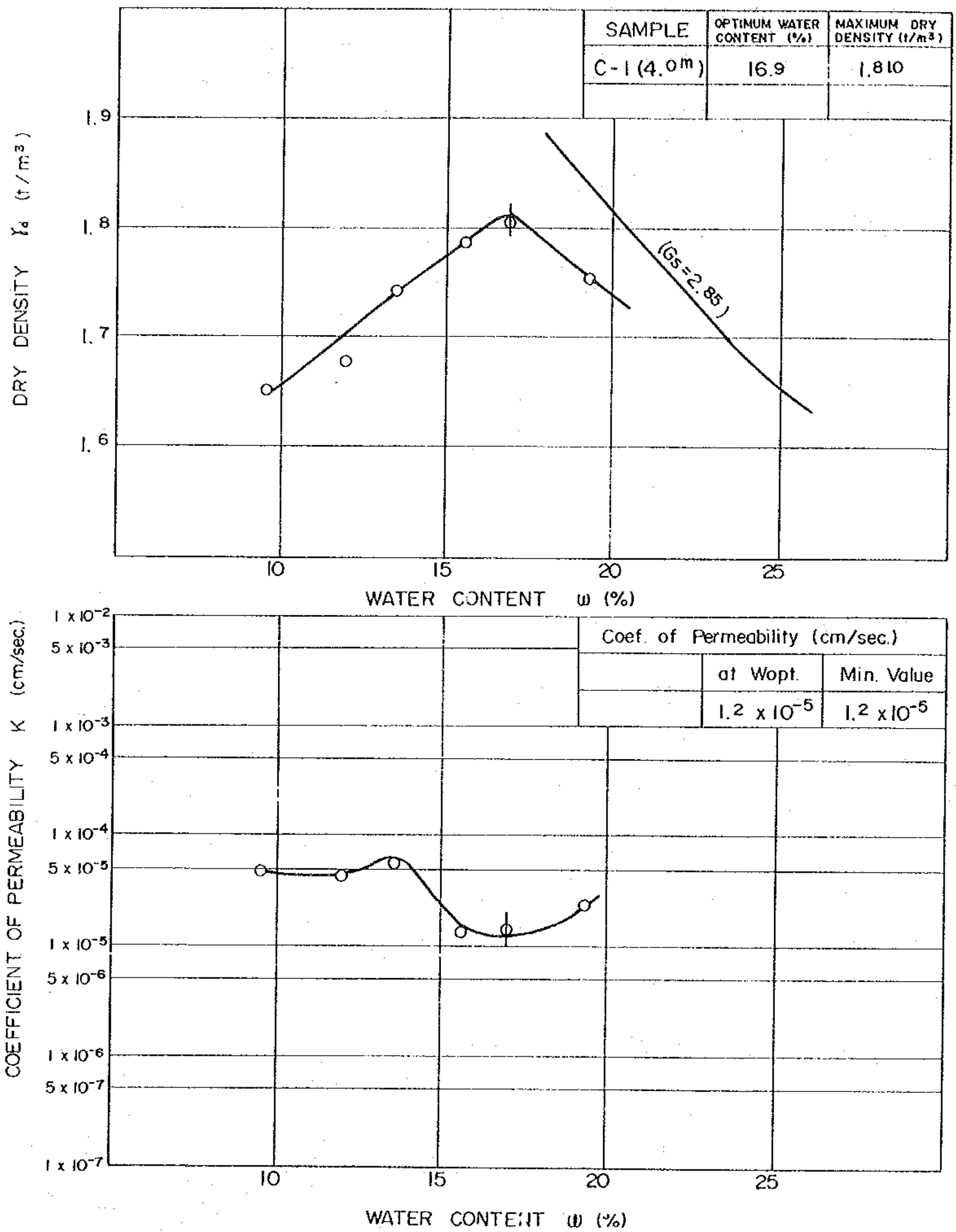

Sample C-1 4.00m

Fig.2-11 Compaction and Permeability Test

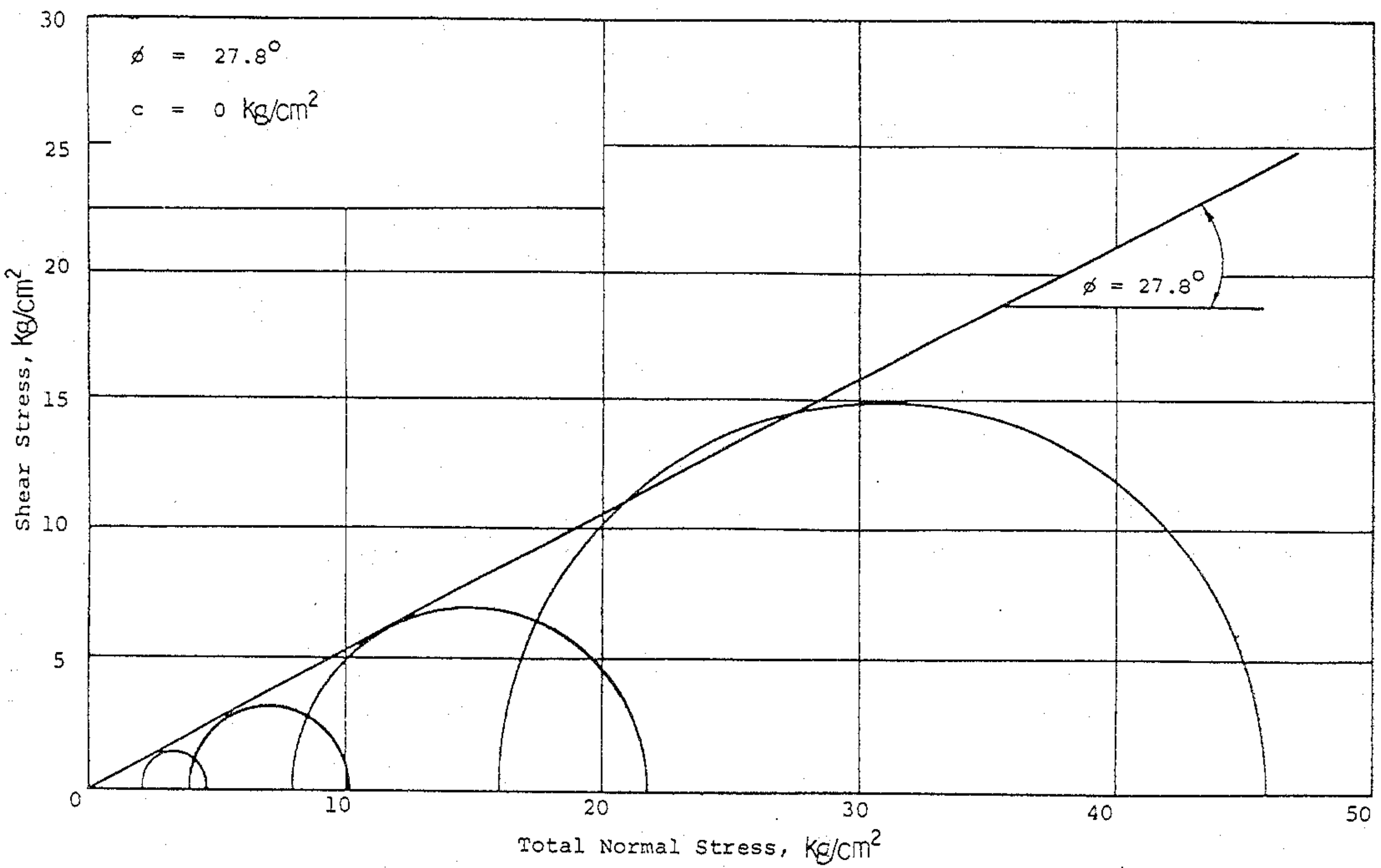

Fig. 3-1 Mohr Envelope in Terms of Total Stresses for $\overline{CU}$ Triaxial Tests on Compacted Samples No. A-1, Depth 1.00 m.

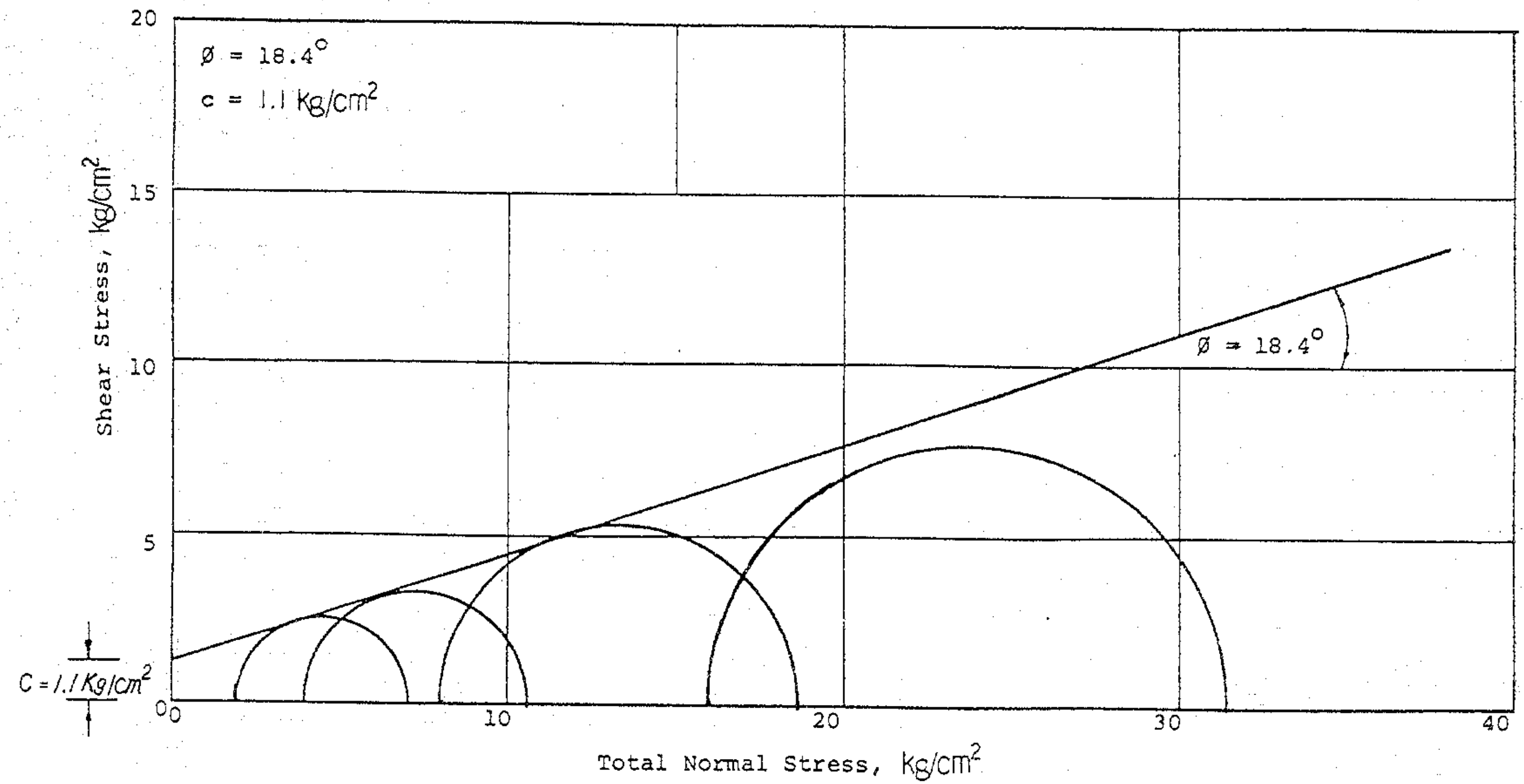

Fig. 3-2 Mohr Envelope in Teams of Total Stresses for $\overline{C}\overline{U}$ Triaxial Tests on Compacted Sample No. A-2, Depth 3.00 m.

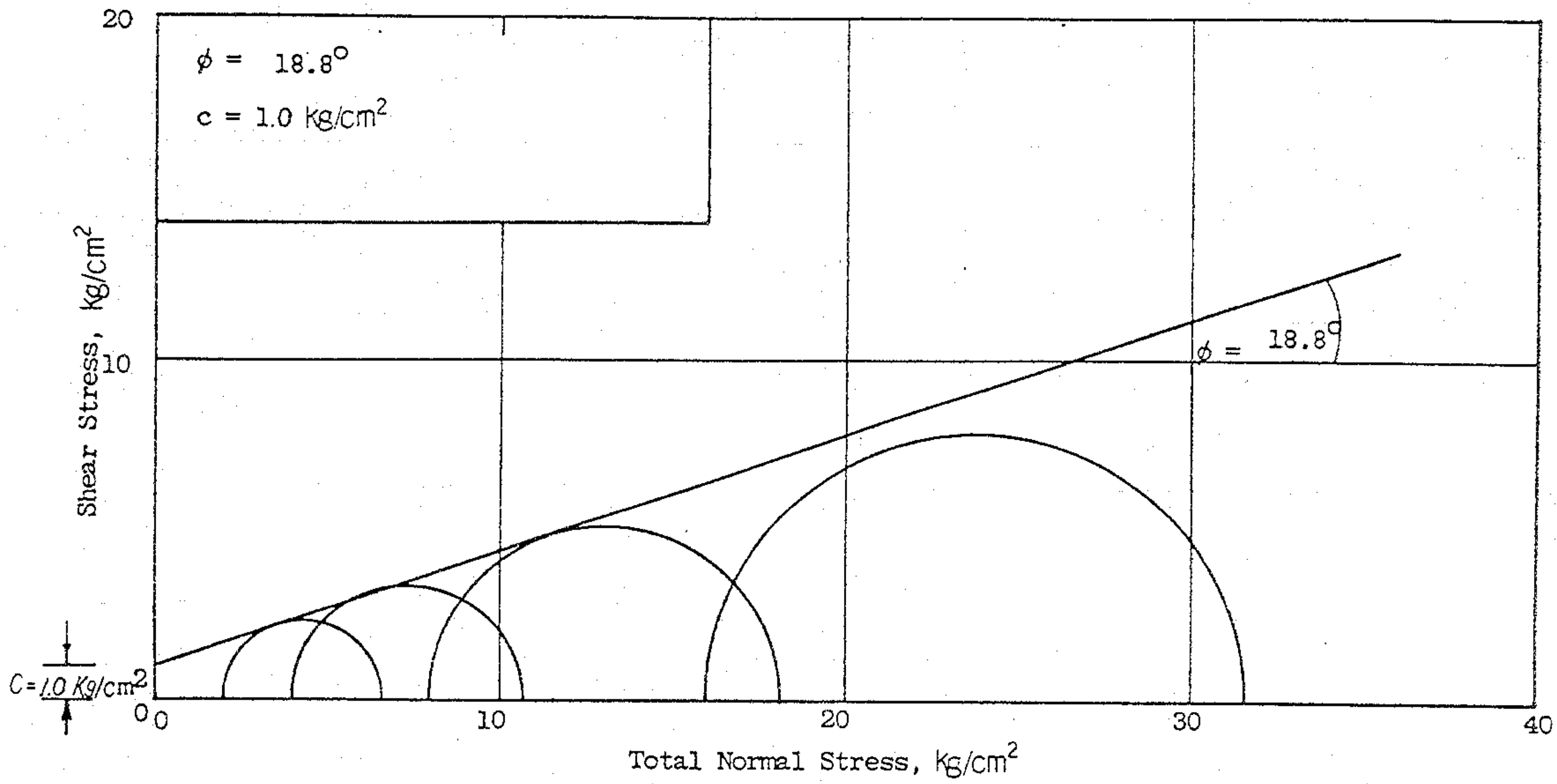

Fig. 3-3 Mohr Envelope in Terms of Total Stresses for $\overline{CU}$ Triaxial Tests on Sample No. A-2, Depth 5.00 m.

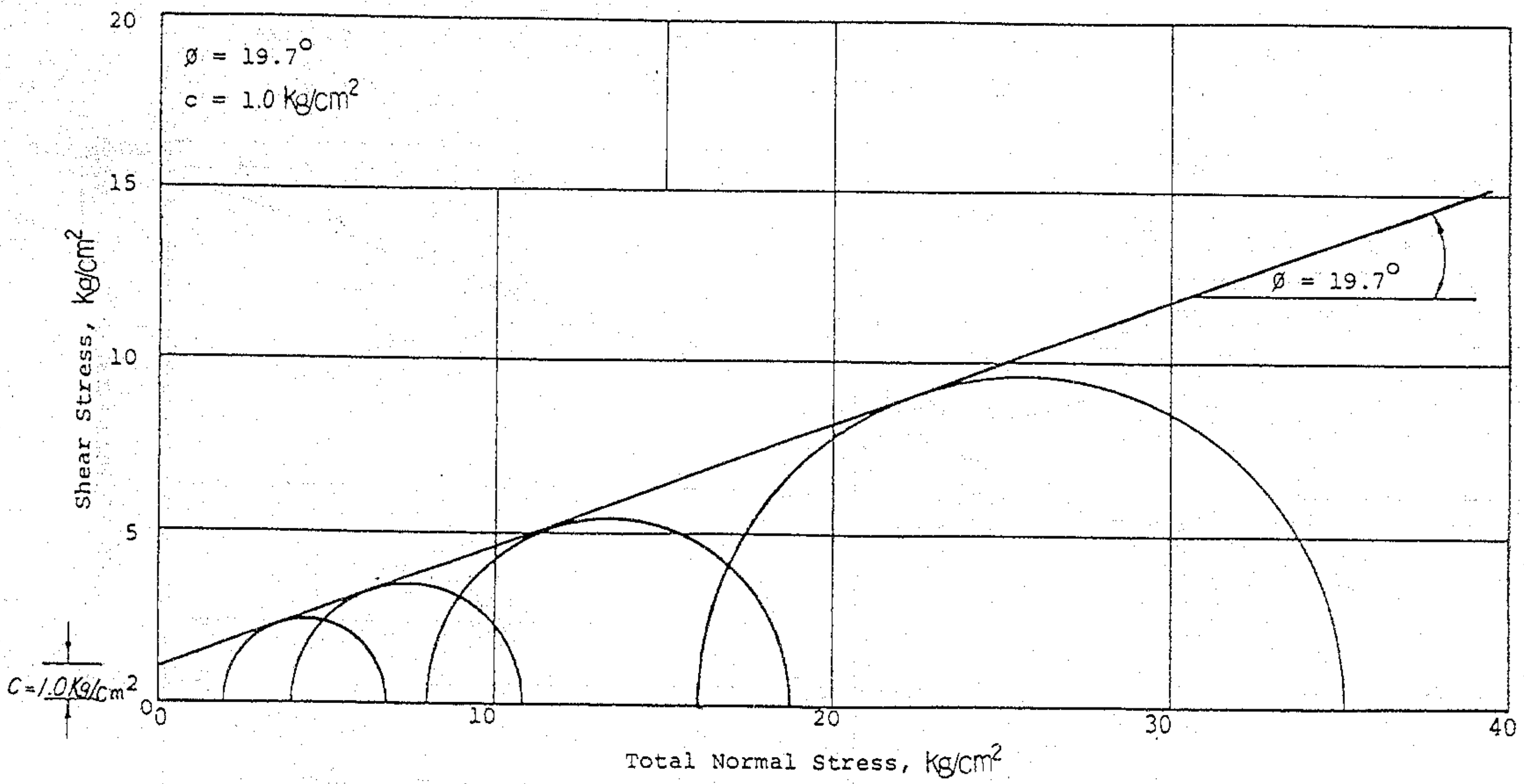

Fig.3-4 Mohr Envelope in Terms of Total Stresses for $\overline{CU}$ Triaxial Tests on Compacted Sample No. A-3, Depth 2.00 m.

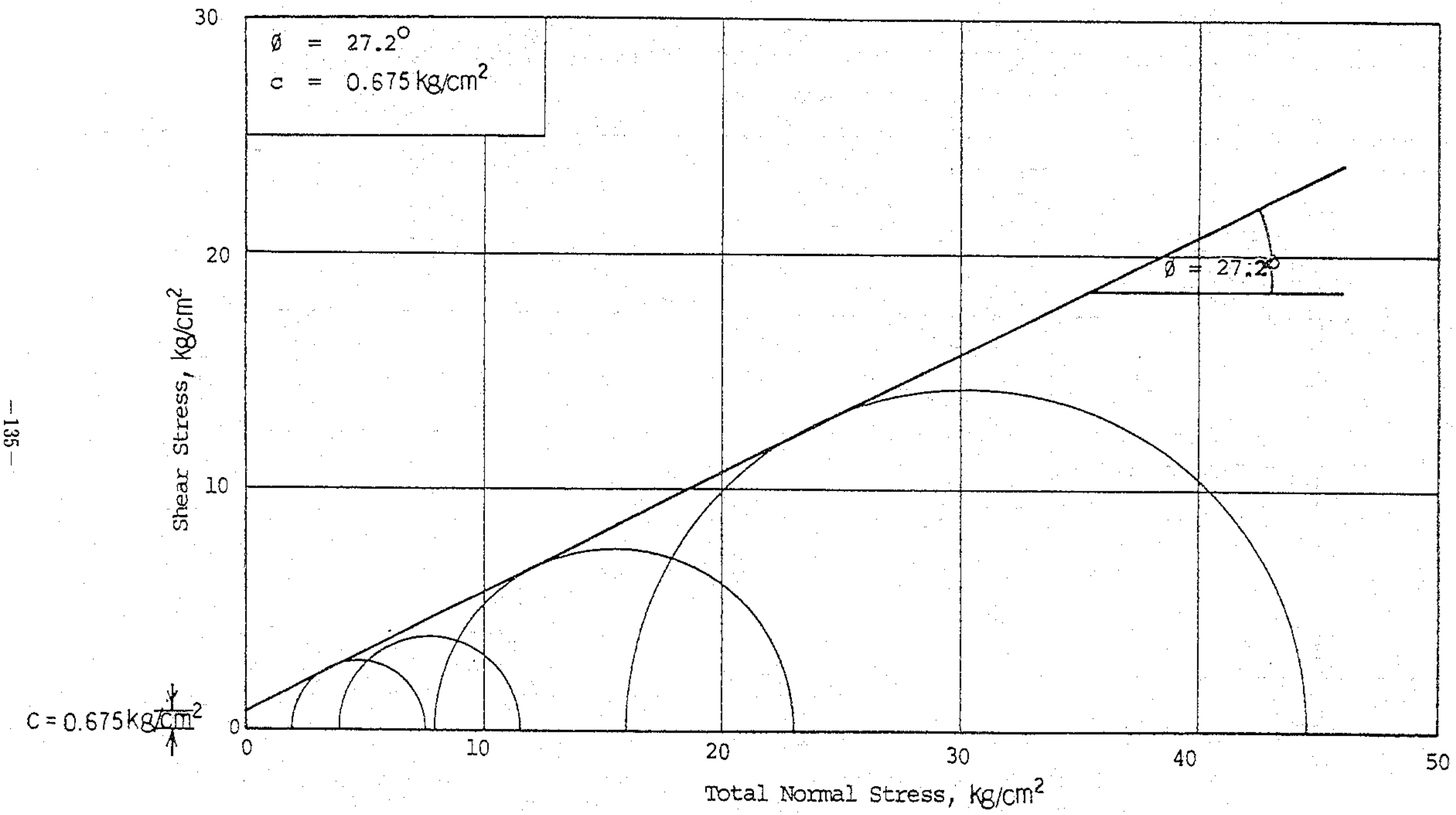

Fig. 3-5 Mohr Envelope in Terms of Total Stresses for $\overline{CU}$ Triaxial Tests on Sample No. A-5, Depth 2.00 m.

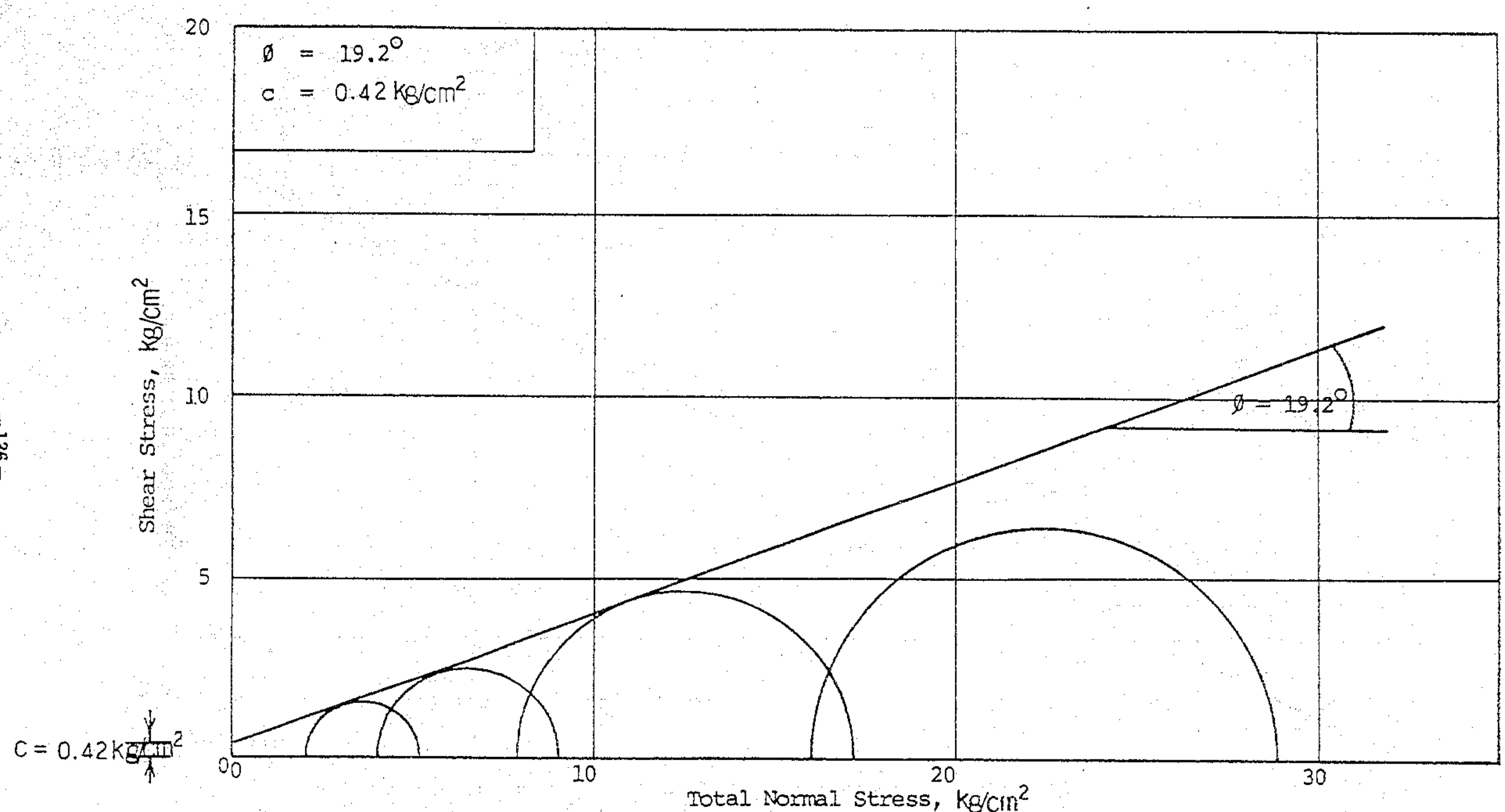

Fig. 3-6 Mohr Envelope in Terms of Total Stresses for $\overline{CU}$ Triaxial Tests on Compacted Sample No. B-1, Depth 2.00 m.

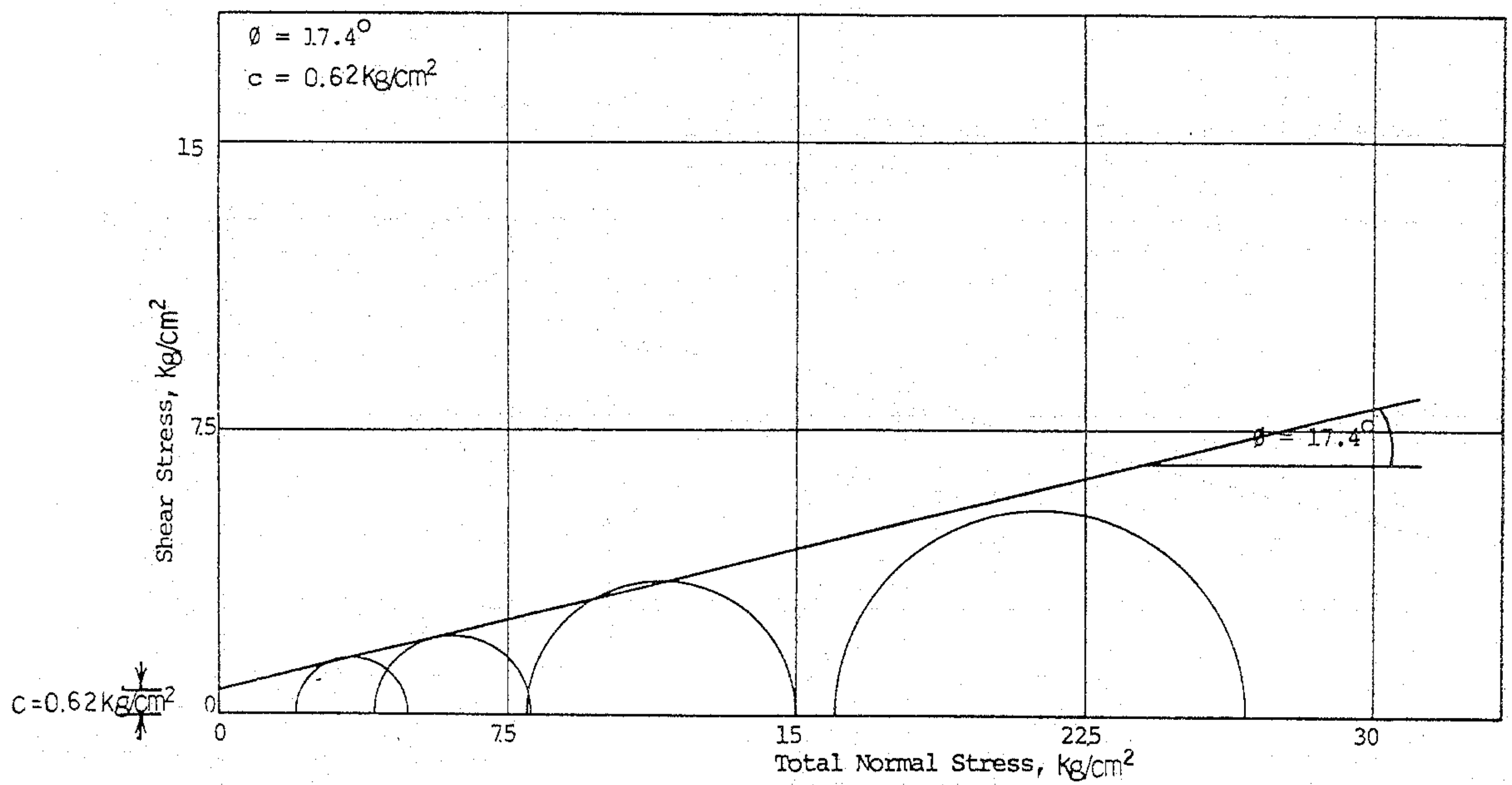

Fig. 3-7 Mohr Envelope in Terms of Total Stresses for $\overline{CU}$ Triaxial Tests on Sample No. C-1, Depth 3.00 m.

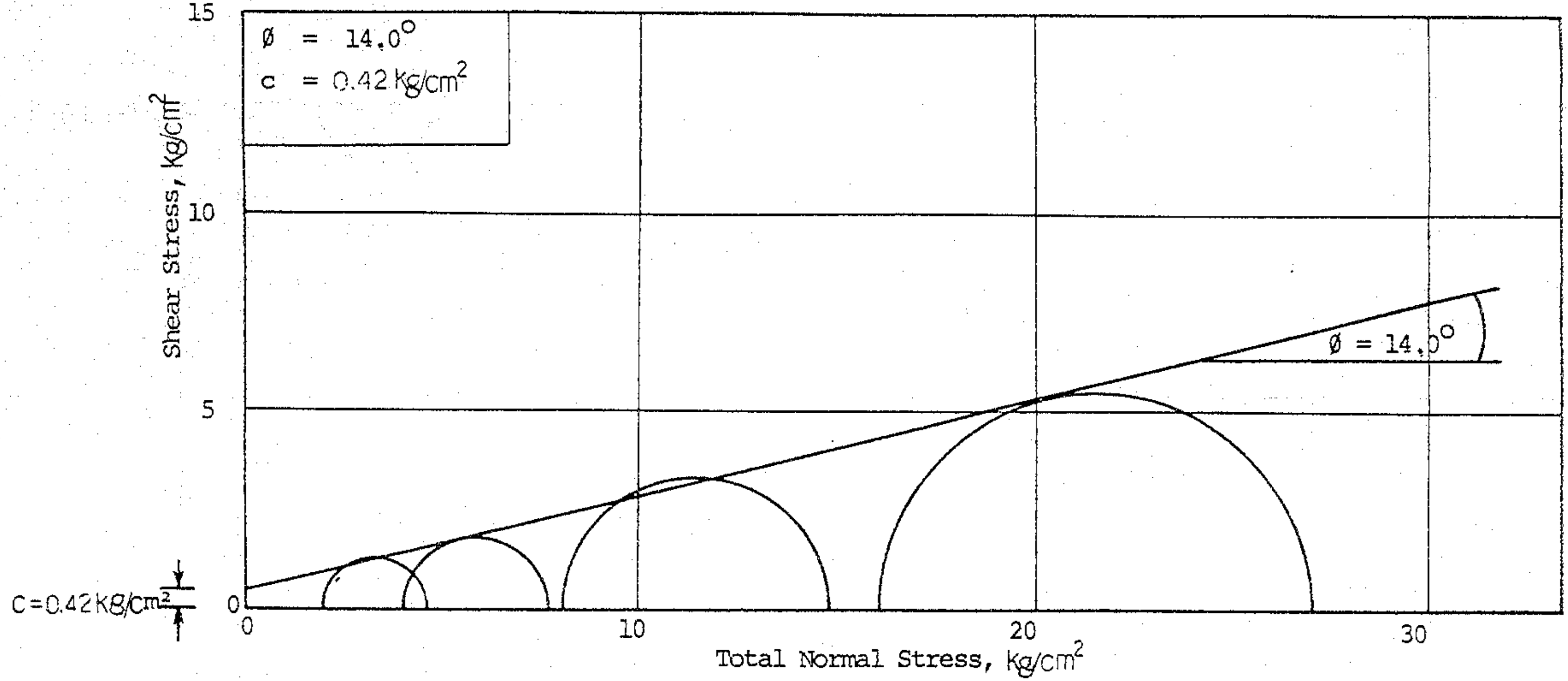

Fig. 3-8 Mohr Envelope in Terms of Total Stress for $\overline{CU}$ Triaxial Tests on Compacted Sample No. C-1, Depth 4.00 m.

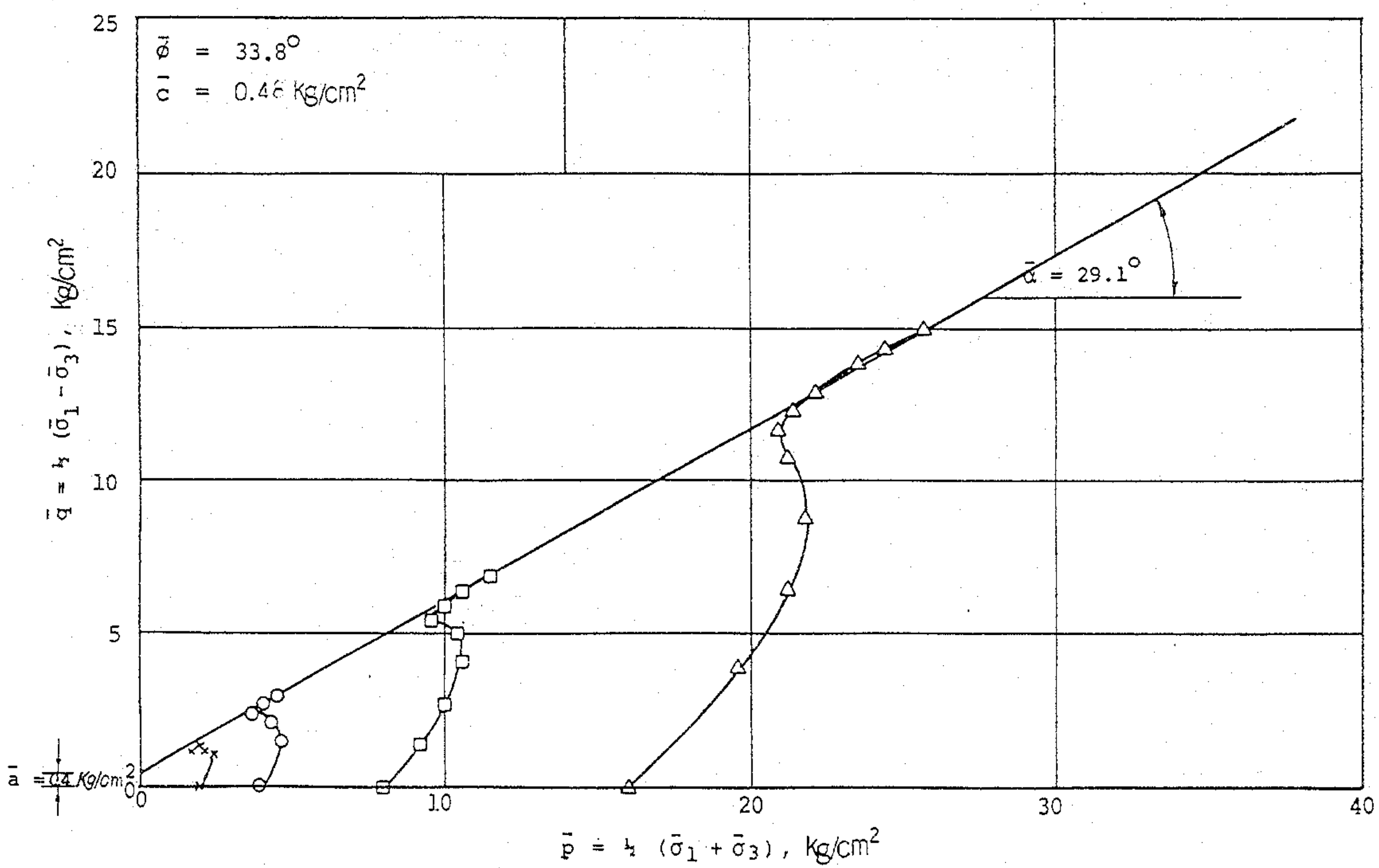

Fig. 4-1 Effective Stress Paths and Strength Envelope for $\overline{CU}$ Triaxial Tests on Compacted Sample No. A-1, Depth 1.00 m.

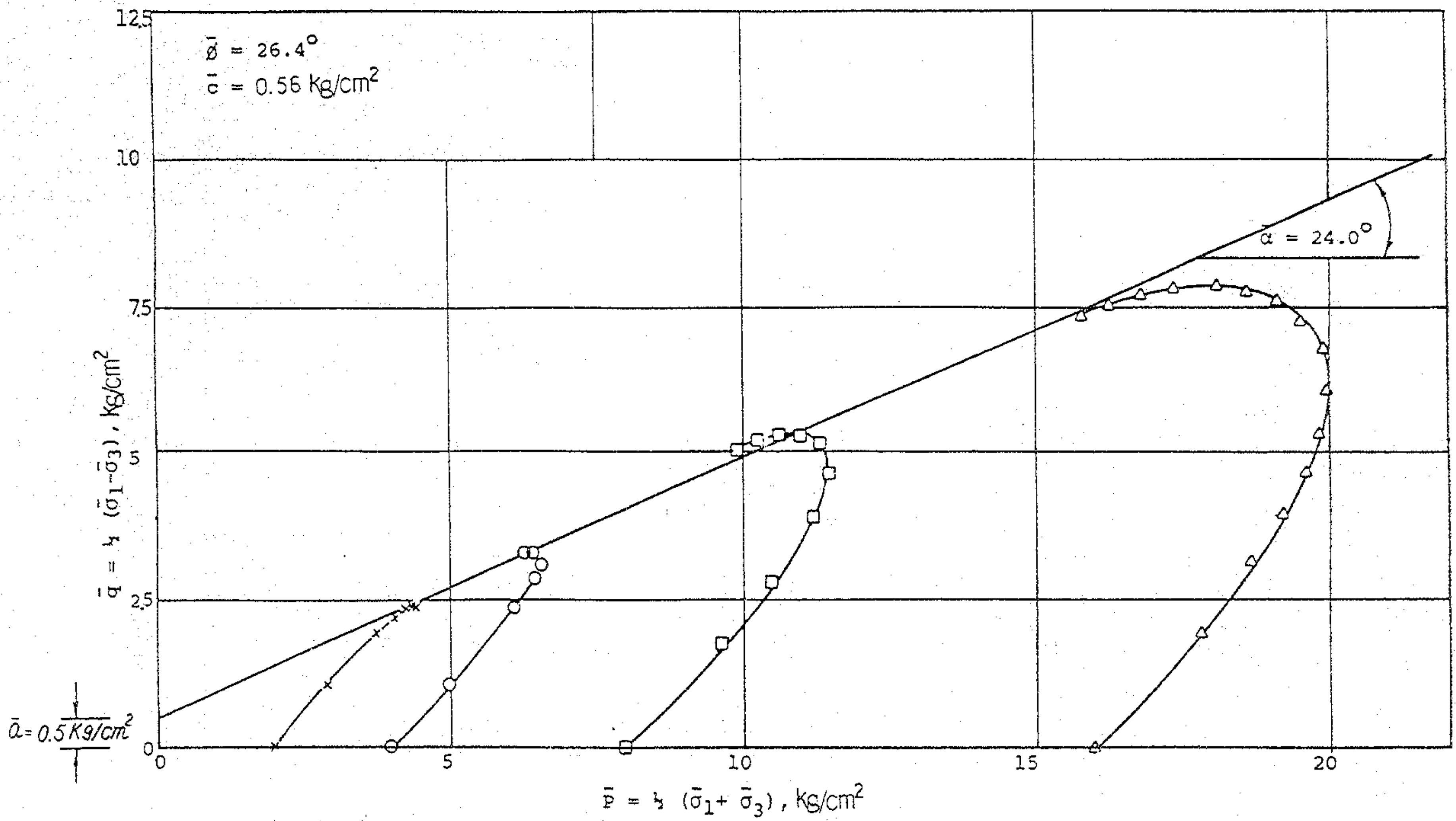

Fig. 4-2 Effective Stress Paths and Strength Envelope for $\overline{CU}$ Triaxial Tests on Compacted Sample No. A-2, Depth 3.00 m.

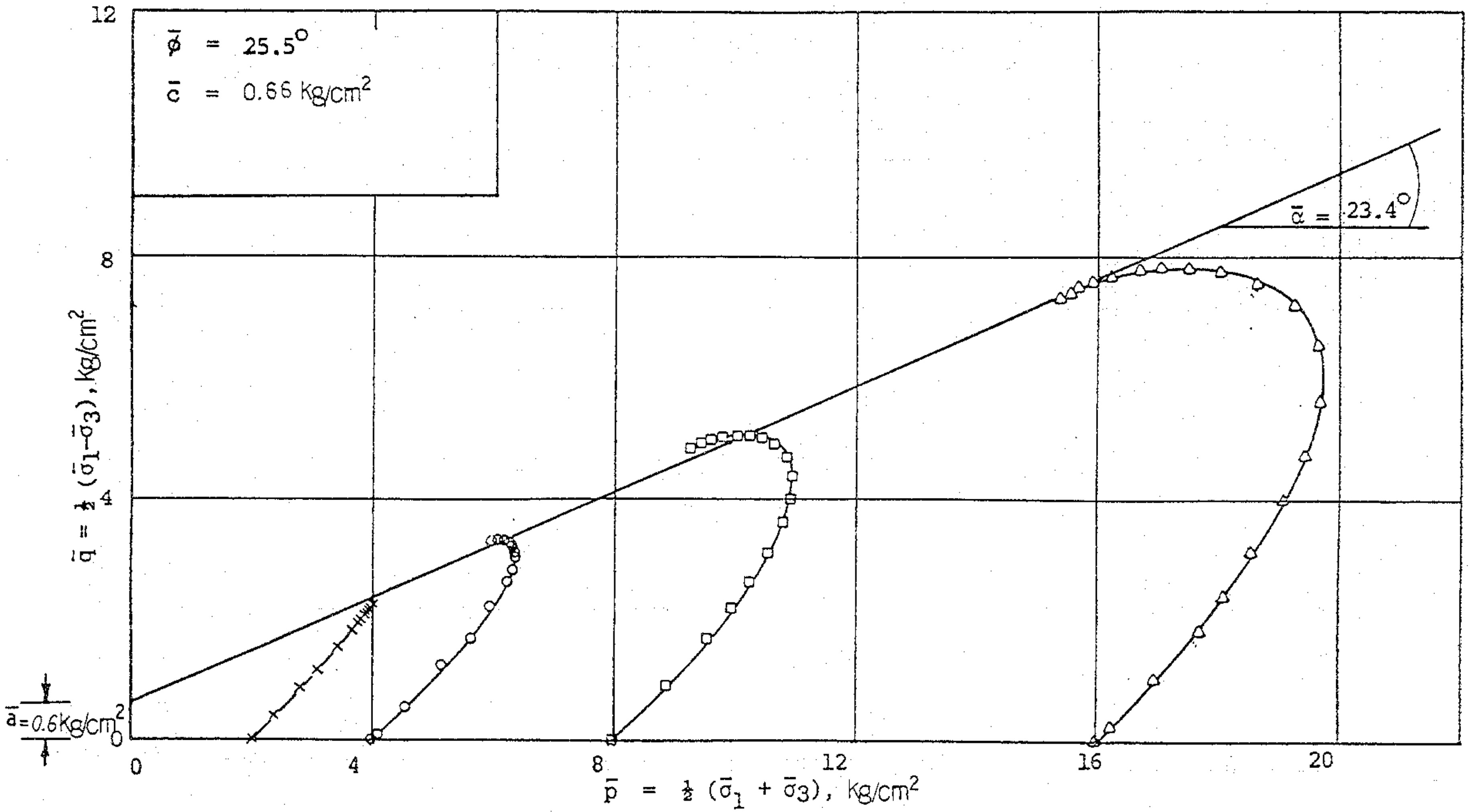

Fig. 4-3 Effective Stress Paths and Strength Envelope for $\overline{CU}$ Triaxial Tests on Sample No. A-2, Depth 5.00 m.

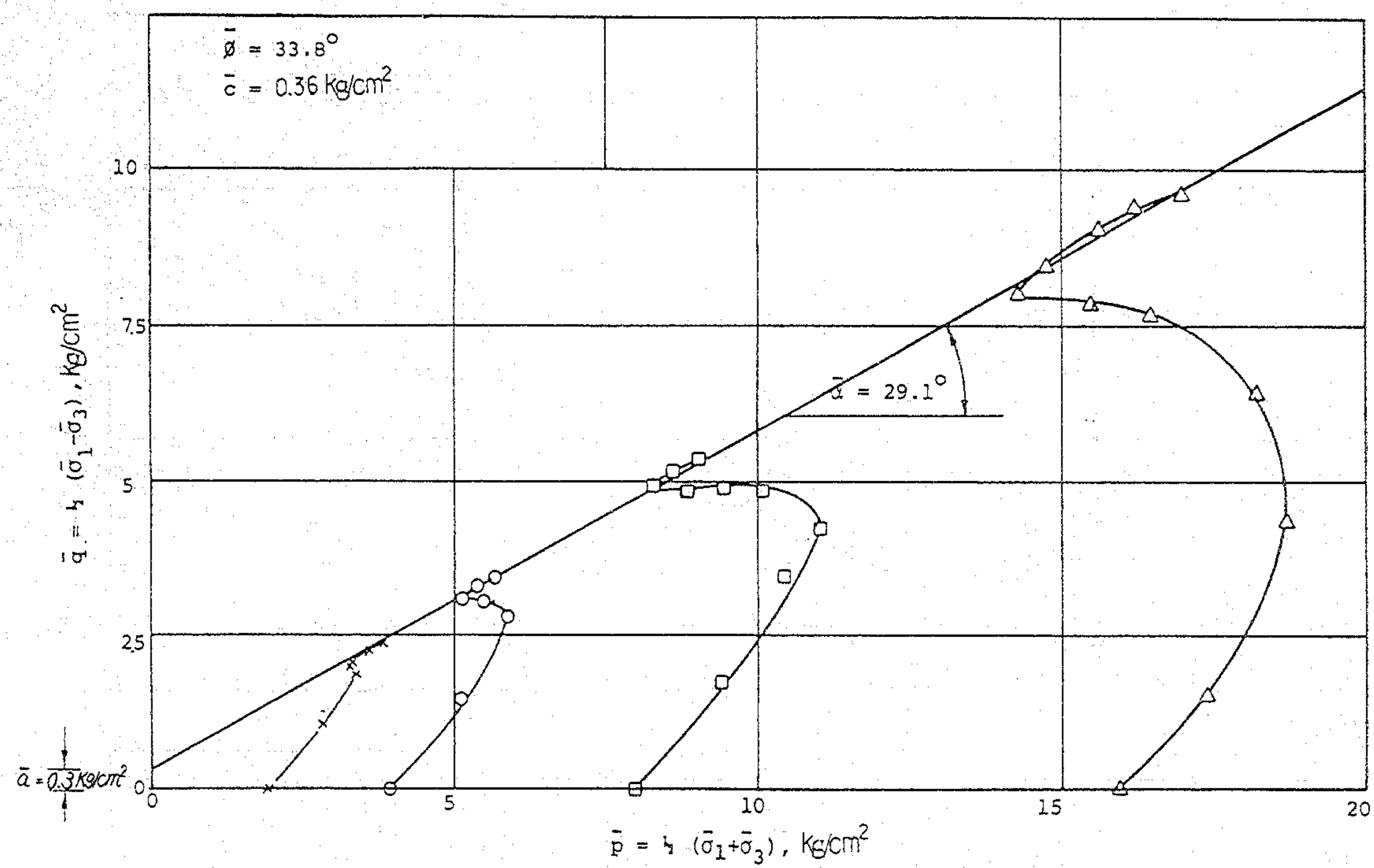

Fig. 4-4 Effective Stress Paths and Strength Envelope for $\overline{CU}$ Triaxial Tests on Compacted Sample No. A-3, Depth 2.00 m.

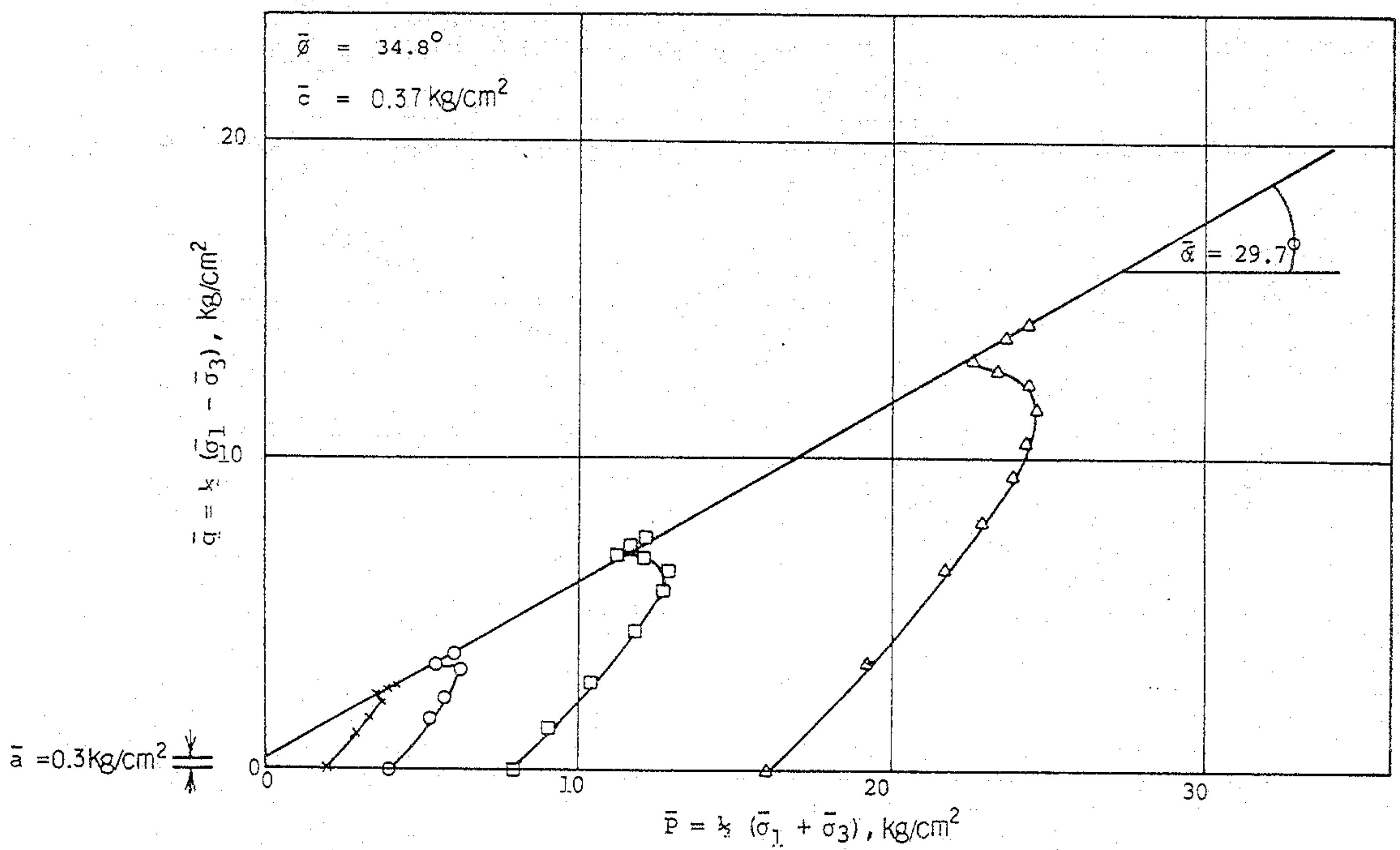

Fig. 4 - 5 Effective Stress Paths and Strength Envelope for $\overline{CU}$ Triaxial Tests on Sample No. A-5, Depth 2.00 m.

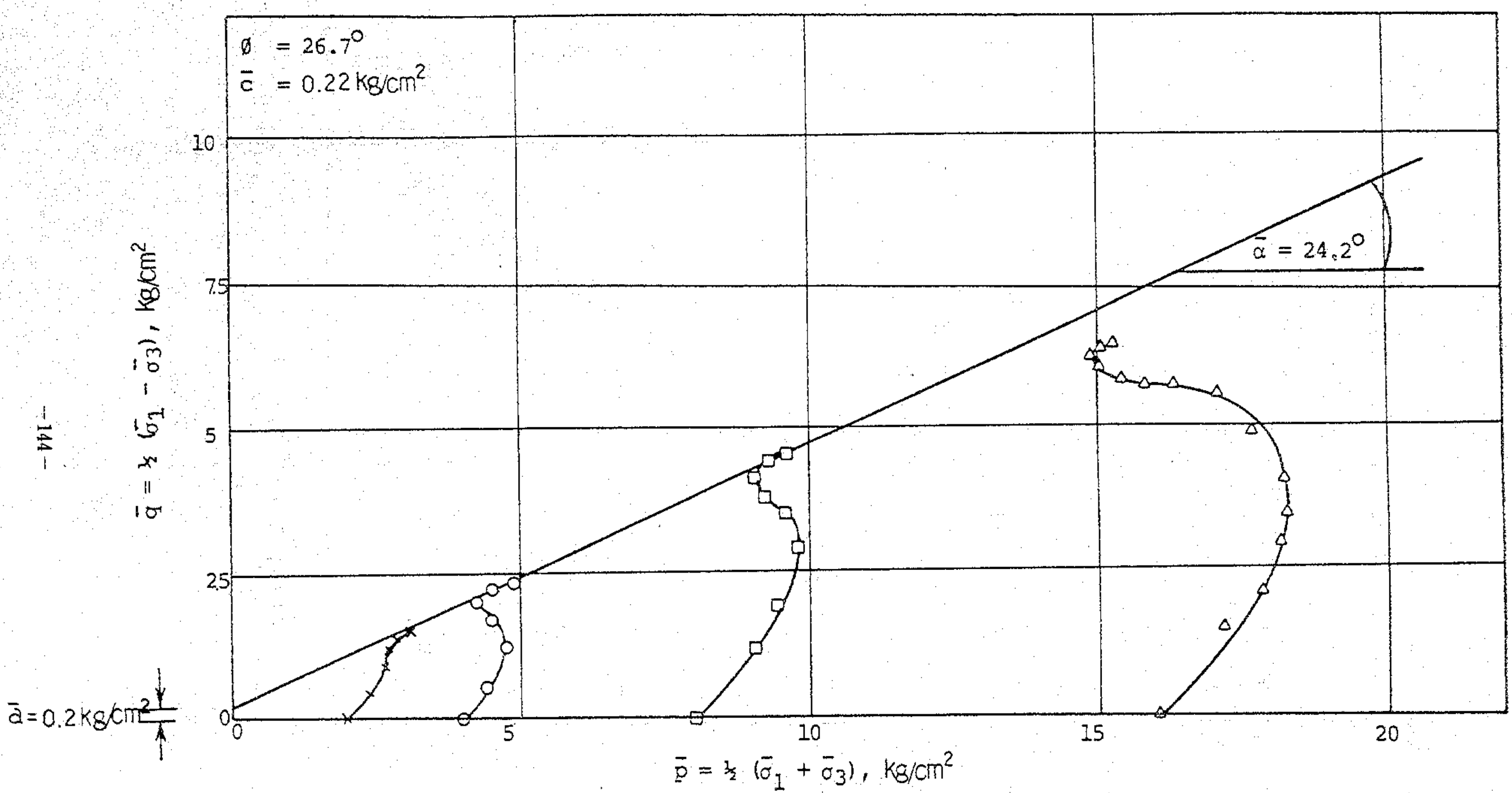

Fig. 4-6 Effective Stress Paths and Strength Envelope for $\overline{CU}$ Triaxial Tests on Compacted Sample No. B-1, Depth 2.00 m.

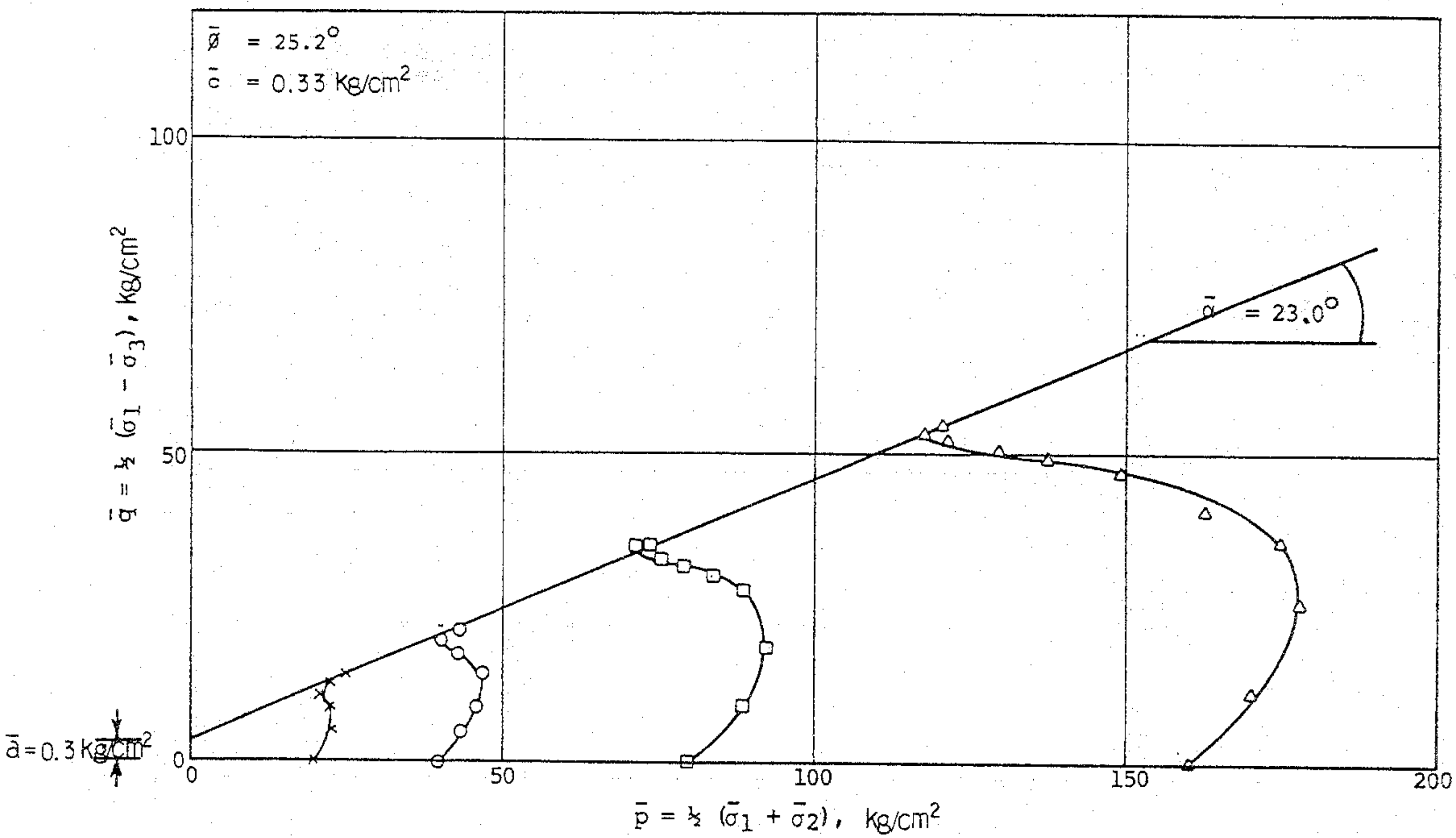

Fig. 4-7 Effective Stress Paths and Strength Envelope for $\overline{CU}$ Triaxial Tests on Sample No. C-1, Depth 3.00 m.

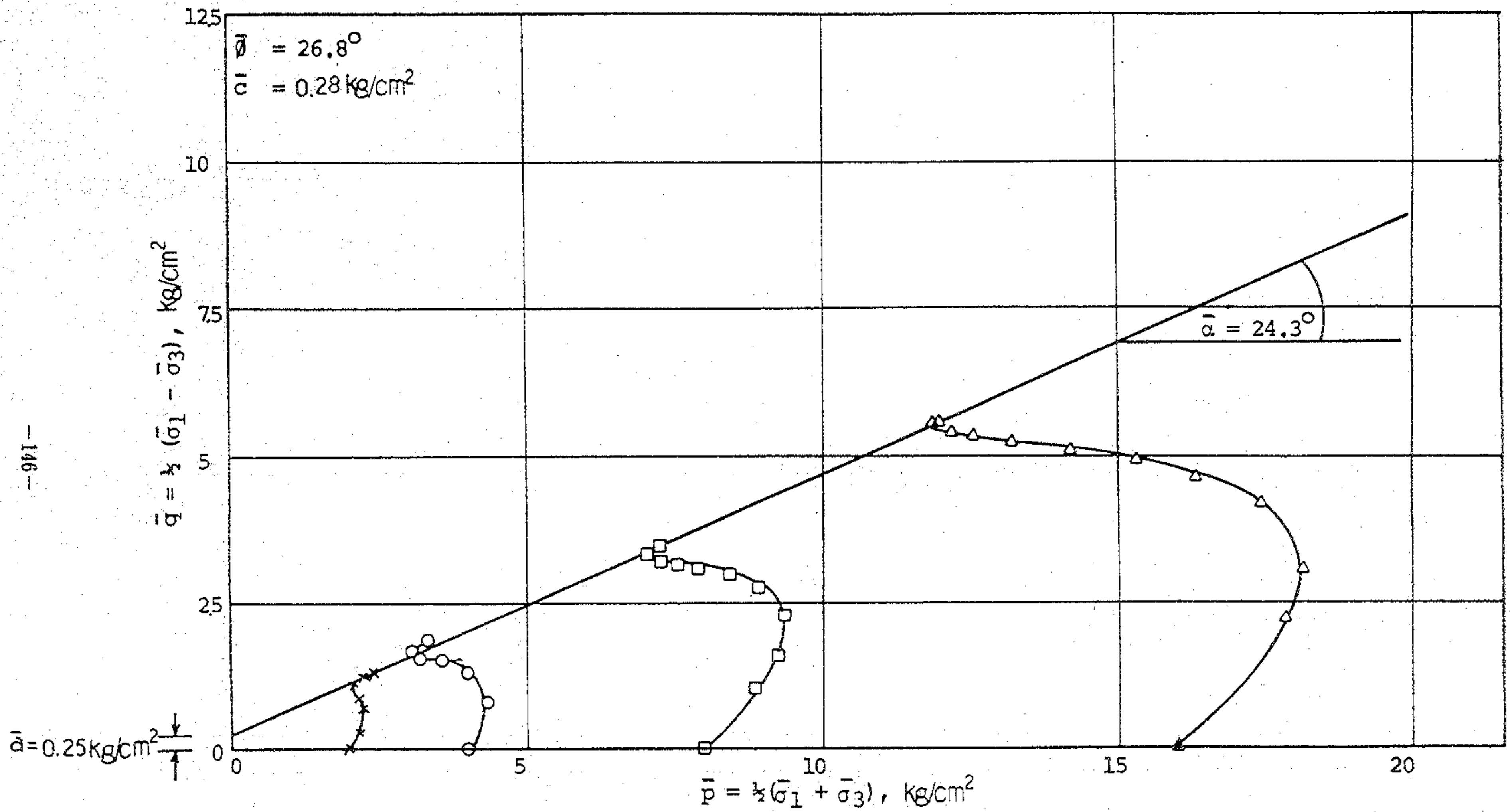

Fig. 4-8 Effective Stress Paths and Strength Envelope for $\overline{CU}$ Triaxial Tests on Compacted Sample No. C-1, Depth 4.00 m.

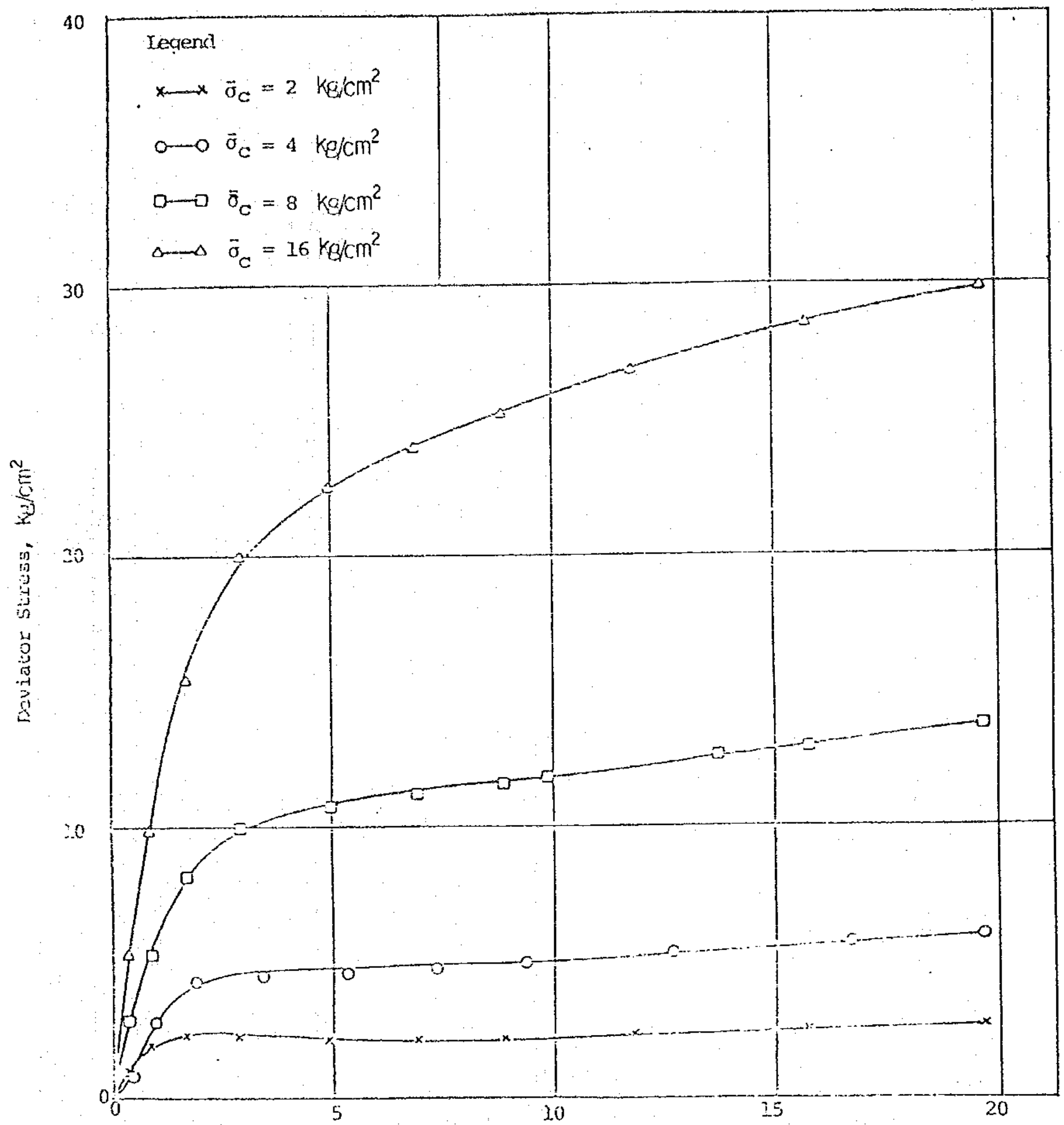

Fig.5-1 Deviator Stress vs Axial Strain for $\bar{CU}$ Triaxial Tests on Compacted Sample No. A-1, Depth 1.00 m.

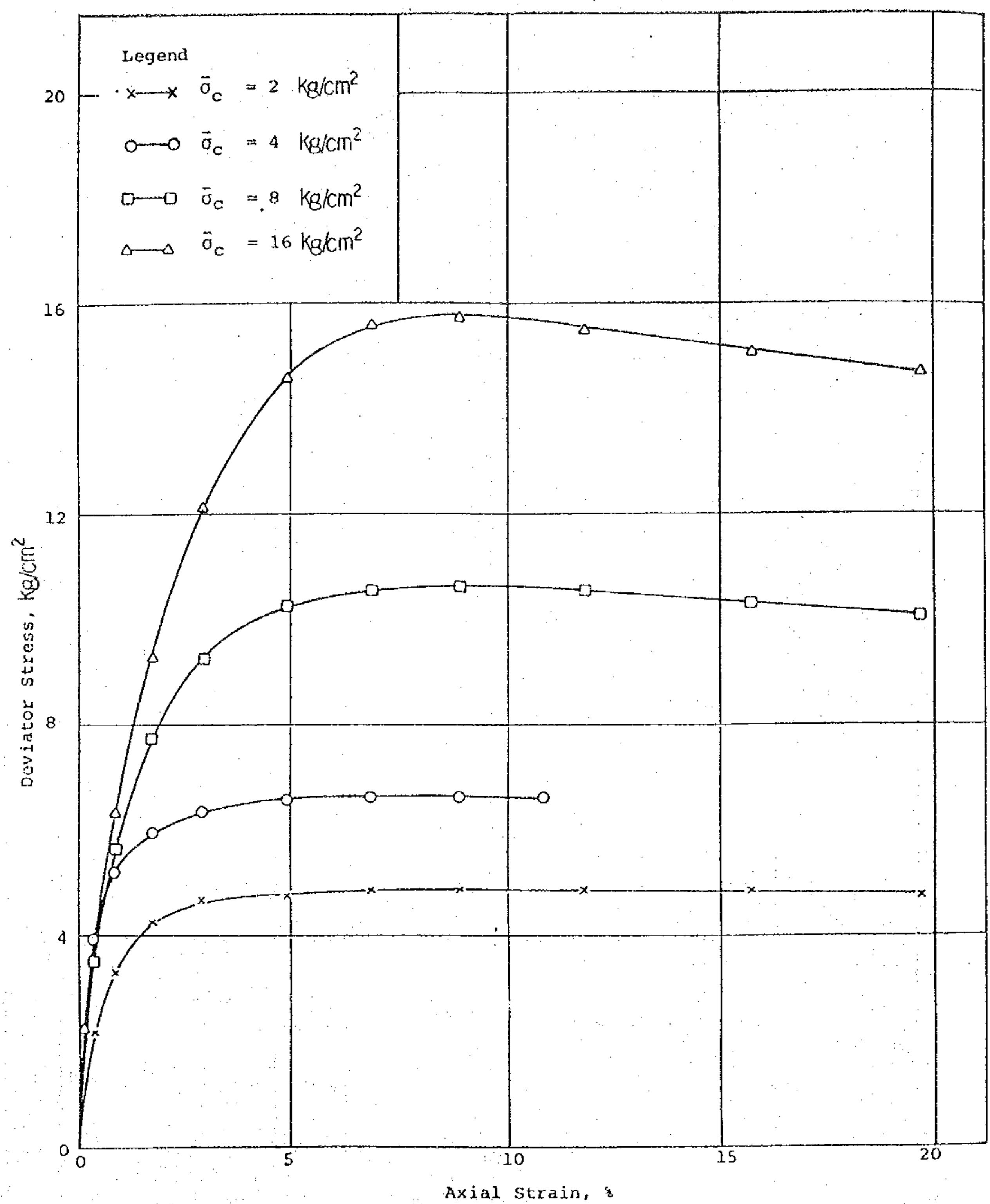

Fig.5-2 Deviator Stress vs Axial Strain for $\overline{CU}$ Triaxial Tests on Compacted Sample No. A-2, Depth 3.00 m.

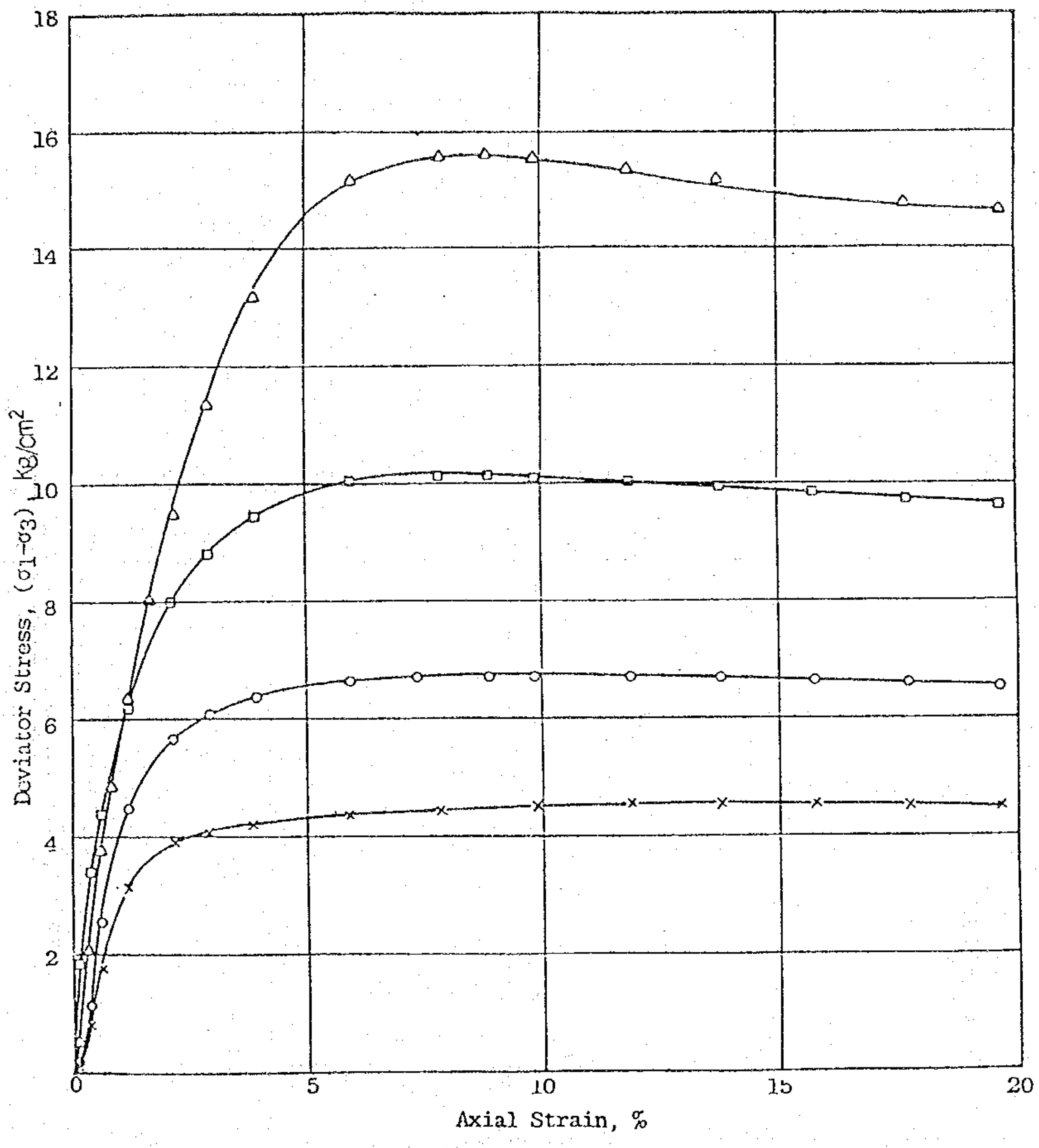

Fig. 5-3 Deviator Stress vs Axial Strain for $\overline{CU}$ Triaxial Tests on Compacted Sample No. A-2, Depth 5.00 m.

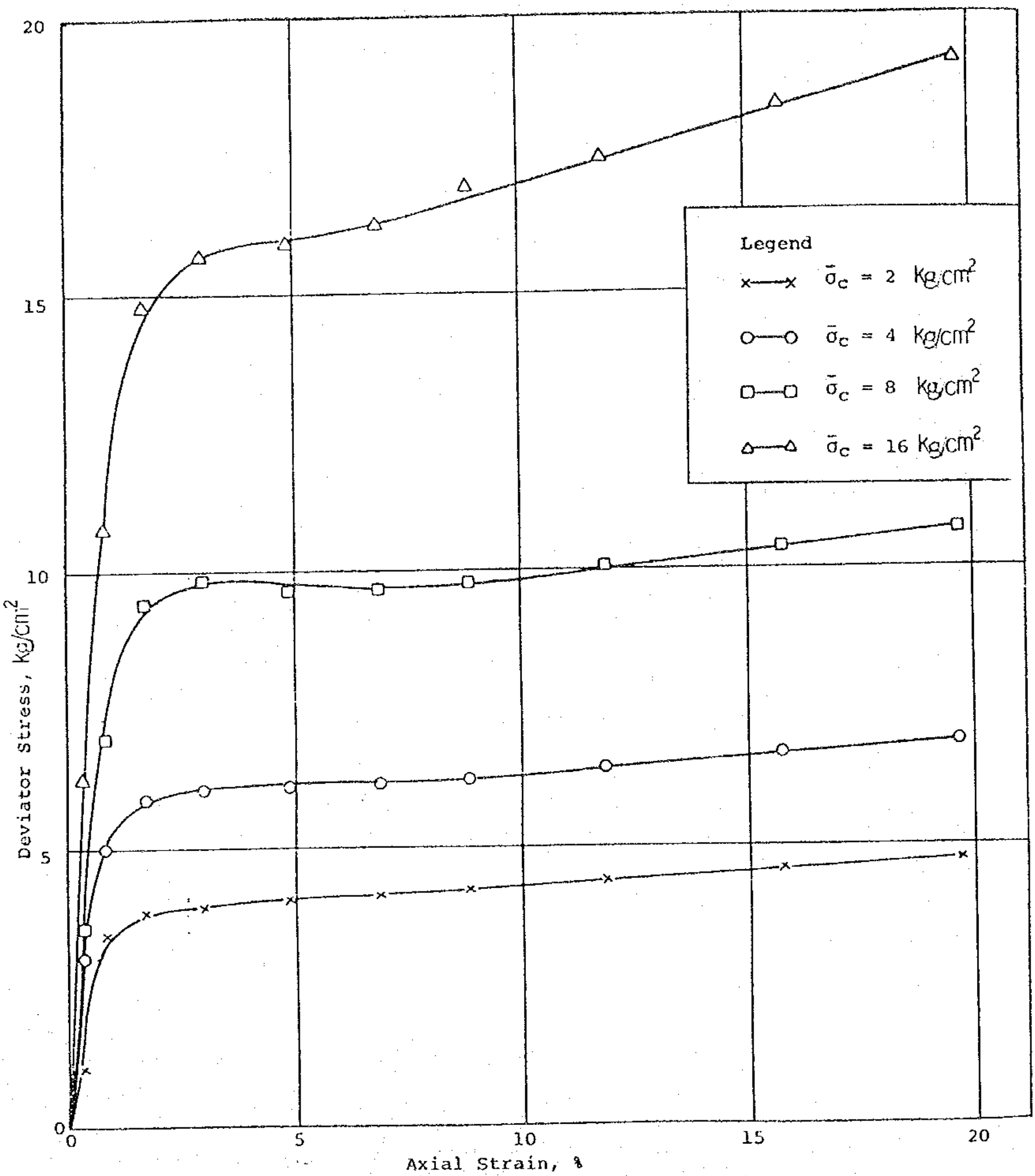

Fig.5-4 Deviator Stress VS Axial Strain for $\bar{C}\bar{U}$ Triaxial Tests on Compacted Sample No. A-3, Depth 2.00 m.

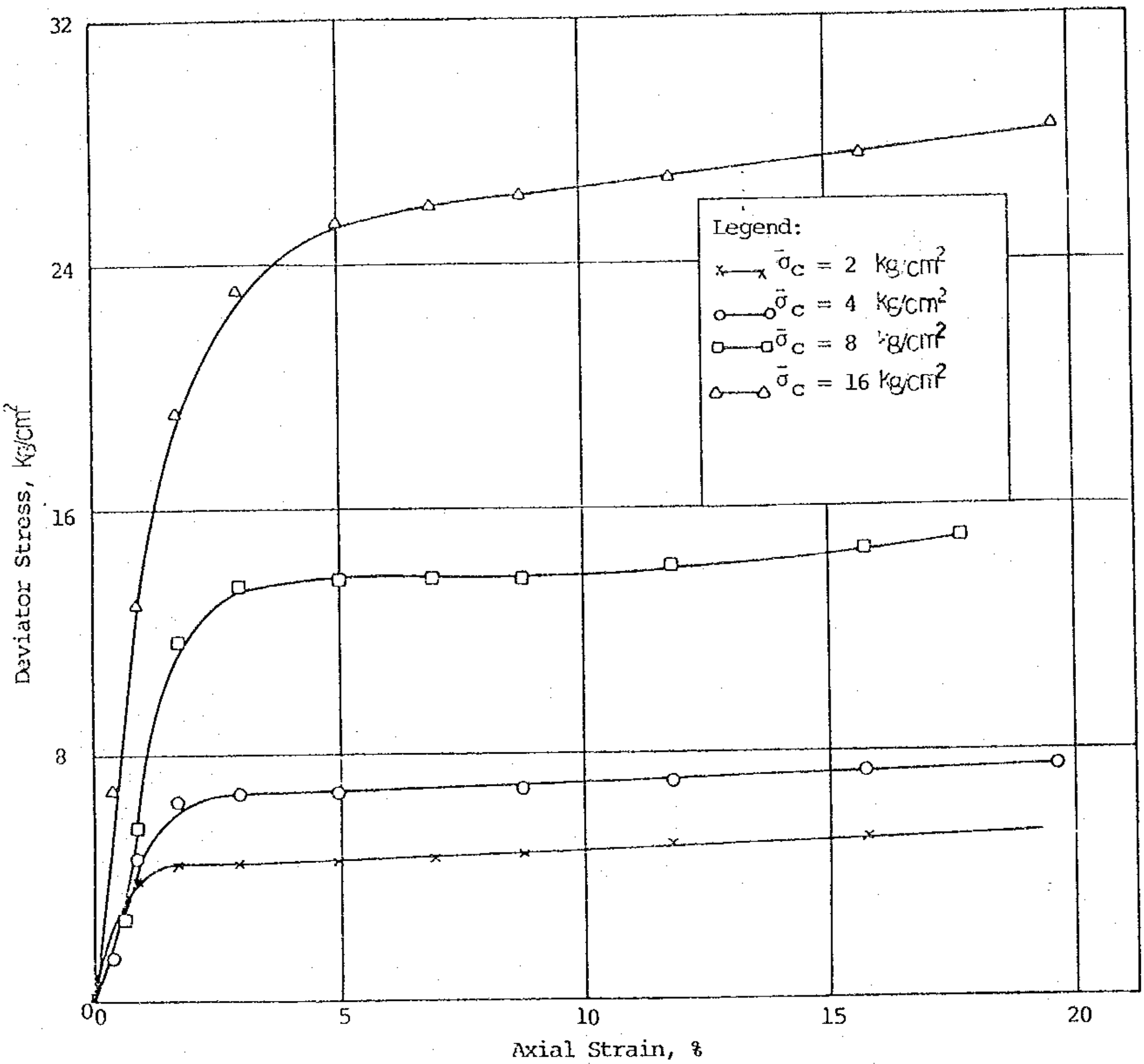

Fig. 5-5 Deviator Stress vs Axial Strain for $\overline{CU}$ Triaxial Tests on Sample No. A-5, Depth 2.00 m.

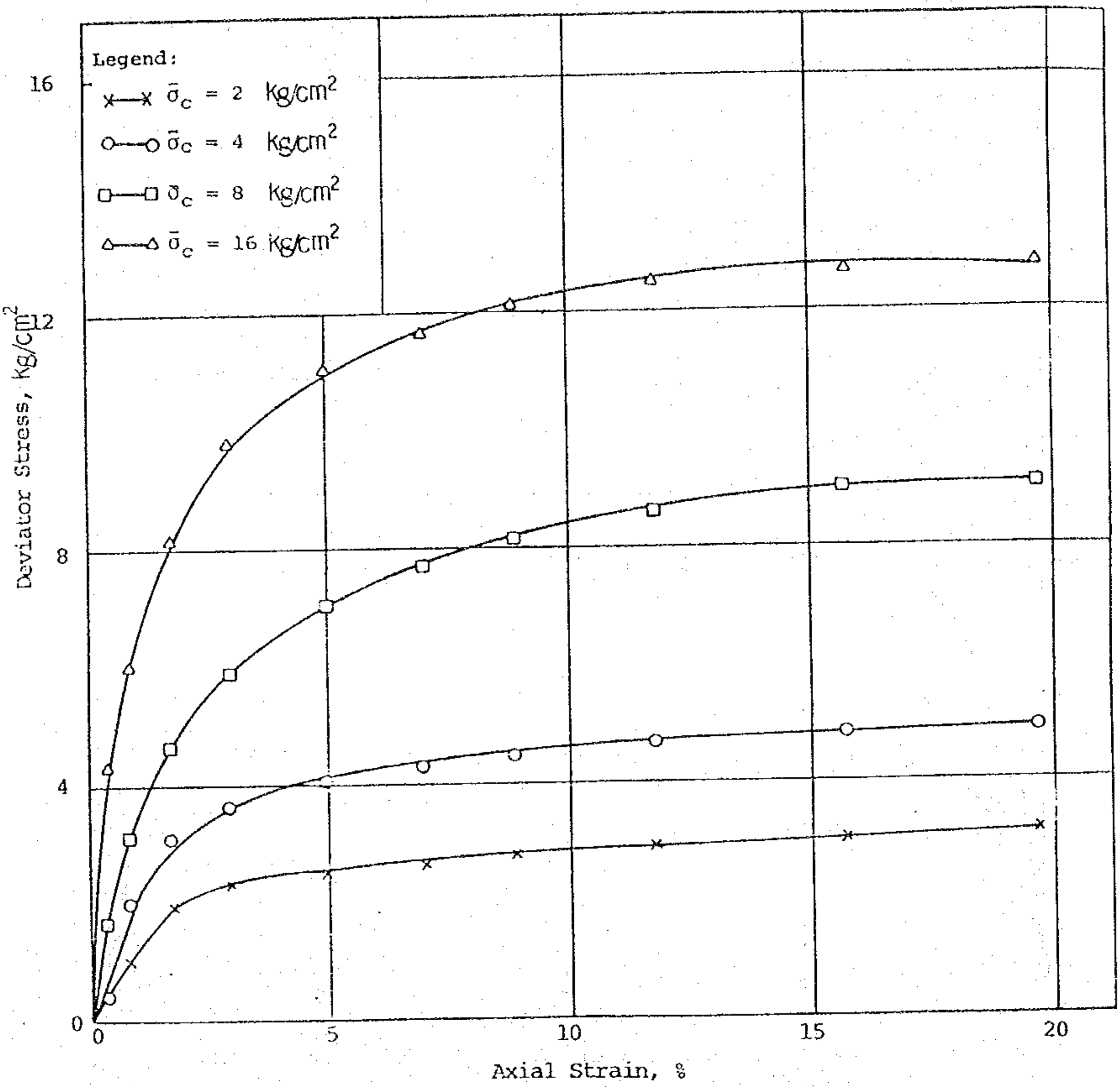

Fig. 5-6 Deviator Stress vs Axial Strain for $\overline{CU}$ Triaxial Tests on Compacted Sample No. B-1, Depth 2.00 m.

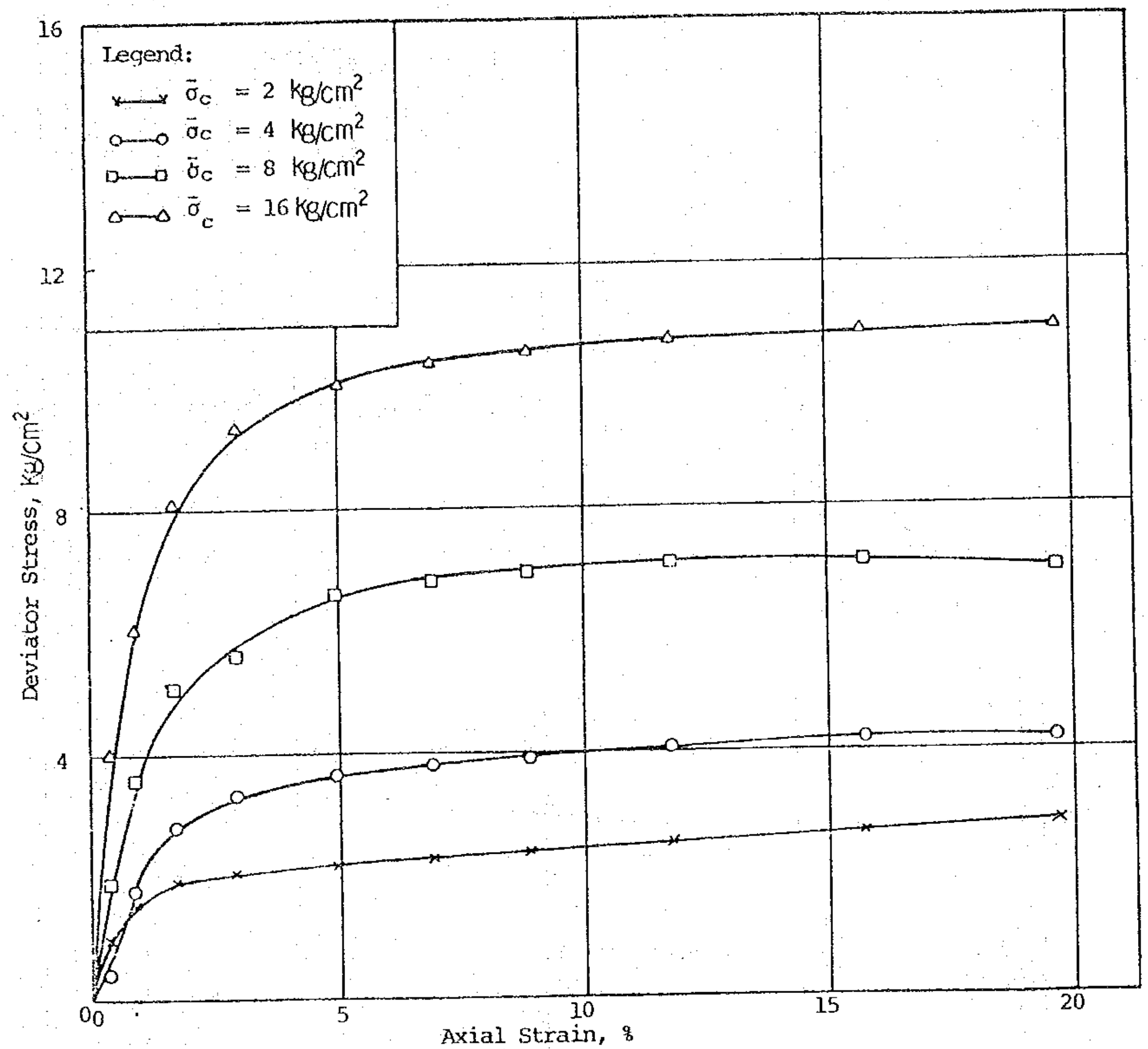

Fig. 5-7 Deviator Stress vs Axial Strain for $\overline{CU}$ Triaxial Tests on Sample No. C-1, Depth 3.00 m.

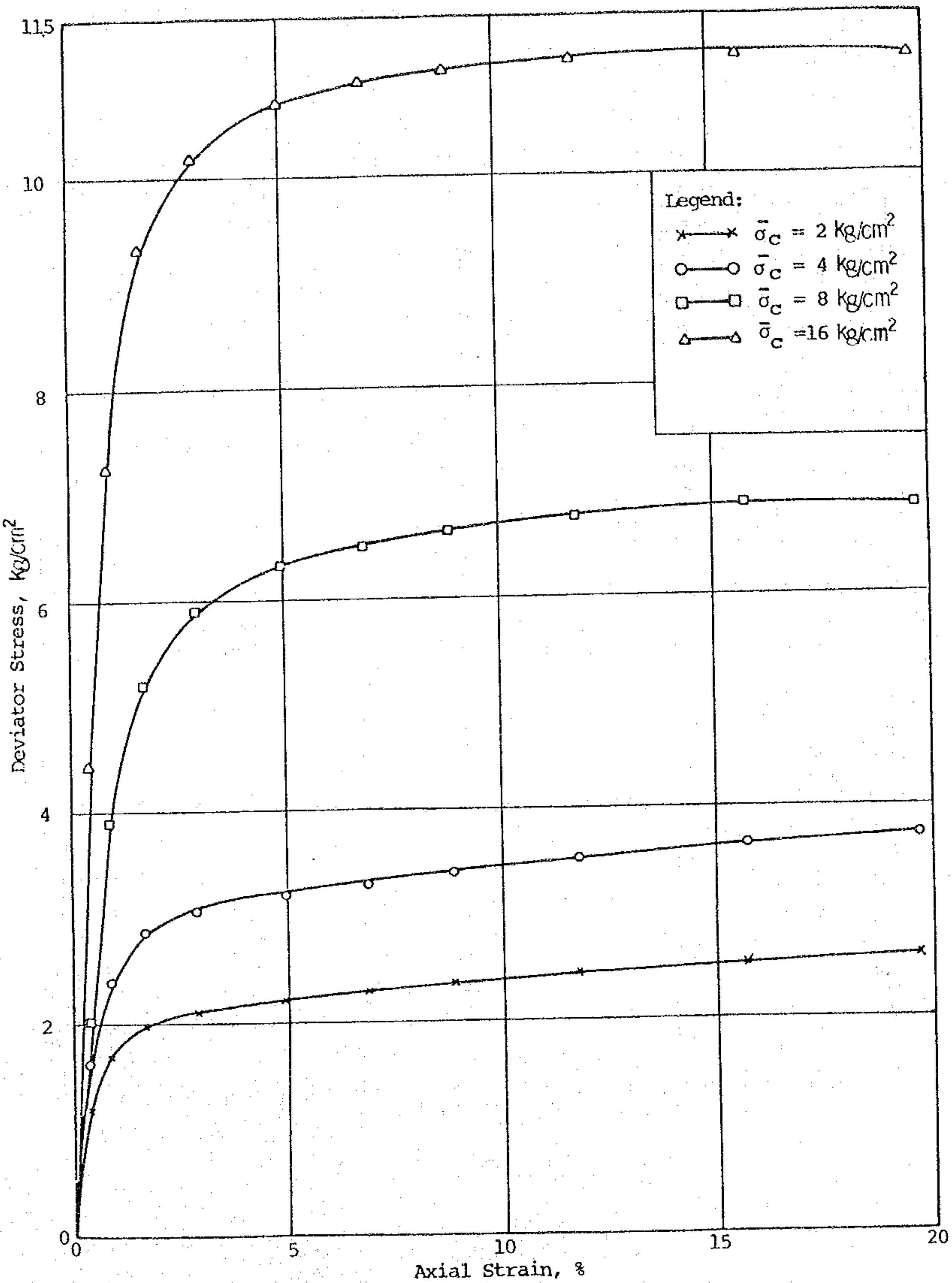

Fig. 5-8 Deviator Stress vs Axial Strain for $\overline{CU}$ Triaxial Tests on Compacted Sample No. C-1, Depth 4.00 m.

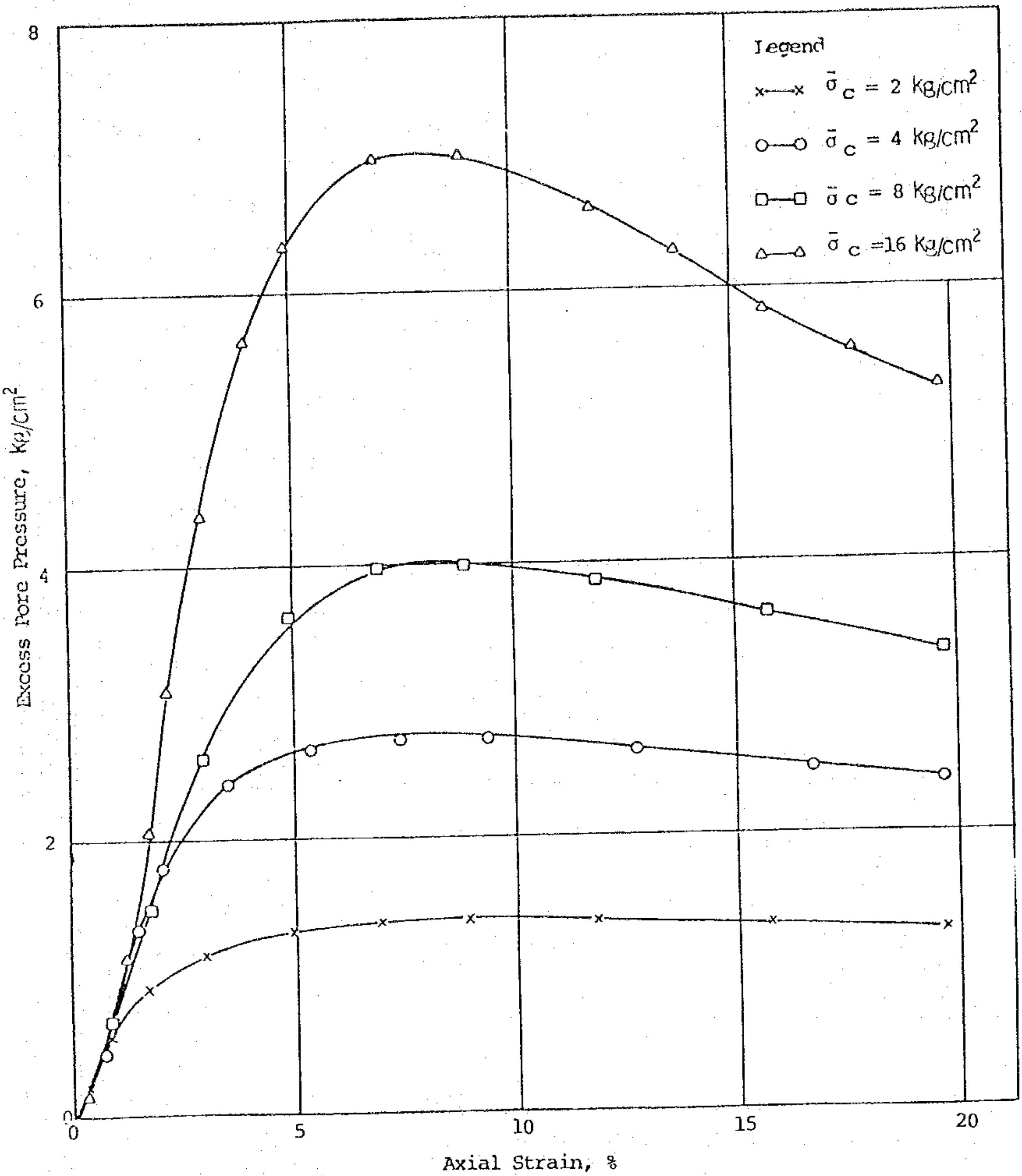

Fig. 6-1 Excess Pore Pressure vs Axial Strain for $\overline{CU}$ Triaxial Tests on Compacted Sample No. A-1, Depth 1.00 m.

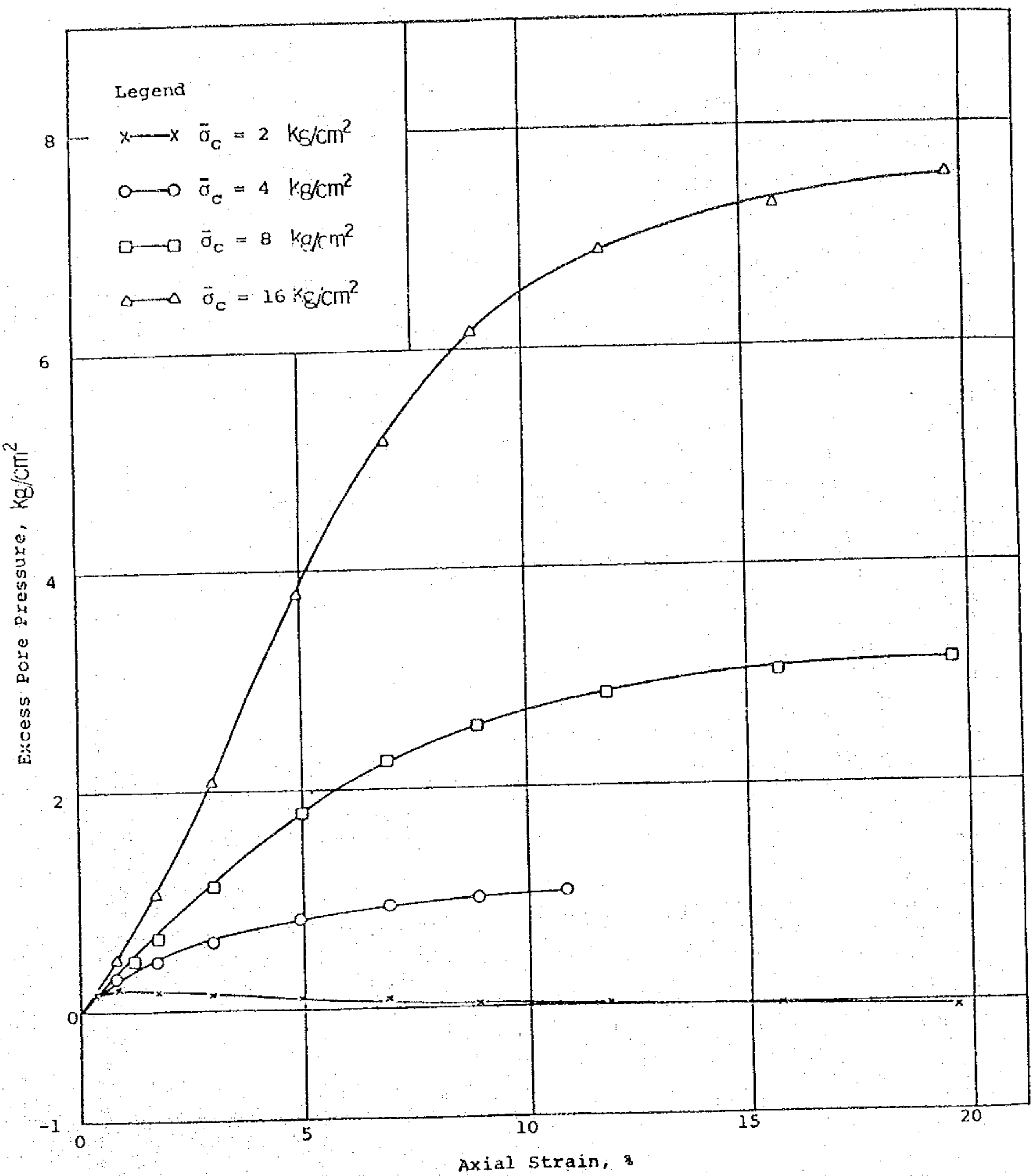

Fig. 6-2 Excess Pore Pressure vs Axial Strain for $\overline{CU}$ Triaxial Tests on Compacted Sample No. A-2, Depth 3.00 m

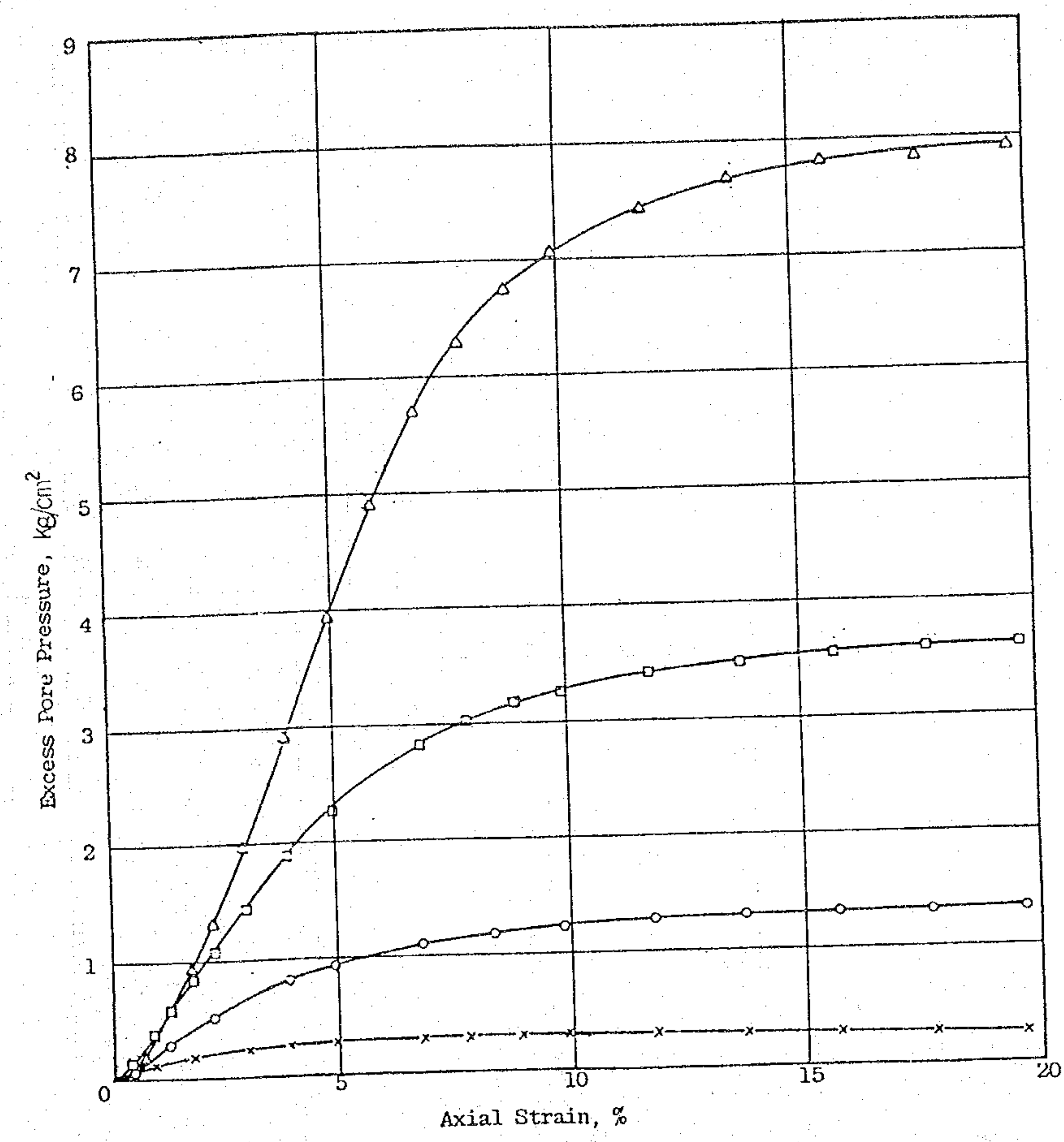

Fig.6-3 Excess Pore Pressure vs Axial Strain for $\overline{CU}$ Triaxial Tests on Sample No. A-2, Depth 5.00 m.

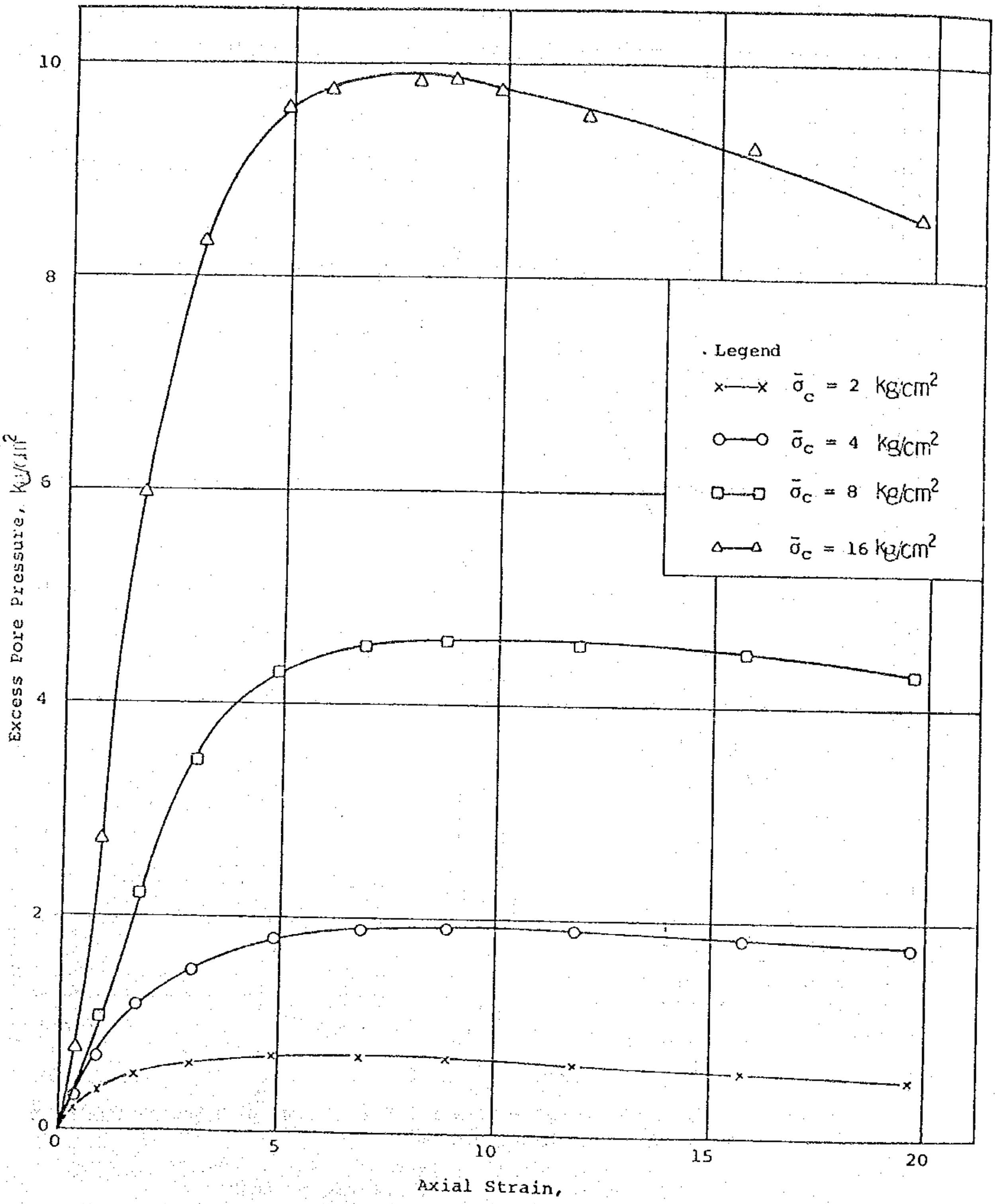

Fig. 6-4 Excess Pore Pressure vs Axial Strain for $\overline{CU}$ Triaxial Tests on Compacted Sample No. A-3, Depth 2.00 m.

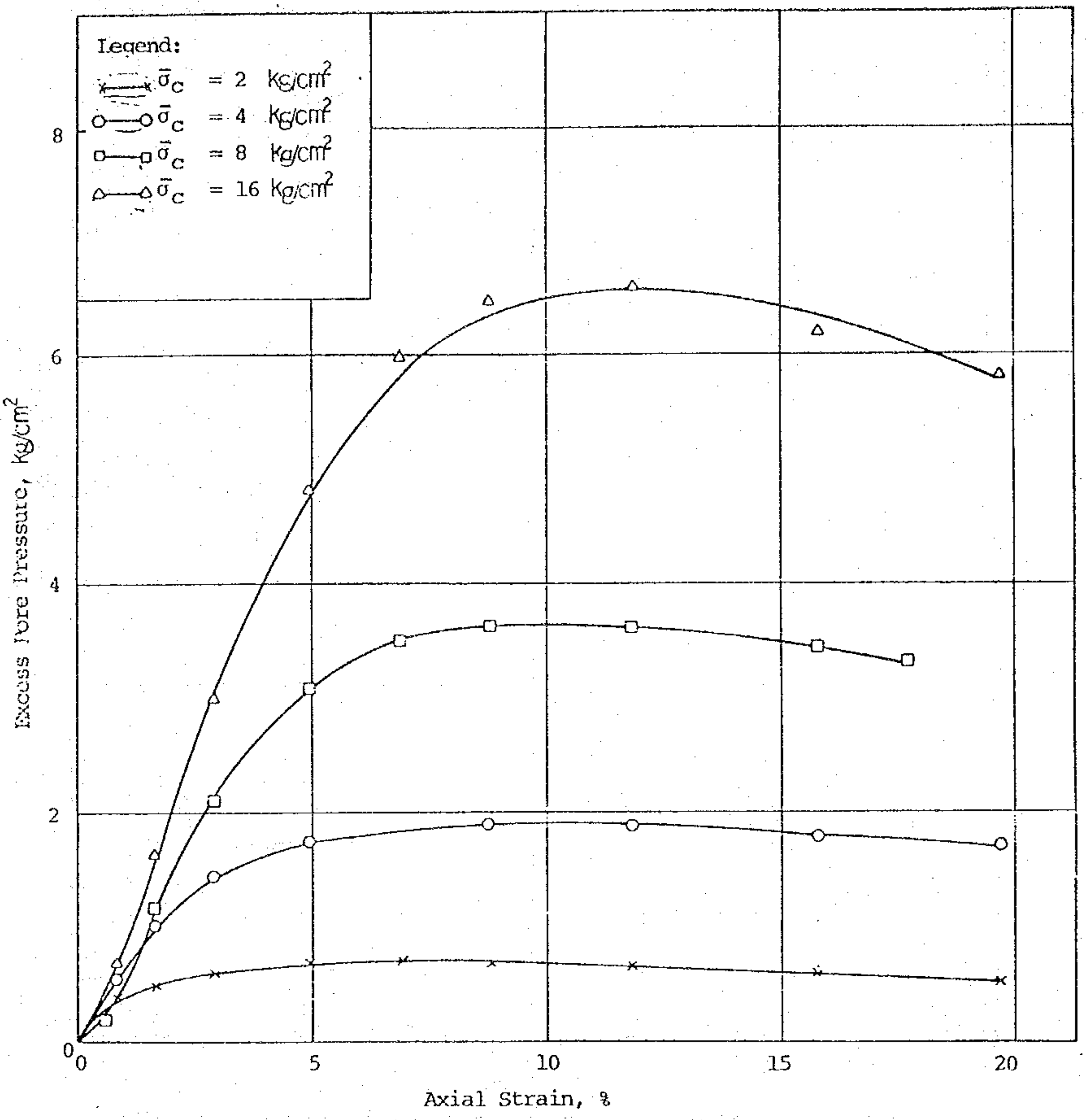

Fig. 6-5 Excess Pore Pressure vs Axial Strain for $\overline{CU}$ Triaxial Tests on Sample No. A-5, Depth 2.00 m.

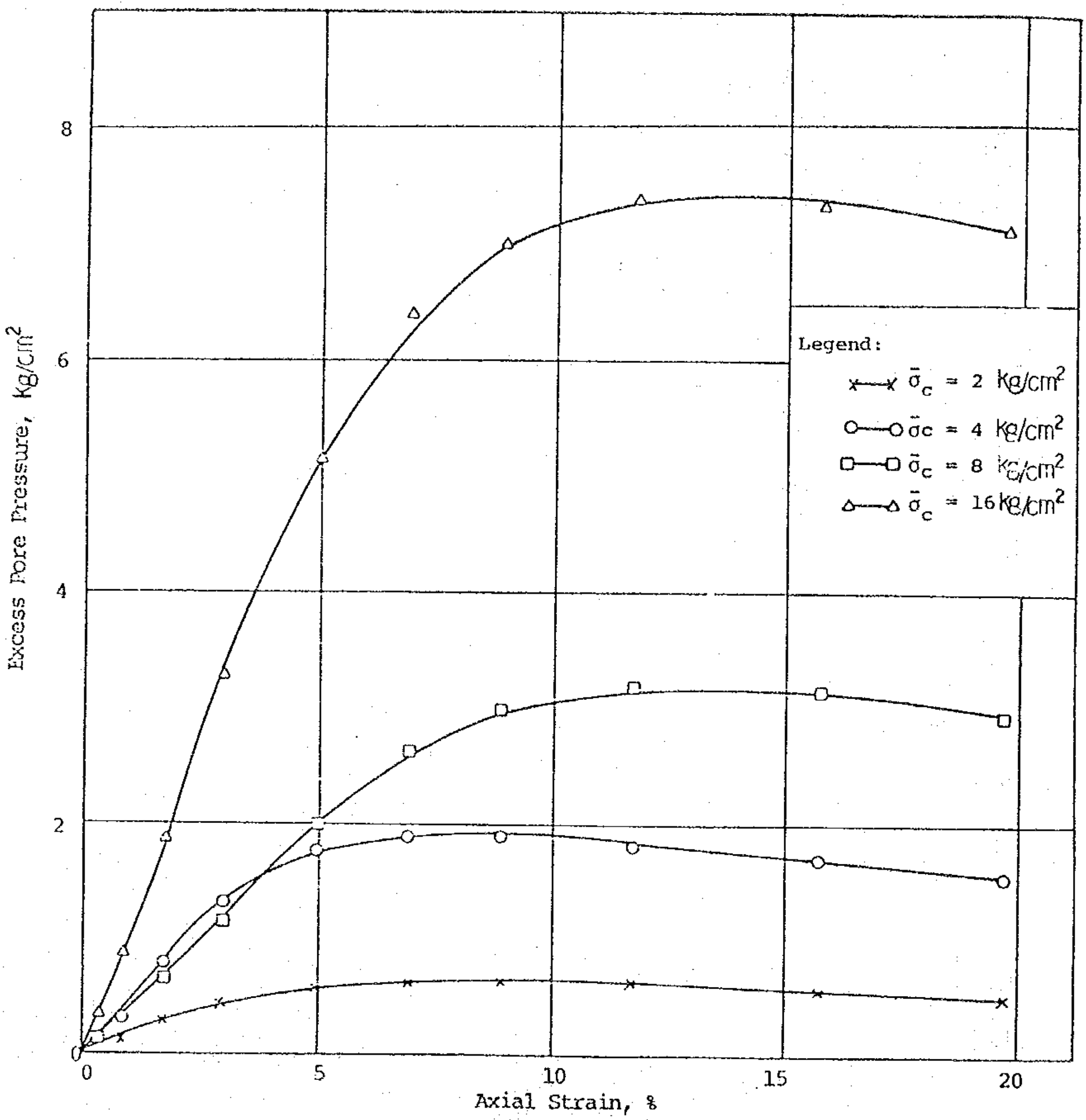

Fig. 6-6 Excess Pore Pressure vs Axial Strain for $\overline{CU}$ Triaxial Tests on Compacted Sample No. B-1, Depth 2.00 m.

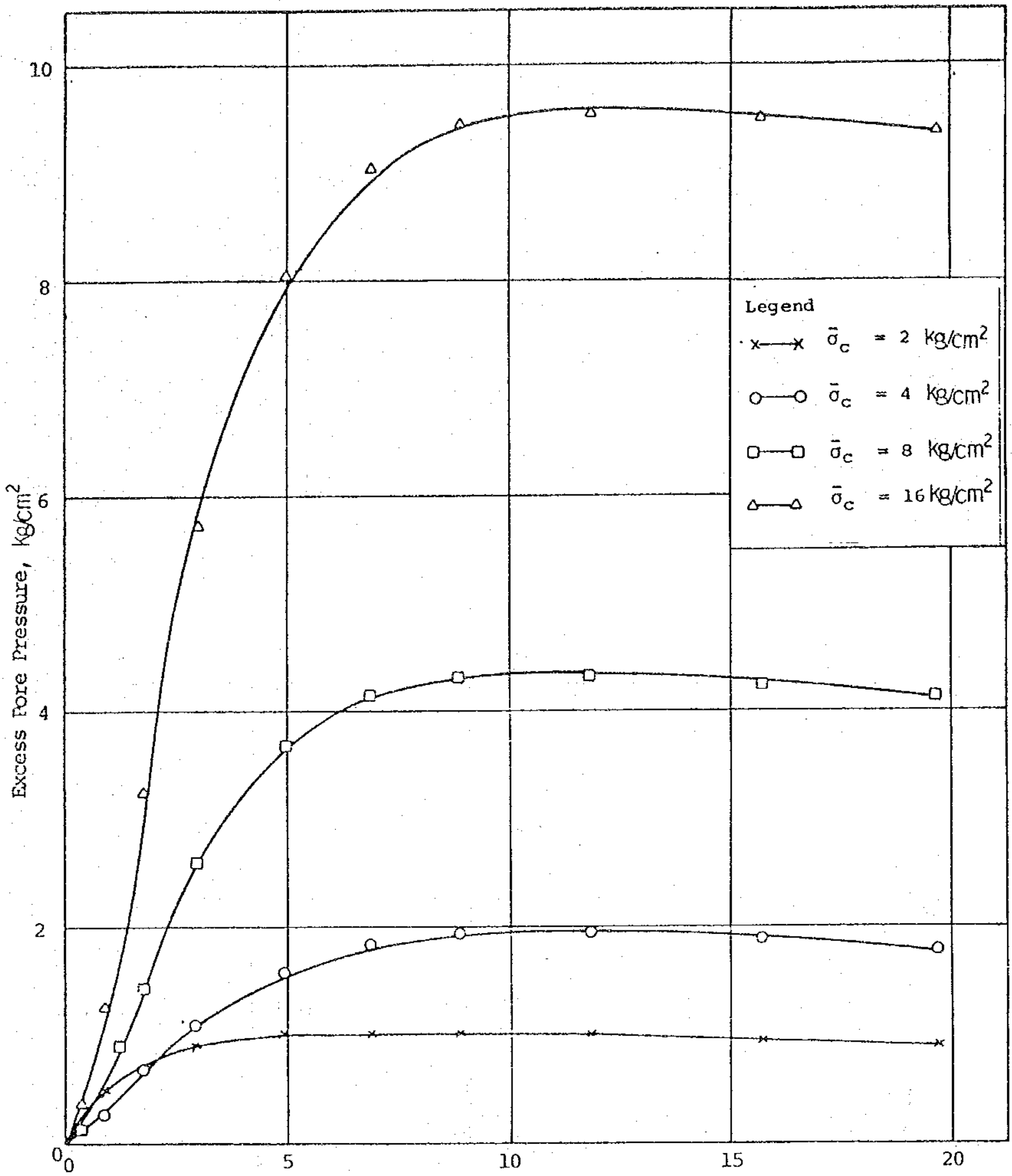

Fig. 6-7 Excess Pore Pressure vs Axial Strain for $\overline{CU}$ Triaxial Tests on Sample No C-1, Depth 3.00 m.

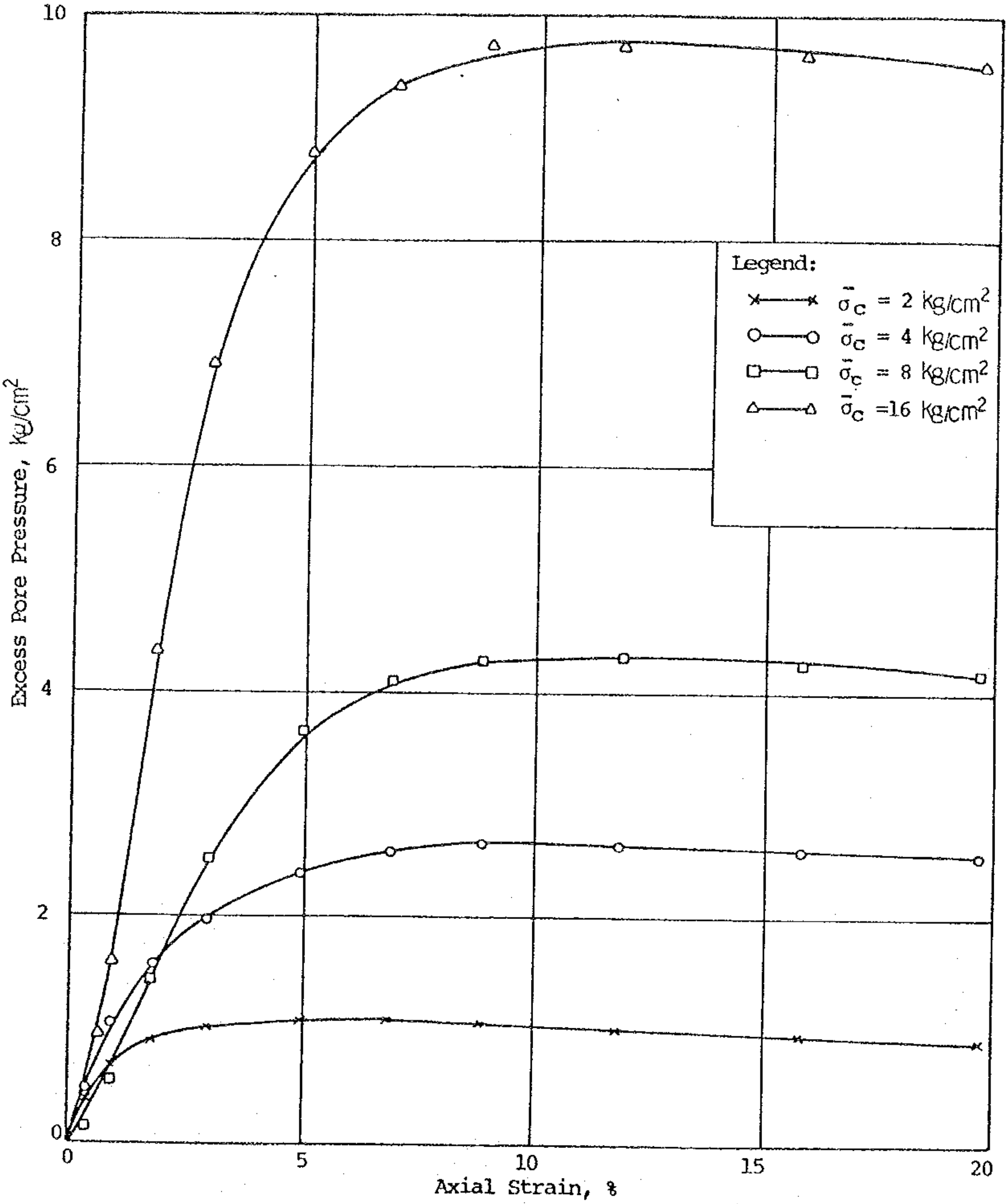

Fig. 6-8 Excess Pore Pressure vs Axial Strain for $\overline{CU}$ Triaxial Tests on Compacted Sample No. C-1, Depth 4.00 m.

A 5 CONSTRUCTION COST

Construction Cost Estimates

As of Dec. 1982 Price Level
Unit: Bath 10^3

Work Items	Unit	Unit Price	Quantities	Total Amount (10^3)	Foreign Currency (10^3)	Local Currency (10^3)
1) Preparation works						
1. Camp facilities	LS		1	122,500	38,700	83,800
2. Compensation	"		1	197,800	12,910	184,910
3. Access road	"		1	213,500	38,075	175,425
4. Clearing	"		1	19,440	-	19,440
5. Contingency	"		1	56,740	8,915	47,825
Sub-total				610,000	98,600	511,400
2) Civil works						
1. Diversion & care of river	LS		1	261,000	58,860	202,140
2. Dam	"		1	893,000	467,700	425,300
3. Spilway	"		1	519,000	81,000	438,000
4. Outlet works	"		1	41,000	5,900	35,100
5. Intake	"		1	25,000	2,700	22,300
6. Head-race	"		1	49,000	10,000	39,000
7. Surge tank	"		1	32,000	2,800	29,200
8. Penstock	"		1	69,000	13,000	56,000
9. Power station	"		1	213,000	20,900	192,100
10. Tail-race	"		1	31,700	5,200	26,500
11. Miscellaneous	"		1	93,800	35,500	58,300
12. Contingency	"		1	222,500	70,440	152,060
Sub-total				2,450,000	774,000	1,676,000
3) Hydraulic equipment						
1. Diversion gate	LS		1	9,800	490	9,310
2. Spillway gate	"		1	43,760	34,188	9,572
3. Intake gate	"		1	25,360	21,556	3,804
4. Tail-race gate	"		1	8,000	6,800	1,200

Construction Cost Estimates

(2)

As of Dec. 1982 Price Level
Unit: Bath 10^3

Work Items	Unit	Unit Price	Quantities	Total Amount (10^3)	Foreign Currency (10^3)	Local Currency (10^3)
(Continue from P-1)						
5. Outlet valve	LS		1	19,550	16,620	2,930
6. Penstock	"		1	90,000	67,500	22,500
7. Surge tank	"		1	66,000	49,500	16,500
8. Contingency	"		1	26,530	19,346	7,184
Sub-total				289,000	216,000	73,000
4) Electric equipment	LS		1	628,800	534,500	94,300
5) Telecommunication & Transmission Line	LS		1	606,600	424,600	182,000
Total				4,584,400	2,047,700	2,536,700
6) Engineering fee	LS			137,600	82,600	55,000
7) Interest during construction	LS			1,026,000	-	1,026,000
Ground-total				5,748,000	2,130,300	3,617,700

(3)

Construction Cost Estimates

As of Dec. 1982 Price Level
Unit: Bath 10^3

2) Civil Works

Work Items		Unit	Unit Price	Quantities	Total Amount (10^3)	Foreign Currency (10^3)	Local Currency (10^3)
1. Diversion & Care of river							
Excavation	Common	m^3	65	22,000	1,430	930	500
"	Rock	"	125	52,000	6,500	1,300	5,200
"	Tunnel	"	900	138,000	124,200	43,470	80,730
Concrete	Linning	"	2,900	28,000	81,200	8,120	73,080
Others		LS		1	47,670	5,040	42,630
Sub-total					261,000	58,860	202,140
2. Dam							
Excavation	Common	m^3	65	210,000	13,650	8,870	4,780
"	Rock	"	140	50,000	7,000	1,400	5,600
Embankment	Rock	"	120	3,550,000	426,000	255,600	170,400
"	Filter	"	200	412,000	82,400	49,440	32,960
"	Core	"	220	690,000	151,800	98,670	53,130
Drilling (not incl. grouting)		m	1,900	50,000	95,000	19,000	76,000
Others		LS		1	117,150	34,720	82,430
Sub-total					893,000	467,700	425,300
3. Spillway							
Excavation	Common	m^3	65	447,000	29,055	18,885	10,170
"	Rock	"	130	1,050,000	136,500	27,300	109,200
Concrete		"	2,300	102,000	234,600	23,460	211,140
Reinforcement		t	14,000	3,700	51,800	2,590	49,210
Others		LS		1	67,045	8,765	58,280
Sub-total					519,000	81,000	438,000

Construction Cost Estimates

(4)

As of Dec. 1982 Price Level
Unit: Bath 10^3

Work Items		Unit	Unit Price	Quantities	Total Amount (10^3)	Foreign Currency (10^3)	Local Currency (10^3)
(Continue from P-3)							
4. Outlet works							
Excavation	Common	m^3	65	3,200	208	135	73
"	Rock	"	140	7,500	1,050	210	840
"	Tunnel Access	"	1,500	1,600	2,400	840	1,560
Concrete	Plug	"	2,500	10,000	25,000	2,500	22,500
"	Linning	"	3,000	800	2,400	240	2,160
		LS		1	9,942	1,975	7,967
Sub-total					41,000	5,900	35,100
5. Intake							
Excavation	Common	m^3	65	6,000	390	254	136
"	Rock	"	140	13,000	1,820	364	1,456
Concrete	Open	"	2,500	6,000	15,000	1,500	13,500
Reinforcement		t	14,000	220	3,080	154	2,926
Others		LS		1	4,710	428	4,282
Sub-total					25,000	2,700	22,300
6. Head-race							
Excavation	Tunnel	m^3	930	17,000	15,810	5,534	10,276
Concrete		"	2,900	5,100	14,790	1,479	13,311
Reinforcement		t	14,500	280	4,060	203	3,857
Drilling		m	1,730	3,200	5,536	1,107	4,429
Grouting		t	7,900	320	2,528	632	1,896
Others		LS		1	6,276	1,045	5,231
Sub-total					49,000	10,000	39,000

Construction Cost Estimates

As of Dec. 1982 Price Level
Unit: Bath 10^3

Work Items		Unit	Unit Price	Quantities	Total Amount (10^3)	Foreign Currency (10^3)	Local Currency (10^3)
(Continue from P-4)							
7. Surge tank							
Concrete	Base	m^3	2,300	9,000	20,700	2,070	18,630
Reinforcement		t	14,000	330	4,620	231	4,389
Others		LS		1	6,680	499	6,181
Sub-total					32,000	2,800	29,200
8. Penstock							
Excavation	Common	m^3	65	140,000	9,100	5,915	3,185
"	Rock	"	140	60,000	8,400	1,680	6,720
Concrete		"	2,300	13,500	31,050	3,105	27,945
Reinforcement		t	14,000	490	6,860	343	6,517
Others		LS		1	13,590	1,957	11,633
Sub-total					69,000	13,000	56,000
9. Power station							
Excavation	Common	m^3	65	22,000	1,430	930	500
"	Rock	"	165	53,000	8,745	1,749	6,996
Concrete		"	2,600	40,000	104,000	10,400	93,600
Reinforcement		t	14,000	2,900	40,600	2,030	38,570
Others		LS		1	58,225	5,791	52,434
Sub-total					213,000	20,900	192,100

Construction Cost Estimates

As of Dec. 1982 Price Level
Unit: Bath 10^3

Work Items	Unit	Unit Price	Quantities	Total Amount (10^3)	Foreign Currency (10^3)	Local Currency (10^3)
(Continue from P-5)						
10. Tail-race						
Excavation Common	m^3	65	31,000	2,015	1,301	714
" Rock	"	125	72,000	9,000	1,800	7,200
Concrete	"	2,600	6,500	16,900	1,690	15,210
Others	LS		1	3,785	409	3,376
Sub-total				31,700	5,200	26,500
11. Miscellaneous (S.Y. & others)						
Excavation Common	m^3	65	252,000	16,380	10,647	5,733
Banking	"	120	250,000	30,000	18,000	12,000
Shotcrete	m^2	740	50,000	37,000	3,700	33,300
Others	LS		1	10,420	3,153	7,267
Sub-total				93,800	35,500	58,300

JICA